

ENERGY CONSUMPTION MODELING OF TURN-MILL SYSTEMS AND  
RELATED MACHINING PROCESSES

A THESIS SUBMITTED TO  
THE GRADUATE SCHOOL OF NATURAL AND APPLIED SCIENCES  
OF  
MIDDLE EAST TECHNICAL UNIVERSITY

BY

MARIYEH MORADNAZHAD

IN PARTIAL FULFILLMENT OF THE REQUIREMENTS  
FOR  
THE DEGREE OF MASTER OF SCIENCE  
IN  
MECHANICAL ENGINEERING

SEPTEMBER 2015



Approval of the thesis:

**ENERGY CONSUMPTION MODELING OF TURN-MILL SYSTEMS AND  
RELATED MACHINING PROCESSES**

Submitted by **MARIYEH MORADNAZHAD** in partial fulfillment of the  
requirements for the degree of **Master of Science in Mechanical Engineering**  
**Department, Middle East Technical University** by,

Prof. Dr. Gülbin Dural Ünver  
Dean, Graduate School of **Natural and Applied Sciences**

Prof. Dr. Tuna Balkan  
Head of Department, **Mechanical Engineering**

Prof. Dr. Metin Akkök  
Supervisor, **Mechanical Engineering Dept., METU**

Assist. Prof. Dr. Hakkı Özgür Ünver  
Co-supervisor, **Mechanical Engineering Dept., TOBB ETU**

**Examining Committee Members:**

Assoc Prof. Dr. Tuba Okutucu Özyurt  
Mechanical Engineering Dept., METU

Prof. Dr. Metin Akkök  
Mechanical Engineering Dept., METU

Assist. Prof. Dr. Hakkı Özgür Ünver  
Mechanical Engineering Dept., TOBB ETU

Assist. Prof. Dr. Ali Emre Turgut  
Mechanical Engineering Dept., METU

Prof. Dr. Engin Kılıç  
Mechanical Engineering Dept., ATILIM University

**Date:** \_\_\_\_\_

**I hereby declare that all information in this document has been obtained and presented in accordance with academic rules and ethical conduct. I also declare that, as required by these rules and conduct, I have fully cited and referenced all material and results that are not original to this work.**

Name, Last name : MARIYEH MORADNAZHAD

Signature :

## **ABSTRACT**

### **ENERGY CONSUMPTION MODELING OF TURN-MILL SYSTEMS AND RELATED MACHINING PROCESSES**

Moradnazhad, Mariyeh

M.S., Department of Mechanical Engineering

Supervisor: Prof. Dr. Metin Akkok

Co-Supervisor: Assist. Prof. Dr. Hakki Ozgur Unver

September 2015, 123 pages

In this thesis, a generic energy consumption model is developed for turn-mill systems which could be adopted for all turn-mill machine tools. Also energy characterization studies is performed to a turn-mill machine tool in order to validate the presented model and a methodology is created to develop a feature based energy consumption model for this turn-mill system considering cutting parameters during cutting operations of 304 stainless steel. This model predicts the energy consumption of the turn-mill machine tool during machining operation based on used features and cutting parameters with an accuracy of 95%. The results of this research work showed that depth of cut is the most significant factor on power consumption during machining processes. Furthermore, the present work outlines an experimental study to investigate the energy consumption of orthogonal turn-milling processes performed on a turn-mill machine tool. Effect of cutting parameters on power requirement and energy consumption of turn-milling processes are analyzed. In addition, conventional turning processes are performed in the same cutting conditions in order to compare their power and energy consumption with orthogonal turn-milling processes. It is concluded that in spite of high power requirement of the turn-milling processes, these processes result in higher material removal rates and are more energy efficient.

Keywords: Energy consumption modeling, Turn-mill systems, orthogonal turn-milling processes

# ÖZ

## ENERGY CONSUMPTION MODELING OF TURN-MILL SYSTEMS AND RELATED MACHINING PROCESSES

Moradnazard, Mariyeh

Yüksek Lisans, Makina Mühendisliği Bölümü

Tez Yöneticisi: Prof. Dr. Metin Akkök

Ortak Tez Yöneticisi: Yrd. Doç. Dr. Hakki Özgür Ünver

Eylül 2015, 123 Sayfa

Bu tezde, tüm turn-mill tezgahlarında kullanılabilir genel bir enerji tüketim modeli geliştirilmiştir. Sunulan modeli doğrulamak için bir turn-mill tezgahı üzerinde enerji karakterizasyon çalışmaları yapılmıştır. Bu turn-mill tezgahı üzerinde kesme parametrelerini göze alarak, 304 paslanmaz çelik kesme işlemleri sırasında, unsur bazlı bir enerji tüketim modeli oluşturmak adına bir metodoloji sunulmuştur. Bu model turn-mill tezgahının kesme işlemleri esnasındaki enerji tüketimini kesme unsurleri ve kesme parametrelerine dayalı 95% oranında bir doğrulukla tahmin etmektedir. Bu çalışmaların sonucunda talaş derinliğinin işleme süreçlerinde güç tüketimini etkileyen en önemli faktör olduğunu tesbit edilmiştir. Ayrıca bu tez kapsamında dikey turn-mill süreçlerinin enerji tüketimini incelemek için deneysel çalışmalar gerçekleştirilmiştir. Kesme parametrelerinin turn-mill işlemlerinin enerji tüketimi ve güç gereksinimi üzerindeki etkisi incelenmiştir. Buna ek olarak, turn-mill işlemlerinin güç ve enerji tüketimini karşılaştırmak için aynı kesme şartlarında geleneksel torna işlemleri gerçekleştirilmiştir. Turn-mill işlemlerinin yüksek güç gereksinimine rağmen, bu işlemlerde talaş kaldırma oranının daha yüksek olduğu ve enerji açısından daha verimli olduğu sonucuna varılmıştır.

Anahtar Kelimeler: Enerji tüketim modelleri, Turn-mill sistemleri, Dikey turn-mill işlemleri

*To my family*

## **ACKNOWLEDGEMENTS**

The author wishes to express his deepest gratitude to his supervisor Prof. Dr. Metin Akkök and co-supervisor Assist. Prof. Dr. Hakkı Özgür Ünver for their guidance, advice, criticism, encouragements and insight throughout the research.

The technical assistance of Mr. Hasan Uz, Mr. Kamil Arslan are gratefully acknowledged.

The author would also like to thank. Dr. Bahram Lotfisdigh for his suggestions and comments.

This study was supported by SAN-TEZ project No. 00979.stz.2011-12 of the Turkish Ministry of Science, Technology and Industry.



# TABLE OF CONTENTS

ABSTRACT.....	I
ÖZ .....	II
ACKNOWLEDGEMENTS.....	IV
TABLE OF CONTENTS.....	V
LIST OF TABLES.....	VIII
LIST OF FIGURES .....	X
CHAPTERS	
1 INTRODUCTION.....	1
2 LITERATURE REVIEW.....	5
2.1 Energy consumption modelling .....	5
2.1.1 Theoretical modelling .....	5
2.1.2 Empirical modelling.....	20
2.2 Design of experiments .....	26
2.2.1 Taguchi methodology.....	26
2.2.2 Response surface methodology.....	27
2.3 Feature Based Design and ISO 10303 (STEP) standard.....	29
2.4 Turn-mill systems .....	31
3 ENERGY CONSUMPTION MODELING OF TURN-MILL SYSTEMS.....	35
3.1 Idle energy .....	36
3.2 Auxiliary energy .....	36
3.3 Cutting energy.....	38

4 ENERGY CHARACTERIZATION OF MAZAK INTEGREX I200-ST TURN-MILL SYSTEM .....	41
4.1 Machine tool properties.....	41
4.2 Energy measurement method .....	43
4.3 Idle energy.....	44
4.4 Auxiliary energy.....	46
4.4.1 Main Spindle .....	47
4.4.2 Sub-Spindle .....	49
4.4.3 Milling Head.....	50
4.4.4 Turret .....	56
4.4.5 Tool change .....	60
4.4.6 Conveyor .....	62
4.4.7 Coolant .....	62
4.4.8 Chiller and lubrication unit.....	65
4.5 Cutting energy.....	65
4.5.1 Outer Diameter turning (OD turning).....	67
4.5.2 Slot milling .....	71
4.5.3 Hole making .....	74
4.5.4 Boss rectangular milling.....	77
5 FIRST CASE STUDY; VERIFICATION OF TURN-MILL ENERGY MODEL .....	83
5.1 Turning .....	86
5.2 Hole making.....	88
5.3 Boss rectangular.....	89
5.4 Slot milling .....	90

6 SECOND CASE STUDY; INVESTIGATION OF THE ENERGY CONSUMPTION OF TURN-MILLING PROCESSES .....	91
7 DISCUSSION OF THE RESULTS .....	97
8 CONCLUSIONS AND FUTURE WORKS.....	101
REFERENCES .....	105
APPENDICES	
A. AVERAGE POWER CONSUMPTION AMOUNT FOR AUXILIARY SUB-UNITS.....	111
B. DERIVED EQUATIONS FOR SUB-UNITS OF MAZAK INTEGREX I200-ST 117	
C. MAZARTOL PROGRAMMING OF FIRST CASE PART .....	119
D. MATERIAL REMOVED DURING CUTTING FEATURES OF CASE STUDY .....	121
E. ISO PROGRAMMING OF SECOND CASE PART .....	123

## LIST OF TABLES

### TABLES

Table 1 A summary of developed theoretical models .....	19
Table 2 A summary of developed empirical models.....	25
Table 3 A summary of energy optimization studies using DOE methods .....	29
Table 4 Specifications of Mazak integrex i200-ST .....	42
Table 5 Pumps of coolant system of Mazak integrex i200-ST.....	63
Table 6 Power consumption of coolant system.....	64
Table 7 Properties of 304 stainless steel.....	67
Table 8 Levels of cutting parameters for design of experiments for OD turning.....	68
Table 9 Taguchi's L9 orthogonal array for OD turning .....	69
Table 10 Modified Levels of cutting parameters for design of experiments.....	69
Table 11 Power consumption values of designed OD turning experiments.....	70
Table 12 Levels of cutting parameters for design of experiments for slot milling.....	72
Table 13 Taguchi's L9 orthogonal array for slot milling .....	72
Table 14 Power consumption values of designed slot milling experiments.....	73
Table 15 Levels of cutting parameters for design of experiments for hole making .....	75
Table 16 Taguchi's L9 orthogonal array for hole making.....	75
Table 17 Power consumption values of designed hole making experiments .....	76
Table 18 Levels of cutting parameters for design of experiments for slot milling.....	79
Table 19 Taguchi's L9 orthogonal array for slot milling .....	79
Table 20 Power consumption values of designed slot milling experiments.....	80
Table 21 Average power consumption amounts for spindle speeds of main spindle.....	111

Table 22 Average power consumption amounts for spindle speeds of sub-spindle .....112

Table 23 Average power consumption amounts for spindle speeds of milling spindle.....113

Table 24 Average power consumption amounts for G00 moves of milling head.....114

Table 25 Average power consumption amounts for G00 moves of milling head.....114

Table 26 Average power consumption amounts for G01 moves of milling head.....115

Table 27 Average power consumption amounts for rotation of milling head .....115

Table 28 Average power consumption amounts for for G00 movess of turret.....116

Table 29 Average power consumption amounts for for G01 movess of turret.....116

Table 30 Derived equations for sub-units of Mazak integrex i200-ST .....117

Table 31 Material removed during cutting features of case study .....121

# LIST OF FIGURES

## FIGURES

Figure 1 Sources of primary energy consumption in the world .....	1
Figure 2 The power consumption of the Cincinnati Milacron automated milling machine represented graphically .....	6
Figure 3 The energy used as a function of production rate for an automobile production machining line . .....	7
Figure 4 Power profile of a turning process .....	9
Figure 5 Average fixed energy breakdown of a reviewed machine tool .....	10
Figure 6 Energy and power demand as a function of M.R.R. ....	14
Figure 7 System influences on the energy losses of machine tool components .....	17
Figure 8 Specific consumed energy as a function of milling parameters .....	22
Figure 9 Material removal power with respect to the tool wear under the specified conditions .	25
Figure 10 a) Coordinate system of an orthogonal turn-mill system, b) Coordinate system of a co-axial turn-mill system .....	31
Figure 11 A view of Mazak integrex i200-ST.....	42
Figure 12 Schematic representation of the energy measurement methods .....	44
Figure 13 Instantaneous power - time graph for basic energy consumption.....	45
Figure 14 Subunits of Mazak integrex i200-ST .....	46
Figure 15 Average power consumption-speed graph for main spindle.....	47
Figure 16 Trend lines of average power consumption-speed graph for main spindle.....	48
Figure 17 Average power consumption-speed graph for sub-spindle.....	49
Figure 18 Trend lines of average power consumption-speed graph for sub-spindle.....	50
Figure 19 Average power consumption-speed graph for milling spindle .....	51

Figure 20 Trend lines of average power consumption-speed graph for milling spindle.....	52
Figure 21 Average power consumption-feed rate graph for feed axis of milling head (G01) .....	53
Figure 22 Average power consumption-feed rate graph for feed axis of milling head (G00) .....	54
Figure 23 Trend lines of average power consumption-feed rate graph for milling head (G01) ...	54
Figure 24 Trend lines of average power consumption-feed rate graph for milling head (G00) ...	55
Figure 25 Average power consumption-rotation graph for B axes of milling head .....	56
Figure 26 Average power consumption-feed rate graph for feed axis of milling head (G01) .....	57
Figure 27 Average power consumption-feed rate graph for feed axis of milling head (G00) .....	58
Figure 28 Trend lines of average power consumption-feed rate graph for turret (G01).....	58
Figure 29 Trend lines of average power consumption-feed rate graph for turret (G00).....	59
Figure 30 Average power consumption-time graph for tool change of milling head .....	60
Figure 31 Average power consumption-time graph for tool change of turret .....	61
Figure 32 Pumps usage of coolant system of Mazak integrex i200-ST.....	63
Figure 33 Selected STEP features.....	66
Figure 34 Schematic of axial depth of cut and radial depth.....	78
Figure 35 Part model of case study .....	83
Figure 36 Power consumption during cutting operation of case study part.....	84
Figure 37 Power consumption and sequence of cutting features of case study part.....	85
Figure 38. Estimated and real power consumption during cutting operation of case study part ..	86
Figure 39 Tool path of OD turning of case study part .....	86
Figure 40. Power-time graph for OD turning .....	87
Figure 41 Power-time graph for center drilling and.....	88
Figure 42 Tool path of boss rectangular milling of case study part.....	89
Figure 43 Real energy consumption and estimated energy consumption for cutting features.....	90

Figure 44 a) orthogonal turn-milling b) co-axial turn-milling ..... 91

Figure 45 Effect of rotational speed on power requirement and energy consumption of turn-milling processes ..... 93

Figure 46 Effect of depth of cut on power requirement and energy consumption of turn-milling processes ..... 93

Figure 47 Effect of depth of cut on power requirement and energy consumption of turn-milling processes ..... 94

Figure 48. Surface plots for power consumption of orthogonal turn-milling process..... 95

Figure 49 . Pictures of turn-milled parts..... 95

Figure 50 Breakdown of energy consumption for cutting operation of the case study part..... 97

Figure 51 Energy consumption of spindle during machining processes of case study part ..... 98

Figure 52 Breakdown of cutting energy consumption for case study ..... 99

Figure 53 Specific cutting energy of the cutting features..... 100



# CHAPTER 1

## INTRODUCTION

The increase of industrialization and human population leads to a rapid increase in world energy consumption. According to the estimations, the primary energy demand is expected to increase by a minimum of 42.7% to the current demand in 2035 in the world [1]. As energy demand is increasing constantly, concerns about the environmental impact of resources used for energy production and the availability of energy is also increasing. Carbon dioxide gas, water vapor and methane in the atmosphere, which are known as greenhouse gases, have the ability to keep the sun's rays reflected from the earth and this is causing the global warming. In order to produce energy, natural energy sources like coal, natural gas and oil, which are called carbon-based or fossil fuels, are burning out and resulting carbon- dioxide raise the temperature of the earth. Sources of primary energy consumption in the world and their usage percentages are shown in Figure 1.

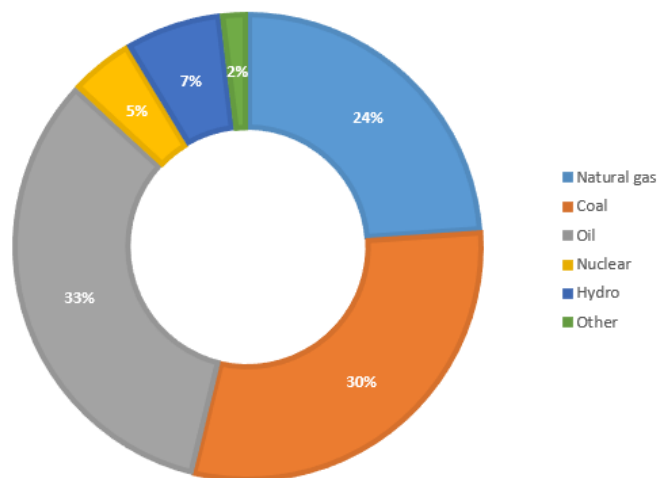


Figure 1 Sources of primary energy consumption in the world [1]

Turkey is located in fifth place in natural gas importing countries and eighth place in coal importing countries in the rankings. In addition, Turkey imports about 90% of crude oil processed in the petroleum refining [2, 3]. According to 2011 data, the 21.9% of the total imports of turkey are energy imports [4]. Therefore, efforts to reduce energy demand should be carried out using existing energy more efficiently. Energy efficiency is defined as a product or service using less energy to produce or provide.

The manufacturing sector is comprised of some of the largest energy consumers and carbon emitters in the world, accounting for about 33% of primary energy use and 38% of CO<sub>2</sub> emissions globally. On the other hand the rising cost of energy also is affecting the manufacturing industry economically. Reducing the amount of consumed energy and implementing more energy efficient manufacturing processes can significantly enhance performance of processes and reduce its undesirable impacts. Therefore, energy saving has become a worldwide hot issue in manufacturing sectors, and energy- efficient machining system will be very promising in metal- working industry and could significantly improve the environmental performance of manufacturing processes. Thus, scholars strongly agree that performing an inclusive review of manufacturing processes to determine overall energy demand is essential [5].

Manufacturing processes are processes carried out on raw material to produce finalized or intermediated products. Casting, welding, surface treatment, heat treatment and machining are the basic manufacturing process [6]. Machining is one of the most fundamental and important manufacturing processes that is widely used in manufacturing industries which is also one of the main energy consuming practices in the manufacturing sector and it has been identified as a main target for energy reduction in recent years. Most existing studies on energy reduction in the manufacturing sector are focused on developing the most energy efficient machining processes. Main machining processes are turning, milling, shaping, planing, grinding, broaching and drilling operations. Machining operations are usually performed on the machine tools. The development of technology has increased the number of machine tools and computer controlled machines developed over time. With development of machine tool

production technologies, machines are capable of reaching a very precise cutting ability. The widespread use of machine tools made it one of the most important energy consumers in the machine tool industry. Machine tools require electrical energy to run and most of the electricity generated in the country is obtained from fossil fuels with high carbon emissions and low energy conversion efficiency. So for efficient use of energy it is important to determine energy consumption of machine tools during machining operations. The energy consumption of each machine tool according to the intended use and different capabilities of subunits is unique. Therefore, obtaining power consumption profile of each machine tool is required. These profiles makes easier to estimate the energy consumption of machining operations and also helps to determine processing strategies in order to more efficient use of energy.

This study has two main objectives. The first one is developing a generic energy consumption model for turn-mill machine tools which will be usable for different machine tools. The other is characterization of a turn-mill machine tool and providing a feature-based energy consumption model which will give the energy consumption of a specific machine tool for different machining features.

In this framework, a generic energy consumption model is presented to estimate the energy consumption amounts of turn-mill machine tools, then this model is further improved with performing experimental studies on Mazak integrex i200-ST located at TOBB ETU Advanced Manufacturing Laboratory and adding constants and parameters to generate an energy consumption model which will be specific to this machine tool.

The second chapter of the thesis contains literature review. In this section, studies on characterization and energy consumption modelling of machine tools, design of experiments for energy efficiency and turn-mill systems are identified furthermore feature based design and STEP standard is summarized. Third Chapter of the thesis includes the development of generic energy consumption model for turn-mill machine tools and details of the model. In fourth chapter energy characterization of Mazak integrex i200-ST turn-mill machine tool is presented and experimental studies are performed to validate the presented generic model and a feature based energy

consumption model is developed. In fifth chapter a case study is presented where results are discussed in sixth chapter and the last chapter includes conclusion and future work.

## **CHAPTER 2**

### **LITERATURE REVIEW**

In this section the studies which are relevant to this thesis work are summarized. Strengths, weaknesses, challenges and limitations of related studies are identified and given in following sections.

#### **2.1 Energy consumption modelling**

Analyzing energy consumption of machine tools is significant and required to reduce the total amount of energy during machining operations. Several efforts have been made for modeling of energy consumption of machine tools. According to existing studies and methodologies, modeling of energy consumption of machine tools can be grouped into two broad categories: theoretical modeling and empirical modeling. Studies in this area have increased considerably in recent years.

##### **2.1.1 Theoretical modelling**

A large number of studies involve the development of a mathematical model for predicting electrical energy requirements of machine tools during machining operations. One of the precursor works to determine the environmental impact of machine tools and energy consumption rate and periods of sub-units was carried out by Kordonowy [7]. In the study power consumption data of 6 different machine tool including injection molding machine, manual and automated milling machines and automated lathe machine were collected. As shown in Figure 2 the ratio of power consumed for metal cutting and power consumed by the sub-units to total power consumed for carrying out the turning operation was measured. In addition, the values of power consumption according to the characters of operation are divided into two groups of variable and constant. Power drawn by sub-units such as computer, fans, servo motors, hydraulic pumps and unloaded motors which are activated as soon as machine start-up are classified as constant part. In this study power measurements were achieved by measuring the voltage and current values with the help of multi-meter. Sub-units of machine were classified and with

specifying how much power is drawn by which sub-unit energy characterization of machine tools was done.

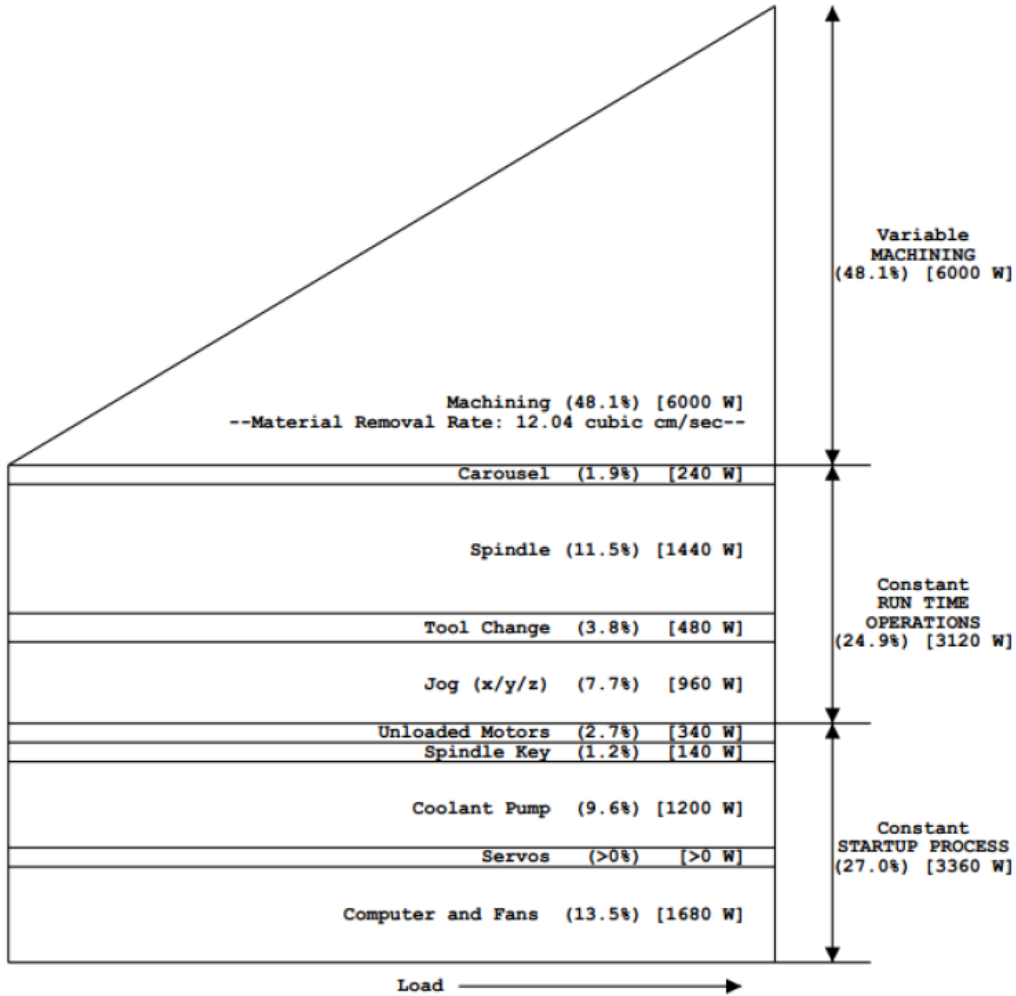


Figure 2 The power consumption of the Cincinnati Milacron automated milling machine represented graphically [7].

In this study, it is assumed that a considerable amount of energy is required to startup and also keeps the machine in a ready status, in addition there is an energy demand which is related to the rate of material processing, so it has been suggested that the energy expended during the machining process could be calculated using Equation (1).

$$E = (P_0 + kQ) \quad (1)$$

Where  $P_0$  is power consumed by machine,  $k$  is specific cutting energy,  $Q$  is Material removal rate and  $t$  is cutting time. Gutowski et al [8] have shown that energy consumed by material removing process is much lower than energy consumed by necessary auxiliary units in order to maintain the metal cutting process using the monitoring system developed by Dahmus and Gutowski [9]. Although this model has paved the way for many other studies, it couldn't provide a full-fledged model for energy consumed by auxiliary sub-units. Because the energy consumed by these sub-units does not stay fixed and is subject to change at the time of operation. There has not been an experimental study In order to measure the consistency of this model. Figure 3 shows the energy used as a function of production rate for an automobile production machining line. It is noticeable that the energy consumed for machining is much exceeded by the energy consumed while machine is idling.

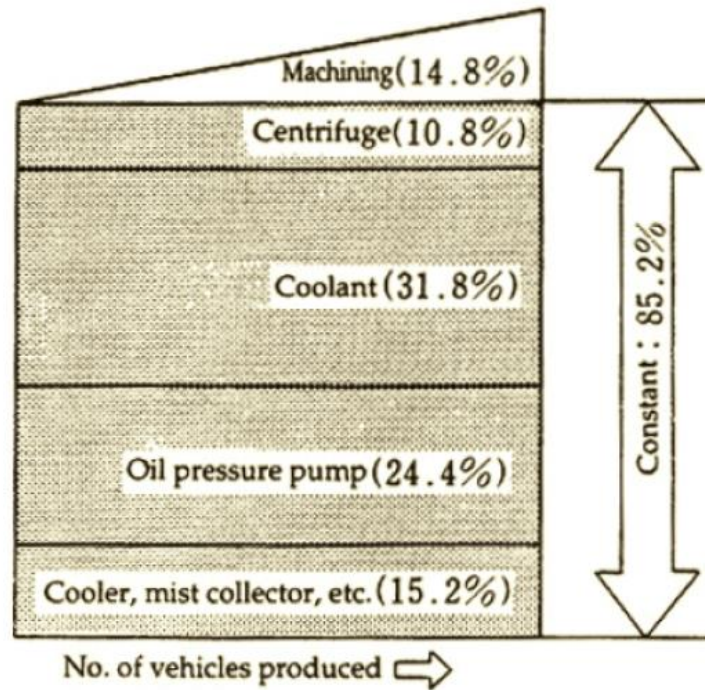


Figure 3 The energy used as a function of production rate for an automobile production machining line [8].

Devoldere et al. [10] also analyzed the energy consumption of machine tools and contributions of sub-units on a five-axis milling machine and as a result of their measurements, machine consumes about 1.7KWenergy in idle or stand-by mode.

Rajemi et al. [11] were modeled the energy expended to produce a part with turning operations as shown in Equation (2).

$$\mathbf{E} = \mathbf{P}_0\mathbf{t}_1 + (\mathbf{P}_0 + \mathbf{kQ})\mathbf{t}_2 + \mathbf{P}_0\mathbf{t}_3 \left(\frac{\mathbf{t}_2}{\mathbf{T}}\right) + \mathbf{Y}_E \left(\frac{\mathbf{t}_2}{\mathbf{T}}\right) \quad (2)$$

where  $P_0$  is power consumed by machine module without cutting  $t_1$  is the machining setup time,  $t_2$  is the actual cutting time  $t_3$  is the tool change time,  $T$  is tool life,  $Y_E$  is energy footprint per tool edge,  $k$  is specific cutting energy and  $Q$  is material removal rate. This model is focused on determining the energy footprint not direct energy demand and also no study has been conducted to investigate the consistency of the created model with experimental measurements. Using developed equation, optimum cutting velocities was evaluated to obtain the optimum tool-life for minimum energy in this study. They also reported that machining at lower production rates decrease the rate of actual energy required for machining processes. Mativenga and Rajemi [12] improved Rajemi et al.'s [11] methodology by taking spindle power consumption into consideration.

In complex NC machine tools, peripheral subunits account for more than 30% of total energy consumption, therefore peripheral subunits could play a significant role in reducing the energy consumption of machine tools [13]. Since the total energy consumption of a machine is greater than the energy consumed during the cutting process, the energy consumed by a peripheral subunit must be taken into consideration. A number of studies have been performed for this purpose. Figure 4 demonstrates the power profile of a turning process presented by Li et al [14].



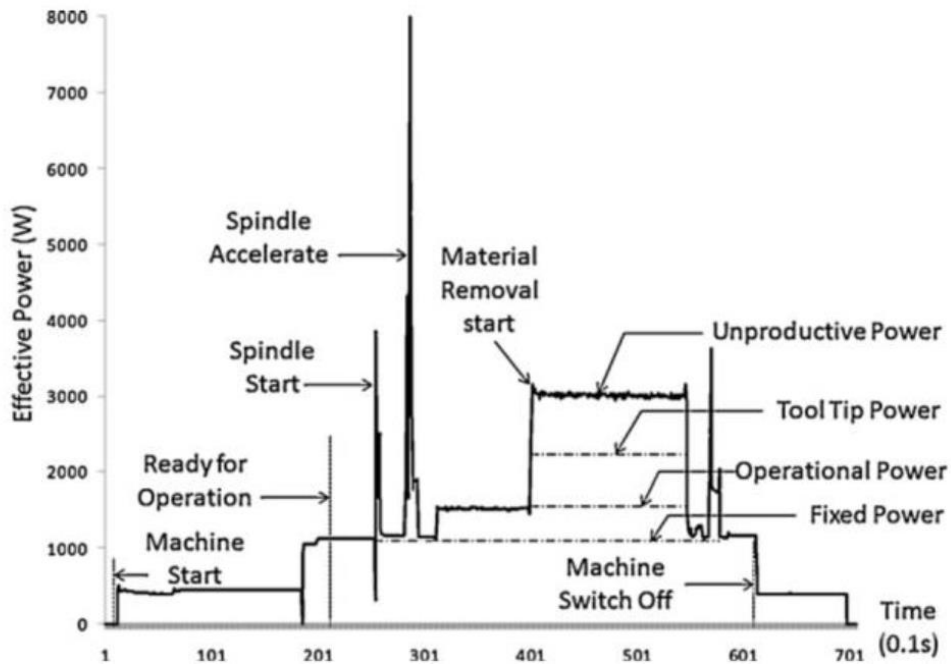


Figure 4 Power profile of a turning process [14].

In this study, Li et al. divided the total power consumption of a machine tool into four main groups:

- Fixed power: power demand of all activated machine components ensuring the operational readiness of the machine.
- Operational power: power demand to distinctively operate components enabling cutting as performed in air cuts
- Tool tip power: power demand at the tool tip to remove the work-piece material
- Unproductive power: power converted to heat mainly due to friction during material removal.

Li et al. also classified the fixed energy consumption of a machine tool, which is shown in Figure 5.

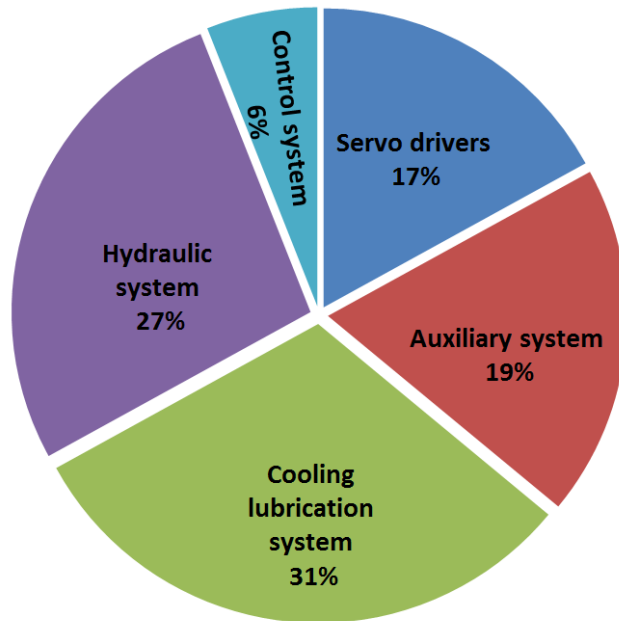


Figure 5 Average fixed energy breakdown of a reviewed machine tool [14].

He et al. [15] have modeled energy consumed in machining operations by associating it with Numerical Control (NC) commands. The model is based on identifying energy consuming sub-units and determining their energy consumption amounts by observing commissioning time of these sub-units. Energy consumption amount of sub-units are calculated with multiplying power consumption amount of each sub-unit by its activation time. The model is shown in Equation (3).

$$\mathbf{E} = \mathbf{E}_{\text{Spindle}} + \mathbf{E}_{\text{Feed}} + \mathbf{E}_{\text{Tool}} + \mathbf{E}_{\text{Coolant}} + \mathbf{E}_{\text{Fix}} \quad (3)$$

Where  $E_{\text{Spindle}}$  is energy consumption of the spindle at the ready position and cutting,  $E_{\text{Feed}}$  is energy consumption of feed axes,  $E_{\text{Tool}}$  is energy consumed for tool change,  $E_{\text{Coolant}}$  is energy consumed by coolant and  $E_{\text{Fix}}$  is energy consumption of machine in ready position such as lightening, fans, computers, etc. For example, operating time of coolant unit is obtained by measuring period of time between coolant activation code in NC code lines (M8) and deactivation code (M9), so energy consumption of coolant sub-unit could be calculated using power consumption amount of this unit. To measure the consistency of the model established in this study, experimental methods was performed

in milling and turning machines. A consistency of about 80% was observed between estimated energy consumption and the measured energy consumption. The energy consumption of sub-units is demonstrated but calculations using theoretical model are not mentioned explicitly. In addition, energy consumption of spindle and axes in different rotational speeds and feed rates is not modeled. Thus, the study is limited to the feed rate and spindle speed value used only on analysis of this special case.

Salonitis and Ball [16] categorized the total energy consumption of machine tools into process energy which is the energy consumed during cutting process and peripheral energy which is the energy consumed by peripheral sub-units. They have also divide peripheral energy into background energy which is the energy consumed by machine tool in ready position irrespective of cutting process is performing or not and load energy which is energy drawn during cutting process and depends on cutting parameters which is shown in Equation (4).

$$\mathbf{E_{Total} = E_{Process} + E_{Background} + E_{Load}} \quad (4)$$

Calvanese et al. [17] also modelled energy consumption based on functional modules including the spindle, axis, chillers, tool change system, auxiliary components and cutting process as shown in Equation (5), but did not consider the effect of tool wear, multiple axis movement, and tool tip energy.

$$\mathbf{E = E_{Fixed} + E_{Axes} + E_{AC} + E_{Spindle} + E_{SC} + E_{Conveyor} + E_{TC} + E_{Clamp}} \quad (1)$$

Where  $E_{Fixed}$  is the energy consumed when machine is switched on,  $E_{Axes}$  is the energy required for axis,  $E_{AC}$  is the energy consumed by axes chillers,  $E_{Spindle}$  is the energy of both the cutting power and the spindle losses,  $E_{SC}$  is the energy consumed by spindle chillers,  $E_{Conveyor}$  is the energy consumed when chip is removed,  $E_{TC}$  is the energy consumed for tool change,  $E_{Clamp}$  is the energy consumed for clamping.

Aramcharoen and Mativenga [18] have suggested a model for calculating total energy consumption of each cutting process considering energy consumed in ready position, tool change, spindle run, material removal, coolant, table movement and cutting feed

which is shown in Equation (6). Energy consumption of sub-units is determined multiplying the amount of power consumed by sub-unit activation time. The energy consumption of metal removal process is obtained as in most studies by multiplying the specific cutting energy by material removal rate.

$$\mathbf{E}_{\text{Total}} = \mathbf{E}_{\text{Basic}} + \mathbf{E}_{\text{Tool}} + \mathbf{E}_{\text{Spindle}} + \mathbf{E}_{\text{Cutting}} + \mathbf{E}_{\text{Feed}} + \mathbf{E}_{\text{Cutting-fluid}} \quad (2)$$

Where  $E_{\text{Basic}}$  is the energy consumption of machine tool in ready position,  $E_{\text{Tool}}$  is energy required for tool change during machining operations,  $E_{\text{Spindle}}$  is the energy consumed for spindle rotation,  $E_{\text{Cutting}}$  is the energy consumed during material removal process,  $E_{\text{Feed}}$  is the energy consumption of feed axis and the  $E_{\text{Cutting-fluid}}$  is the energy consumed by fluid pump motor for cutting fluid delivery to cutting region. The power consumption of sub-units specified in energy model is determined, power consumption profiles are obtained and average power consumptions are found by performing experimental studies within the research work. Comparing the energy consumption amount estimated by means of model and energy measured in the performed experiment in order to measure consistency of the model, a difference at a rate of 5% was determined. Aramcharoen and Mativenga have also analyzed the effect of alternative tool paths on energy consumption.

Uluer et al. [19] have suggested a model for energy consumption of turning a part which is shown in Equation (7). They have analyzed energy consumption at the system level and divided it to the direct and indirect energy. Uluer et al. unlike other models obtained metal cutting energy by multiplying the volume of the chip removed with specific cutting energy and this provides an option of consistency of this model with component-based modeling. They didn't perform any experiments in order to validate the suggested model.

$$\mathbf{E}_{\text{part}} = \mathbf{E}_{\text{th}} + \mathbf{E}_{\text{aux-var}} + \mathbf{E}_{\text{aux-const}} + \mathbf{E}_{\text{handling}} + \mathbf{E}_{\text{indirect}} \quad (3)$$

where  $E_{\text{th}}$  is theoretical energy which is consumed during the actual metal removal processes,  $E_{\text{aux-var}}$  is variable auxiliary which may change during the operation of the machine tool,  $E_{\text{aux-const}}$  is constant auxiliary energy which is due to the auxiliary

components of the machine tools which consume energy even if the machine is in standby mode,  $E_{handling}$  is the energy consumed by the automated material handling equipment and  $E_{indirect}$  is the allocated indirect energy consumed by the services to maintain the environment for the production activities of the part.

Mori et al. [20] divided a machining process into number of various operations to model power consumption of the machine tool which includes: positioning the spindle after tool change and acceleration, metal cutting, turning back of the spindle to the tool exchange location at the end of metal cutting and spindle stop. Based on this classification, the model is shown in Equation (8).

$$\mathbf{E} = \mathbf{P}_1(\mathbf{T}_1 + \mathbf{T}_2) + \mathbf{P}_2\mathbf{T}_2 + \mathbf{P}_3\mathbf{T}_3 \quad (8)$$

Where  $P_1$  is power consumption of machine in ready position,  $P_2$  is power consumed by spindle and servo motors during metal cutting process,  $P_3$  is power drawn for positioning and accelerating the spindle,  $T_1$  is waiting time of the machine in ready position,  $T_2$  is metal cutting time and  $T_3$  is the time required for positioning and accelerating the spindle. In the study energy consumption of different machining methods including face milling, shoulder milling and drilling in various cutting conditions was measured. Experimental data was obtained by performing Taguchi methodology and it has been concluded that machining in optimized cutting conditions decreases energy consumption. But a verification study between theoretical model and experimental data hasn't performed. Since this model do not take into account the energy change of tool tip according to the material being processed, the energy expenditure of feed axis and energy change of spindle depending on the spindle speed, is not seen as a realistic model.

Diaz et al. [21] have modeled total energy consumption of a milling machine tool during a milling operation. For this purpose, they have used the energy drawn by machine when cutting operation is performed for cutting the air which is shown in Equation (9), where  $P_{Cut}$  is Power drawn for cutting,  $P_{Air}$  is power drawn for air cut and  $T$  is processing time.

$$\mathbf{E} = (\mathbf{P}_{Cut} + \mathbf{P}_{Air})\mathbf{T} \quad (9)$$

In this study a number of experiments with varying depth of cut and width of cut were conducted to demonstrate the effect of material removal rate on energy consumption of a 3-axis machining center which is shown in Figure 6. The interchange between power consumption and machining time was investigated and it was affirmed that although power consumption increases with higher material removal rates, but the total energy consumption of machining center do not increase due to reduction of total machining time. The effect of work piece material on the amount of power drawn by machine was also examined in this work. Diaz et al. model's handicap is its failure to consider the power drawn of machine in ready position and also power consumption of auxiliary units and also no comparison between theoretical model and experimental data has been carried out in order to prove the consistency of the model. In a previous work Diaz et al. [22] analyzed the effect of cutting speed on energy consumption comparing high speed and conventional machining, as a result reduced machining time in high speed machining makes it more energy efficient.

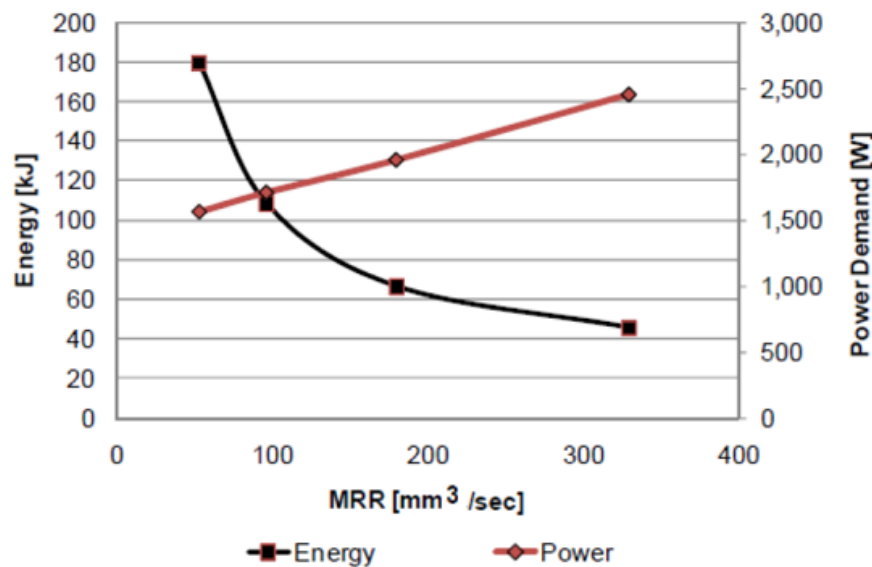


Figure 6 Energy and power demand as a function of M.R.R.

Kong et al. [23] have developed a model for estimating energy consumption of a CNC machine tool which consists of constant part, run-time and cutting stage as shown in Equation (10) they have investigated the effect of different tool paths on the energy consumption of machine tool using introducing a web-based and application programming interface (API) based process analysis software tool. The effect of tool change, individual motion of feed axis and coolant were not considered in this model.

$$\mathbf{E} = \mathbf{E}_{\text{const}} + \mathbf{E}_{\text{run-time-transuent}} + \mathbf{E}_{\text{run-time-steady}} + \mathbf{E}_{\text{cut}} \quad (10)$$

$E_{\text{const}}$  is the energy consumed not related to machining,  $E_{\text{run-time-transuent}}$  is energy consumed by spindle, machine axes and tool change when accelerating or decelerating to reach specified values,  $E_{\text{run-time-steady}}$  is energy consumed by spindle, machine axes and tool change when the spindle motor and the axis drives keep a specified value and  $E_{\text{cut}}$  is energy consumed by material removal action.

Avram and Xirouchakis [24] have developed a model that calculates energy consumed in a metal cutting process by means of reading feed rates and spindle speed values from CATIA V5 R15 program output files which is one of Computer Aided Design (CAD) and Computer Aided Manufacturing (CAM) software packages. Calculations are performed by considering not only feed rate and spindle speed values but also the number of cutting mouth, helix angle, plow angle, cutting depth, cutting width and specific cutting energy of selected material information into model. This study is based on data read from the output files of tool paths which is created to perform 2.5 axis milling operations. In this study, an equation modeling the total energy consumption of machine tool is presented. Also the metal cutting energy consumed by a milling process performed in Y axis of a machine tool is modeled based on power drawn by spindle and feed axes. These are shown in Equations (11) and (12).

$$\mathbf{E}_{\text{DE}} = \mathbf{E}_{\text{aY}} + \mathbf{E}_{\text{SY}} + \mathbf{E}_{\text{dY}} + \mathbf{E}_{\text{Run}} + \mathbf{E}_{\text{Cut}} \quad (4)$$

$$\mathbf{E}_{\text{DE}} = \int_{t_0}^{t_1} \mathbf{P}_{\text{aY}} dt + \int_{t_1}^{t_2} \mathbf{P}_{\text{SY}} dt + \int_{t_2}^{t_3} \mathbf{P}_{\text{dY}} dt + \int_{t_0}^{t_3} \mathbf{P}_{\text{Run}} dt + \int_{t_1}^{t_2} \mathbf{P}_{\text{Cut}} dt \quad (5)$$

$E_{aY}$  is energy consumption of spindle positive acceleration during the motion of spindle in Y axes,  $E_{SY}$  is energy consumption of spindle moving in Y axes,  $E_{dY}$  is energy consumption of spindle negative acceleration during the motion of spindle in Y axes,  $E_{Run}$  is energy consumption of the rotating spindle while it is not interacting with the material being cut and  $E_{Cut}$  is energy consumption of the rotating spindle during metal cutting process. When calculating the power drawn by the spindle torque and angular velocity values were used. Experimental studies carried out in order to verify the model. By performing milling operations at low and high cutting speeds energy consuming units and the amount of energy they consume are determined. The energy consumed is divided into four main groups of constant, feed axes, the spindle and auxiliary energy. Thus, this model gets out of auxiliary and metal cutting classification as observed in other studies. Metal cutting energy consumption is classified into spindle and axis energy consumption and energy drawn by these units in ready position has been included into metal cutting energy class. Also it is demonstrated that a process occurs 43% faster and consumes 25% less energy in high speed removing equal volume of chip. . Experimental studies carried out in order to verify the model. The results obtained in low speeds are more promising compared with high speeds.

Neugebauer et al. [25] have modeled the energy consumption of machine tools in their system-level study in order to using machine tools more efficiently which is shown in Equation (13).

$$\mathbf{E}_{Total} = \mathbf{E}_{use,prim} + \mathbf{E}_{use,sec} + \mathbf{E}_{loss} \quad (13)$$

$E_{use,prim}$  is the energy consumed by sub-units such as coolant and shaping during a metal cutting operation to improve the process characteristics,  $E_{use,sec}$  is the energy consumption which does not have direct impact on the metal cutting process, but is necessary for the realization of the logistics activities and cooling sub-units of the machine tool and  $E_{loss}$  is the energy losses due to inefficiency of sub-units that perform primary and secondary energy consumption. These losses resources are classified as in Figure 7. Neugebauer et al. have determined the energy efficiency of the machine tool as the ratio of useful primary energy consumption to total energy consumption.



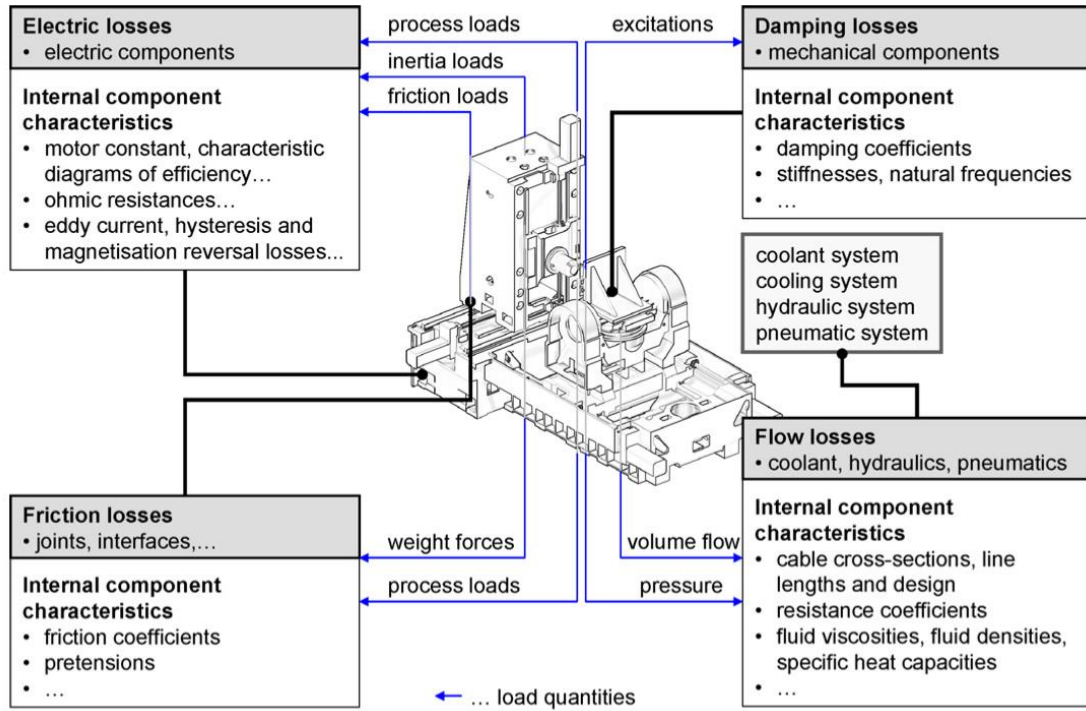


Figure 7 System influences on the energy losses of machine tool components [25]

Hu et al. [26] have modelled the energy consumption of machine tools through the energy consumption of spindle and divided the power drawn by the spindle into three sub-groups of idle power, Cutting power and Additional load loss. As shown in Equation (14), total power drawn by the spindle is defined as  $P_{in}$ , the power drawn by the rotating spindle when the metal cutting process is not performing is defined as  $P_u$ , the power drawn during cutting operation is defined as  $P_c$  and power consumption resulting from mechanical and electrical losses that occurs during metal cutting is defined as  $P_a$ .

$$P_{in} = P_u + P_c + P_a \quad (14)$$

Hu et al. [27] were also modeled their defined power consumption resulting from additional losses as a quadratic function as shown in Equation (15) in another work and combining in Equation (14) and Equation (15) Equation (16) is obtained.  $a_0$  and  $a_1$  are defined as coefficients of additional losses and are determined using experimental data and least square method.

$$P_a = a_0 P_c + a_1 P_c^2 \quad (15)$$

$$P = P_u + (1 + a_0) P_c + a_1 P_c^2 \quad (16)$$

Hu et al. [26] have been carried out experiments in order to validate the presented model. Experiments were performed in a CNC controlled turning machine using torque sensor and the power sensor. Data obtained from Torque sensor multiplying the angular velocity of the spindle the total power drawn by spindle is calculated and compared with the data obtained from power sensor. These values (in 6 tests conducted under different cutting conditions) compared directly, the error rates ranged from 24.09% to 16.75% was observed. Following the proposed procedure, additional loss coefficients of turning machine are determined. Removing the additional losses from the power drawn during cutting, error rate of 3% was obtained. In this study, the energy model provide the information such as instant energy efficiency, instantaneous power drawn, the total energy consumed during the operation, the energy used for metal cutting and operation time as an embedded computer software. This model is for classification of current energy consumption rather than a predictive model, because the additional losses are extrapolated from the amount of online power drawn.

Balogun and Mativeng [28] have constitute their own energy consumption model within the scope of Cooperative Effort in Process Emission (CO2PE) using the classification of Ostade and Kellens et al.'s proposed methodology which is shown in Equation (17) where  $E_t$  is the direct total energy requirement,  $E_r$  is ready state power,  $P_{tc}$  is power demand for tool change  $t_{tc}$  is time required for tool change,  $T$  is tool life,  $P_{air}$  is the average power requirements for a non-cutting approach and retraction moves over the component,  $t_{air}$  is the total duration of non-cutting moves,  $P_{cool}$  is coolant pumping power requirements,  $k$  is specific cutting energy,  $\dot{v}$  is the rate of material processing and  $t_c$  is cutting time.

$$E = E_b + E_r + P_{tc} t_{tc} [INT(t_2/T) + 1] + P_{air} t_{air} + (P_s + P_{cool} + k\dot{v}) t_c \quad (17)$$

In this model, the energy consumed is divided into three groups of basic, ready for cutting and metal cutting energy. Basic energy is defined as energy required for starting up and energy consumption for activation of computer units, lighting, cooling fans, lubrication and energy consumed by the unloaded motors, etc. influence of feed rate and undeformed chip thickness was also analyzed in this study. Table 1 provides a summary of the developed models.

Table 1 A summary of developed theoretical models

Reference	Mathematical model	Remark
Gutowski et al. (2006) [8]	$E = (P_0 + kQ)t$ <i>P<sub>0</sub>: power consumed by machine, k: specific cutting energy, Q: material removal rate, t: cutting time</i>	<ul style="list-style-type: none"> <li>• A precursor work to determine energy consumption</li> <li>• Does not provide information about energy consumption of auxiliary subunits</li> <li>• No model validation studies</li> </ul>
Rajemi et al. (2010) [11]	$E = P_0t_1 + (P_0 + kQ)t_2 + P_0t_3 \frac{t_2}{T} + y_E \frac{t_2}{T}$ <i>P<sub>0</sub>: power consumed by machine, t<sub>1</sub>: machining setup time, t<sub>2</sub>: actual cutting time, t<sub>3</sub>: tool change time, T: tool life, y<sub>E</sub>: energy footprint for tool edge, k: specific cutting energy, Q: material removal rate</i>	<ul style="list-style-type: none"> <li>• A new model and methodology for optimizing the energy footprint</li> <li>• The most effective parameters for minimizing energy consumption are identified</li> </ul>
Mori et al. (2011) [20]	$E = P_1(T_1 + T_2) + P_2(T_2) + P_3(T_3)$ <i>P<sub>1</sub>: constant power during machining, P<sub>2</sub>: power for cutting by spindle and servo motor, P<sub>3</sub>: power to position the work to accelerate/decelerate the spindle to the specified speed, T<sub>1</sub>: cycle time during non-cutting state, T<sub>2</sub>: cycle time during cutting state, T<sub>3</sub>: time required to position the work and accelerate the spindle</i>	<ul style="list-style-type: none"> <li>• Does not provide information about the power calculation of each process.</li> <li>• Effects of feed axis, spindle speed and tool life are not considered in the model</li> <li>• No model validation studies</li> </ul>
Diaz et al. (2011) [21]	$E = (P_{cut} + P_{air}) \cdot \Delta T$ <i>P<sub>cut</sub>: power demand for cutting, P<sub>air</sub>: power demand for air cut, ΔT: processing time</i>	<ul style="list-style-type: none"> <li>• Introduced an interesting approach by considering air cut power consumption</li> <li>• Does not provide information about energy consumption of auxiliary subunits</li> <li>• Requires measuring the air cutting time for the toolpath</li> <li>• No model validation studies</li> </ul>
Kong et al. (2011) [23]	$E = E_{const} + E_{run-time-transient} + E_{run-time-steady} + E_{cut}$ <i>E<sub>const</sub>: energy consumed not related to machining, E<sub>run-time-transient</sub>: energy consumed by spindle, machine axis and tool changes when accelerating or decelerating to reach specified values, E<sub>run-time-steady</sub>: energy consumed by spindle, machine axis and tool changes when the spindle motor and axis drives maintain a specified value, E<sub>cut</sub>: energy consumed by material removal action</i>	<ul style="list-style-type: none"> <li>• Investigation of the effect of different tool paths on energy consumption</li> <li>• Does not provide information about energy consumption of coolant and tool changes</li> </ul>
He et al. (2012) [15]	$E = E_{spindle} + E_{feed} + E_{tool} + E_{coolant} + E_{fix}$ <i>E<sub>spindle</sub>: energy consumption of spindle, E<sub>feed</sub>: energy consumption of axis feed, E<sub>tool</sub>: energy consumption of tool change, E<sub>coolant</sub>: energy consumption of coolant, E<sub>fix</sub>: energy consumption of fan motor and servo system</i>	<ul style="list-style-type: none"> <li>• Not a general model for all machine tools</li> <li>• Fails to model the energy consumption related to the number of tool changes and spindle speed.</li> </ul>

Calvanese et al. (2013) [17]	$E = E_{fixed} + E_{axes} + E_{axis\ chillers} + E_{spindle} + E_{spindle\ chiller} + E_{chip\ conveyor} + E_{tool\ change} + E_{pallet\ clamp}$ <p><math>E_{fixed}</math>: the energy required when machine is switched on, <math>E_{axes}</math>: the energy required by the axis, <math>E_{axis\ chillers}</math>: the energy consumed by axis chillers, <math>E_{spindle}</math>: the energy of both the cutting power and the spindle losses, <math>E_{spindle\ chiller}</math>: the energy consumed by spindle chillers, <math>E_{chip\ conveyor}</math>: the energy consumed when chip is removed, <math>E_{tool\ change}</math>: the energy consumed during tool change, <math>E_{pallet\ clamp}</math>: the energy consumed during clamping</p>	<ul style="list-style-type: none"> <li>The effects of tool wear, multiple axis movement, and tool tip energy not taken into consideration.</li> </ul>
Balogun and Mativenga (2013) [28]	$E = E_b + E_r + P_{tc}t_{tc}[INT(t_2/T) + 1] + P_{air}t_{air} + (P_s + P_{cool} + k\dot{v})t_c$ <p><math>E_b</math>: the direct total energy requirement, <math>E_r</math>: ready state power, <math>P_{tc}</math>: power demand for tool change, <math>t_{tc}</math>: time required for tool change, <math>T</math>: tool life, <math>P_{air}</math>: the average power requirements for a non-cutting approach and retraction moves over the component, <math>t_{air}</math>: the total duration of non-cutting moves, <math>P_s</math>, <math>P_{cool}</math>: coolant pumping power requirements, <math>k</math>: specific cutting energy, <math>\dot{v}</math>: the rate of material processing, <math>t_c</math>: cutting time</p>	<ul style="list-style-type: none"> <li>Reported the effect of machine tool selection and geographic location on energy and carbon footprint</li> <li>Model validation studies have been performed</li> </ul>
Salonitis and Ball (2013) [16]	$E_{total} = E_{process} + E_{background} + E_{load}$ <p><math>E_{process}</math>: energy required for the physical process to occur, <math>E_{background}</math>: energy consumed by the machine tool in ready position, irrespective whether a cutting process is being performed, <math>E_{load}</math>: energy drawn during cutting process based on cutting parameters</p>	<ul style="list-style-type: none"> <li>Does not provide information about energy consumption of auxiliary subunits</li> </ul>
Uluer et al. (2013) [19]	$E_{part} = E_{th} + E_{aux-var} + E_{aux-const} + E_{handling} + E_{indirect}$ <p><math>E_{th}</math>: theoretical energy consumed during the actual metal removal processes, <math>E_{aux-var}</math>: variable auxiliary energy, which may change during the operation of the machine tool, <math>E_{aux-const}</math>: constant auxiliary energy consumed by auxiliary components of the machine tools even when the machine is in standby mode, <math>E_{handling}</math>: energy consumed by automated material handling equipment, <math>E_{indirect}</math>: allocated indirect energy consumed by services to maintain the production environment</p>	<ul style="list-style-type: none"> <li>No model validation studies</li> </ul>
Avram and Xirouchakis (2011) [24]	$E_{DE} = E_{ay} + E_{sy} + E_{dy} + E_{run} + E_{cut}$ <p><math>E_{DE}</math>: total energy consumption, <math>E_{ay}</math>: energy consumed for positive acceleration of spindle, <math>E_{sy}</math>: steady state energy consumption of spindle in y-axis, <math>E_{dy}</math>: energy consumed for negative acceleration of spindle in y-axis, <math>E_{run}</math>: steady state energy consumption of spindle, <math>E_{cut}</math>: energy consumption of spindle during metal cutting process</p>	<ul style="list-style-type: none"> <li>Fails to model the energy consumption of auxiliary components</li> <li>Verification studies have been performed and accuracy of about 75-85% has been obtained</li> </ul>
Neugebauer et al. (2011) [25]	$E_{total} = E_{use,prime} + E_{use,sec} + E_{loss}$ <p><math>E_{use,prime}</math>: energy consumed by auxiliary subunits, <math>E_{use,sec}</math>: energy consumed for metal cutting processes buy machine tool components</p>	<ul style="list-style-type: none"> <li>Fails to model the energy consumption of auxiliary components</li> <li>The effect of machining operations such as dry machining, roughing or finishing is advertised</li> </ul>
Hu et al. (2010) [26]	$P = P_u + (1 + a_0)P_c + a_1P_c^2$ <p><math>P_u</math>: idle power, <math>P_c</math>: cutting power, <math>a_0</math> and <math>a_1</math>: additional load loss coefficient</p>	<ul style="list-style-type: none"> <li>Fails to model the energy consumption of auxiliary components</li> <li>Requires more detailed information about power consumption of auxiliary components</li> <li>Verification studies have been performed</li> </ul>

## 2.1.2 Empirical modelling

Empirical approaches have been efficient for providing a reliable prediction of energy use of machine tools and characterizing the relationship between energy consumption

and cutting parameters. Dragenescu et al. [29] have introduced a detailed model of the specific energy consumption based on cutting parameters during milling operations as shown in Equation (18), where  $E_{cs}$  is specific consumed energy (kWh/cm<sup>3</sup>),  $D$  is cutting tool diameter,  $F_t$  is tangential component of the cutting force,  $s_z$  feed per tooth,  $t$  depth of cut,  $B$  is cutting width,  $z$  is the number of cutting edge and  $\mu$  is productivity rate. Multiplying specific consumed energy by cutting volume ( $Y$ ) gives consumed energy ( $E_c$ ) as seen in Equation (19).

$$E_{cs} = \frac{\pi D F_t}{3.672 \times 10^6 s_z t B z \mu} \quad (18)$$

$$E_c = Y E_{cs} \quad (19)$$

They have also obtained efficiency-cutting parameters, the tangential cutting forces-cutting parameters and specific energy consumption- cutting parameters graphs in the scope of the work by machining the same material with the same cutting tool in the same machine tool but varying cutting parameters. Specific consumed energy as a function of milling parameters is shown in Figure 8. Although this model is a good basis for further study, but this model only calculates energy consumed for the cutting process and does not take into account the energy consumption of sub-units and also this is not a generic model for other processes and machine tools.

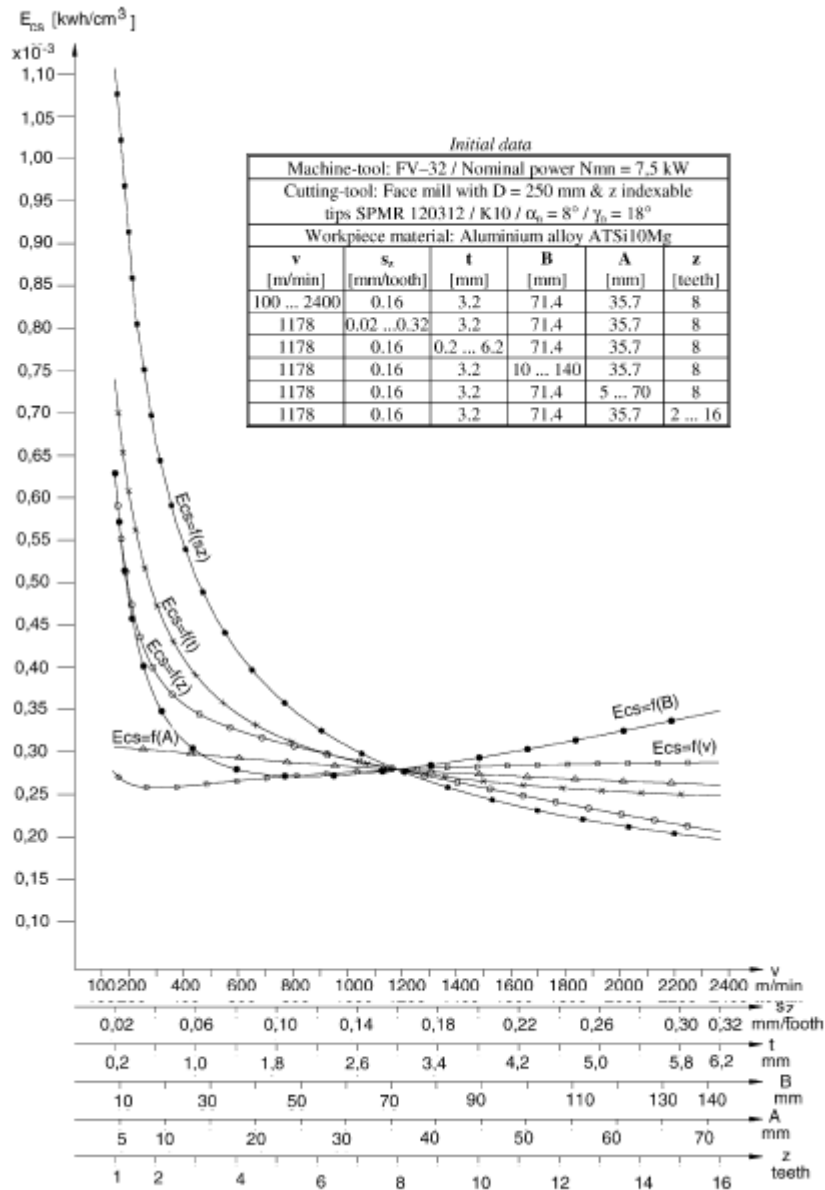


Figure 8 Specific consumed energy as a function of milling parameters [29]

Kara and Li [30] have developed a unit process energy consumption model using experimental methods for observing energy consumption related to process parameters, in order to determine the relation between these parameters and energy consumption. They have identified constants specific to each machine tool and revealed an empirical model based on these machine specific coefficients to achieve a reliable prognostication of unit process energy consumption. They have created their model in following four stages. Initially experiments were designed based on process variables and response

surface methodology was used for this purpose. The next stage was experimental set-up. In this stage a monitoring platform was constructed by means of LabVIEW programming interface. Then, statistical analysis of unit process energy consumption was performed using SPSS software in the next stage, and finally the model is derived as shown in Equation (20) where SEC is specific energy consumption, MRR is material removal rate and  $C_0$  and  $C_1$  are machine specific coefficients. Here total energy consumption is obtained by multiplying SEC with cutting volume Equation (21).

$$\text{SEC} = C_0 + \frac{C_1}{\text{MRR}} \quad (20)$$

$$\mathbf{E} = \text{SEC. cutting volume} \quad (21)$$

The model validation tests have been done in four different milling and turning machine tools. Comparing estimated energy using model and measured energy amount presented model reached a consistency level of 90%. However the estimated energy does not include the start-up, standby, clamping and positioning energy consumption. In the study SEC formulation is derived separately for the operations with and without coolant, but it has not been demonstrated that changes taking place in other auxiliary sub-units how will affect the total energy consumption. According to this study lower energy consumption is obtained in higher material removal rates.

Guo et al [31] developed an empirical model with respect to cutting parameters which is shown in Equation (22), where  $v_c$  is cutting speed,  $f_r$  is feed rate,  $a_p$  depth of cut,  $d$  is final workpiece diameter in the turning operation,  $\alpha, \beta, \gamma, \phi$ ,  $C_0$  and  $C_1$  are empirical constants.

$$\text{SEC} = C_0 \cdot v_c^\alpha \cdot f_r^\beta \cdot a_p^\gamma \cdot d^\phi + \frac{C_1}{v_c \cdot f_r \cdot a_p} \quad (22)$$

Also optimal cutting parameters in order to get minimum energy consumption and precise surface finish are obtained.

Yoon et al. [32] further break down the energy consumption of the machine tool into basic energy, spindle energy, stage energy, and material-removal energy. Basic energy

represents the energy consumption of auxiliary sub-units and control systems which are assumed to be constant, material removal energy is also the energy consumed during material removing process. Stage energy and spindle energy, which are energy required for spindle rotation and stage movement, had a power relationship depend on the rotational speed and feed. An empirical model developed by performing experimental studies and fitting the observed data which is shown in Equation (23).  $E_{\text{basic}}$  includes the basic energy consumption used when turning on the machine,  $E_{\text{stage}}$  represents energy required for moving the stage during the air-cutting state,  $E_{\text{spindle}}$  represents the energy consumed for rotating the spindle and  $E_{\text{machining}}$  an additional process energy consumed in material removal.

$$\mathbf{E}_t = \mathbf{E}_{\text{basic}} + \mathbf{E}_{\text{stage}} + \mathbf{E}_{\text{spindle}} + \mathbf{E}_{\text{machining}} \quad (23)$$

Yoon et al. [33] also divided the energy consumption of the energy consumption during milling operations into particular sections. Also in this study an empirical modeling of material-removal power depending on cutting parameters and tool wear as shown in Figure 9.

Pervaiz et al. [34] used finite element modelling simulation to model energy consumption. Experimental verification revealed that experimental results approximated measured power consumption values quite well. Dietmair and Verl [35] presented an energy consumption model which was improved later [36]. This model predicts energy consumption based on different design and operations strategies. Larek et al. [37] also presented a power consumption prediction approach in which all components of a machine tool are assumed to be either “on” or “off”. Table 2 provides a summary of empirical models of machine tool energy consumption.



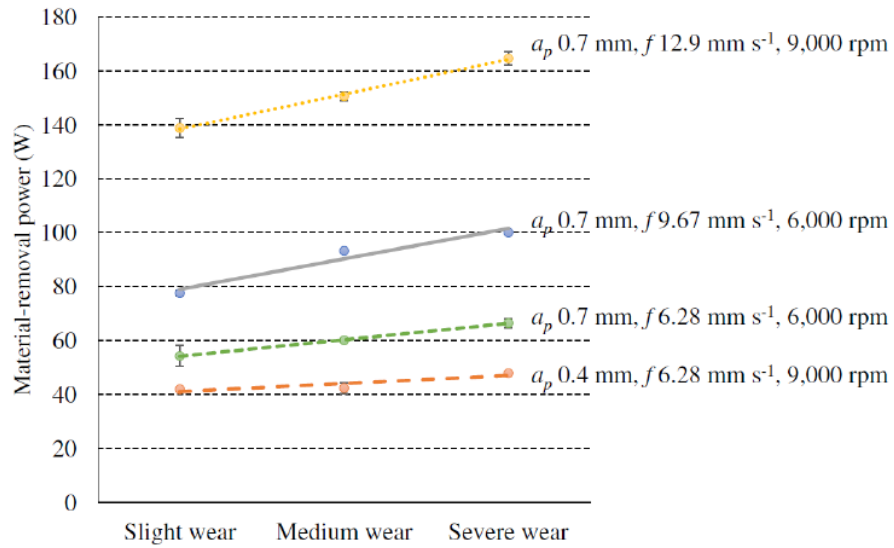


Figure 9 Material removal power with respect to the tool wear under the specified conditions [33]

Table 2 A summary of developed empirical models

Model	Model	Process	Work material
Draganescu et al. (2003) [29]	$E_{cs} = \frac{\pi D F_t}{3.672 \times 10^6 s_z t B z \mu}, \quad E_c = Y E_{cs}$ <p><math>D</math>: diameter of the mill, <math>s_z</math>: feed per tooth, <math>t</math>: depth of milling, <math>B</math>: contact length of the milling tool, <math>z</math>: number of teeth of the milling tool, <math>F_t</math>: tangential component of the cutting force, <math>E_{cs}</math>: specific consumed energy, <math>Y</math>: total volume of material removed, <math>E_c</math>: consumed energy</p>	Milling	<ul style="list-style-type: none"> <li>• ATSi10Mg</li> </ul>
Kara and Li (2011) [30]	$E = SEC \cdot \text{cutting volume}$ $SEC = C_0 + \frac{C_1}{MRR}$ <p><math>SEC</math> is specific energy consumption, <math>C_0</math> and <math>C_1</math> are machine specific coefficients, and <math>MRR</math> is material removal rate</p>	Milling Turning	<ul style="list-style-type: none"> <li>• Brass</li> <li>• Mild Steel</li> <li>• High Tensile</li> </ul>
Guo et al. (2012) [31]	$SEC = C_0 \cdot v_c^\alpha \cdot f_r^\beta \cdot a_p^\gamma \cdot d^\varphi + \frac{C_1}{v_c \cdot f_r \cdot a_p}$ <p><math>v_c</math>: cutting speed, <math>f_r</math>: feed rate, <math>a_p</math>: depth of cut, <math>d</math>: final work-piece diameter (mm) in the turning operation, <math>\alpha, \beta, \gamma, \varphi, C_0</math> and <math>C_1</math> are empirical constants</p>	Turning	<ul style="list-style-type: none"> <li>• Steel</li> <li>• Aluminium</li> </ul>
Yoon et al. (2013) [32]	$E_t = E_{basic} + E_{stage} + E_{spindle} + E_{machining}$ <p><math>E_{basic}</math>: energy consumed when turning on the machine, <math>E_{stage}</math>: energy consumed when moving the stage, during the air-cutting state, <math>E_{spindle}</math>: energy consumed by rotating the spindle, <math>E_{machining}</math>: additional process energy consumed in material removal</p>	Drilling	<ul style="list-style-type: none"> <li>• PCB (Printed Circuit Boards)</li> </ul>

## **2.2 Design of experiments**

It has long been known that to optimize the economics and quality of machining processes which are determined by productivity, total energy consumption, total cost and some other criteria, cutting parameters such as feed rate, cutting speed and depth of cut in machining processes should be selected [38]. Energy consumption of machine tools as a function of cutting processes are required for improving energy efficiency [39]. Statistical design of experiments refers to the process of planning the experiment so that the appropriate data can be analyzed by statistical methods, resulting in valid and objective conclusions [38]. A number of studies have been previously performed in order to optimize machining process taking into account cutting parameters and employing DOE methods such as factorial design, full factorial design, response surface methodology and Taguchi methods where the most widely used ones are response surface methodology and Taguchi methods.

### **2.2.1 Taguchi methodology**

Classical experimental design methods are too complicated and using these methods are not simple. Furthermore, as the number of the process parameters increases, the number of experiments to be performed also increases. The Taguchi method utilizes a specific design of orthogonal arrays in order to study the whole parameter interval performing lower number of experiments. Then the experimental results are turned into a signal-to-noise (S/N) ratio. Taguchi recommends the use of the S/N ratio to measure the quality characteristics deviating from the desired values. Taguchi methodology can significantly decrease the required time for experimental research. Also the effects of factors on response can be determined and compared with other factors. [40]

Taguchi methodology is widely used for obtaining optimum cutting parameters. Obtaining optimal cutting parameters using Taguchi method was first presented by Yang et al. [41] In this study the optimal cutting parameters are found exerting an orthogonal array, the signal-to-noise (S/N) ratio, and the analysis of variance (ANOVA) for turning S45C steel bars using tungsten carbide cutting tools. In addition, the cutting parameters which influence cutting performance in turning operations are identified. Several studies

have been carried out to minimize the power consumption obtaining optimized cutting parameters using Taguchi techniques. Fratila and Caizar also used Taguchi methodology in their work to optimize the cutting parameters in face milling in order to minimize power consumption. An orthogonal array, signal to noise (S/N) ratio and ANOVA are employed to investigate the effect of cutting parameters during machining AlMg3 (EN AW 5754) with HSS tool. The experiments were performed under different conditions of dry cutting, minimal quantity lubrication and flood lubrication. It is mentioned in the study that using Taguchi method requires minimum number of trials as compared with a full factorial design [42]. Bhattacharya et al. [43] and Hanafi et al. [44] try to achieve best surface roughness and minimum cutting power as objective of experiments. Bhattacharya et al. performed experimental study to analyze the contribution and effects of cutting speed, feed rate and depth of cut on surface roughness and power consumption during high speed machining of AISI 1045 steel based on Taguchi techniques. An orthogonal array and analysis of variance (ANOVA) were employed for this purpose. It is concluded that the cutting speed has the main effect on power consumption and consequently optimized cutting parameters for minimizing power consumption was obtained [43].

In the work of Hanafi et al. Taguchi's orthogonal array, S/N ratio and grey relational analysis are employed to achieve best surface roughness and minimum cutting power during dry turning of PEEK-CF30 using TiN tools under. It is concluded that the depth of cut and have the main effect on power consumption following by cutting speed and feed rate [44].

### **2.2.2 Response surface methodology**

Response Surface Methodology (RSM) is a set of mathematical and actuarial techniques for modeling and analysis of problems in which a response of interest is influenced by several parameters and the objective is to optimize this response [38]. RSM was introduced by Box and Wilson [45] and later popularized by Montgomery [38]. Abhang and Hameedullah developed a model to predict the power consumption during turning operation of EN-31 Steel Using RSM. ANOVA was used for data analysis and RSM was employed to develop the first order and second order models in order to

prognosticate the power consumption. Consequently the optimum values of cutting speed, feed rate, depth of cut and nose radius for minimizing power consumption was achieved [46]. Campatelli employed response surface methodology to optimize the cutting parameters in order to minimize the power consumption during a milling operation of carbon steel [47].

The work of Bhushan outlines experimental studies to investigate the effects of cutting speed, feed rate, depth of cut and nose radius in CNC turning of 7075 Al alloy SiC composite. The optimized cutting parameters are obtained in order to get minimum power consumption and maximum tool life using response surface methodology [48].

Some studies have been carried out using both methods or comparing the results. Yan et al. applied weighted grey relational analysis and response surface methodology (RSM) to perform a multi-objective optimization. Three objectives of the work are surface roughness, material removal rate and cutting energy, which are to be optimized concurrently. Taguchi methodology was also employed in order to confirm the developed method [49]. Aggarawal et al. have used both RSM and Taguchi techniques and present a comparative analysis in order to optimize power consumption of CNC turning operation of AISI P-20 tool steel in different cutting environments. An orthogonal array and face centered central composite are employed to design experiments. Although the results of both methods were similar, RSM took nearly twice time which Taguchi need to design the experiments. Also the model developed by RSM is in respect of parameters, their interactions and square terms but in Taguchi method only three interactions are investigated and also RSM 3D surface provide a better visualizing of the effect of parameters [50]. Jou et al. have integrated Taguchi and RSM method in order to optimize process parameters of injection molding. In this work Taguchi method is employed to obtain significant parameters and RSM is employed for develop a model for optimization [51].

Table 3 A summary of energy optimization studies using DOE methods

Author	Work piece material	Cutting tool	Cutting parameters						Method
			Cutting speed	Feed rate	Depth of cut	Width of cut	Nose Radius	Cutting fluid	
Yang et al. (1998) [41]	S45C steel	Tungsten carbide	✓	✓	✓				Taguchi
Aggarwal et al. (2008) [50]	AISI P-20 tool steel	TiN coated tungsten carbide	✓	✓	✓		✓		RSM + Taguchi
Bhattacharya et al. (2009) [43]	AISI 1045	Coated carbide	✓	✓	✓				Taguchi
Abhang and Hameedullah (2010) [46]	EN-31 steel	Tungsten carbide	✓	✓	✓		✓		RSM
Fratila and Caizar (2011) [42].	AlMg3 (EN AW 5754)	HSS	✓	✓	✓			✓	Taguchi
Hanafi et al. (2012) [44]	PEEK-CF30	TiN coated	✓	✓	✓				Taguchi
Bhushan (2013) [48].	7075 Al alloy 15	Tungsten carbide	✓	✓	✓		✓		RSM
Yan and Li (2013) [49]	Carbon steel	Carbide	✓	✓	✓	✓			RSM + Taguchi
Campatelli et al. (2014) [47]	AISI 1050 carbon steel	Carbide	✓	✓	✓	✓			RSM

### 2.3 Feature Based Design and ISO 10303 (STEP) standard

CAD software packages have the opportunity to design geometrical and topological models of parts. But this low-level data representation is insufficient to represent part models at the CAM and CNC stage. Feature based design was developed to provide a high level of data transmission. Features in addition to geometric and topological data transfer, has the ability to transfer data like tolerances, material properties and surface roughness. A feature can be created in two different ways, including: Feature Based Design (FBD) and design with feature recognition. In FBD dimension, tolerance and material properties data is kept as variables and utilizing the variables the geometry of the desired workpiece is created [52, 19].

FBD gains the ability to be represented in the downstream applications creating explicit product data and design has enabled a better understanding of the purpose [52].

Many systems are used to manage technical product information in the production and design phases. Each system has its own unique data format and comprises information on this format. This requires the input of the same information many times to many different systems. This situation leads to errors caused by the excess of information and information abundance. To solve this mismatch and ensure data exchange, standards have been formed. Formats such as 'SET' in France, 'VDAFS' in Germany and 'IGES' in America have been created and later, merging under the International Standards Organization (ISO), 10303 known as the STEP (Standard for the Exchange of Product Model Data) was introduced.

The overall objective of STEP is to provide an independent mechanism for defining the product independently of any system in the life cycle of the product which allows the neutral file exchange and also provides a basis for sharing and archiving of database products. STEP's ultimate goal is to create database which is accessible to the resources in interaction and integrated and useful product information in the product life cycle. [53]

STEP consists of the series which each of them released separately. Series such as application protocol, definition of methods, integrated resources, application interpretive structures, abstract test series, perform method and compliance testing are included in the STEP.

STEP AP224 is one of the application protocols located in the STEP which includes identification information of mechanical products for process planning using processing features. In STEP AP224 manufacturing features are defined as shapes representing the volume to be removed from the material using machining processes.

The aim of the STEP to represent a single format in all stages of the product life cycle makes inferences in CAD/CAM software package companies. More are expected to be widely used in STEP format in the coming years.

## 2.4 Turn-mill systems

Modern CNC machine tool industry has been trying to fulfill the demand towards high productivity, precision, efficiency and flexibility with its advances on cutting technology. Turn-mill technology, by combining classical turning setup with a milling head provides great advantages along with aforementioned demands from industries such as automotive, aerospace etc. The distinguishing advantage of a turn-mill center is that, turning, milling, drilling and tapping processes can be combined in a single machine tool [54]. As set-up time is reduced, combining multiple processes into single machine increases productivity, and provides great flexibility in the part features that can be combined in a single part.

One of the pioneer studies on turn-milling systems is carried out by Schulz et al. [55]. In their study turn-milling operations are divided to two groups: orthogonal turn-milling and co-axial turn-milling. In orthogonal turn-milling the axes of the cutter is perpendicular the workpiece where in co-axial turn-milling are parallel to each other as shown in Figure 10. Orthogonal turn-mill system is a lathe with a milling head. In some complex machine tools a turret and also a second spindle on the other side of the lathe are optionally added. Co-axial turn-mill system is mainly a machining center that turning operations can be performed by rotating work piece table with a locked spindle. Both types of turn-mill machine tools have been developed by many machine tool manufacturers, such as Mazak and Deckel Maho.

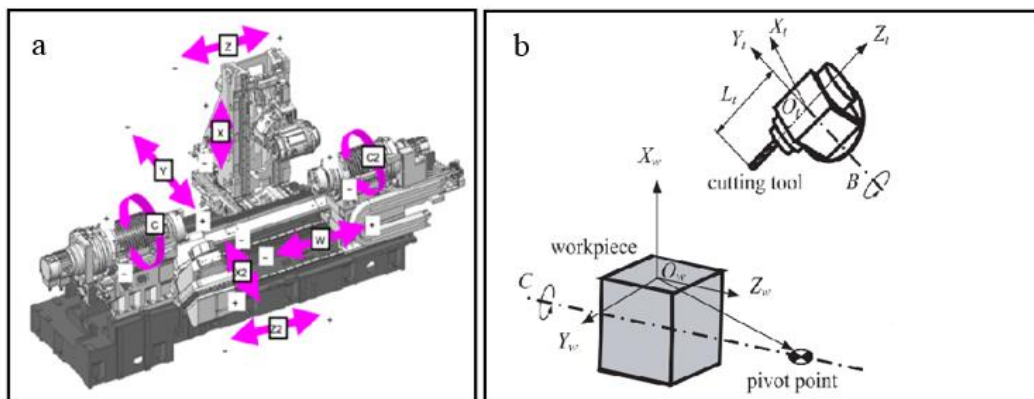


Figure 10 a) Coordinate system of an orthogonal turn-mill system, b) Coordinate system of a co-axial turn-mill system

Turning and milling processes are widely used conventional machining processes. Turn-milling process is a novel process which combines turning and milling processes. Research on turn-mill process and availability of machines tools on market which have capability of turn-milling is relatively new, with an increasing popularity. The pioneering research on turn-milling is carried out by Schulz et al. [56] focusing on production of shafts of hard materials with improved surface quality.

Recent studies about turn-milling processes are focused on analyzing the effect of the turn-milling processes and comparing with conventional processes. Most of these studies are evaluating the surface roughness of the turn-milled parts. Choudhury and Mangrulkar [57] performed experimental studies in order to compare surface roughness quality obtained from orthogonal turn-milling process and conventional turning. They have concluded that the surface quality of turn-milled parts are 10 time better than the turned parts. Choudhury et al. [58] have also compared the surface roughness quality obtained from turn-milling processes and milling processes. The effect of cutter diameter and depth of cut and also optimum cutting speed in order to minimize surface roughness are obtained. They have also concluded that the turn-milled parts have better surface quality. In this study surface roughness is modeled using response surface methodology. Savas et al [59] have concluded that a better surface roughness obtained from tangential turn-milling compared with grinding.

Kopac and Pogacnik [60] further investigated optimal eccentricity of the tool in orthogonal turn-milling for surface roughness. They concluded that a cutting eccentricity value of  $d/2 - L_n$  yields to best surface finish where  $d$  is the tool diameter and  $L_n$  is the length of the cutting edge of the tool. Zhu et al. [61] have modelled topography and surface roughness during orthogonal turn- milling processes. Verification studies also performed to validate the presented model.

In addition to surface roughness studies, the effect of cutting parameter on tool wear during turn-milling processes are analyzed [62]. kinematics of orthogonal turn-milling is investigated by Neagu et al. [63] and it is concluded that the productivity of turn-milling for roughing of straight shafts is 20 times better than conventional turning. Filho et al.



[54] have also developed an analytical model to predict cutting forces in plunge turn-milling.

Karaguzel et al. [64] have presented a study on orthogonal, tangential and co-axial turn-milling operations where surface quality, cutting forces, chip thickness and kinematics of turn-milling processes are investigated. In this study, material removal rate (MRR) is specified and also optimized taking tool wear and surface quality into consideration.



## CHAPTER 3

### ENERGY CONSUMPTION MODELING OF TURN-MILL SYSTEMS

In this section a generic energy consumption model for orthogonal turn-mill systems is presented considering idle energy, auxiliary energy and cutting energy as shown in Equation (24).

$$E_{\text{total}} = E_{\text{idle}} + E_{\text{cutting}} + E_{\text{auxiliary}} \quad (24)$$

Where  $E_{\text{idle}}$  is the energy consumption of machine tool when it is in a ready state to perform a machining operation. This part includes energy consumptions of controller, lightening systems, machine start-up and etc.  $E_{\text{cutting}}$  is tool tip energy consumption for material removal process during cutting operation.  $E_{\text{auxiliary}}$  is the energy consumption of sub-units of the machine tool. This part includes all auxiliary components of machine tool such as main spindle, sub-spindle, milling head, turret and etc. which are given in Equation (25). The sub-spindle and turret may not exist in all orthogonal turn-mill systems, if they are not existing in an orthogonal turn-mill system the values of the energy consumption for turret and sub-spindle in the equation will be zero.

$$E_{\text{auxiliary}} = E_{\text{main spindle}} + E_{\text{sub-spindle}} + E_{\text{milling spindle}} + E_{\text{milling head-feed}} + E_{\text{turret-feed}} \quad (25)$$

$$+ E_{\text{tool change}} + E_{\text{coolant}} + E_{\text{conveyor}} + E_{\text{chiller}} + E_{\text{Lubrication}}$$

$E_{\text{main spindle}}$  is energy consumed for rotation of spindle,  $E_{\text{sub-spindle}}$  is the energy consumed for rotations of the other spindle if existed in orthogonal turn-mill system,  $E_{\text{milling spindle}}$  is the energy required for rotation of the milling spindle of machine tool,  $E_{\text{milling head-feed}}$  is energy consumption of travel of milling head in feed axes of orthogonal turn-mill system,  $E_{\text{turret-feed}}$  is energy consumption of travel of turret in

feed axes of system,  $E_{\text{tool change}}$  is the energy consumption for automatic tool change of milling spindle. If the turn-mill system has a turret, the tool change energy consumption for automatic tool change of turret should be included in this part.  $E_{\text{conveyor}}$  is energy consumed by the conveyor to remove chips from machining region,  $E_{\text{coolant}}$  is the energy consumed by coolant system of the machine tool,  $E_{\text{chiller}}$  is the energy consumption of chiller which is for keeping the temperature of spindles under control and  $E_{\text{Lubrication}}$  is the energy consumption of lubrication unit for lubricating spindles and gears.

The energy consumption of each part of the model could be determined for different turn-mill systems by obtaining power consumption amount of each part. So the energy consumption values can be determined using the power consumption amounts and the activation time of each part.

### 3.1 Idle energy

Power consumption during idling is constant so the energy consumption for idling time could be determined multiplying the constant power consumption value of idling by the time that machine has started up which is shown in Equation (26).

$$E_{\text{idle}} = P_{\text{idle}} \cdot \Delta t_1 \quad (26)$$

Where  $P_{\text{idle}}$  is power consumed during idling and  $\Delta t_1$  is the total run time of machine.

### 3.2 Auxiliary energy

The energy consumption of all auxiliary sub-units are determined separately in this section. The energy consumption of spindles are given in Equations (27), (28) and (29).  $P_{\text{main-spindle}}$  and  $P_{\text{sub-spindle}}$  are equation of power consumption of main spindle and sub-spindle with respect to rotational speed when work piece is rotating and  $t_1$  and  $t_2$  are the rotations times of the main spindle and sub-spindle.  $P_{\text{milling-spindle}}$  is also equation of power consumption of milling spindle with respect to rotational speed when cutting tool is rotating and  $t_3$  is the rotation times of the milling spindle.

$$E_{\text{main-spindle}} = \int_0^{t_1} P_{\text{main-spindle}} dt \quad (27)$$

$$\mathbf{E}_{\text{sub-spindle}} = \int_0^{t_2} \mathbf{P}_{\text{sub-spindle}} \mathbf{dt} \quad (28)$$

$$\mathbf{E}_{\text{milling-spindle}} = \int_0^{t_3} \mathbf{P}_{\text{milling-spindle}} \mathbf{dt} \quad (29)$$

The energy consumption of travels of milling head and turret are given in Equations (30) and (31) where  $\mathbf{P}_{\text{milling head-feed}}$  and  $\mathbf{P}_{\text{turret-feed}}$  are equations of power consumption of milling head and turret travels on feed axes with respect to feed rate and  $t_4$  and  $t_5$  are the traveling times of the milling head and turret.

$$\mathbf{E}_{\text{milling head-feed}} = \int_0^{t_4} \mathbf{P}_{\text{milling head-feed}} \mathbf{dt} \quad (30)$$

$$\mathbf{E}_{\text{turret-feed}} = \int_0^{t_5} \mathbf{P}_{\text{turret-feed}} \mathbf{dt} \quad (31)$$

The energy consumption of automatic tool change for the machine tools that tool change is not manual should be determined. The energy consumption for tool change is given in Equation (32) where  $\mathbf{P}_{\text{tool change}}$  is equation of power consumption for automatic tool change with respect to feed rate and  $t_6$  is the time duration of tool change.

$$\mathbf{E}_{\text{tool change}} = \int_0^{t_6} \mathbf{P}_{\text{tool change}} \mathbf{dt} \quad (32)$$

If the speed of tool change operation is not adjustable and is running on a constant speed, the power consumption of tool change will be constant and the energy consumption could be determine by multiplying the constant value of power consumption by the time duration of tool change. The tool change energy consumption should be calculated for milling head and turret separately for machine tools which contains turret.

Power consumption of coolant and conveyor are constant since their not dependent to any parameter, so the energy consumption of coolant and conveyor could also be determined multiplying the constant power consumption value by their activation time, which is shown in Equation (33) and (34) where  $\mathbf{P}_{\text{coolant}}$  is coolant power consumption,  $\Delta t_7$  is the coolants activation time,  $\mathbf{P}_{\text{conveyor}}$  is the power consumption of conveyor and  $\Delta t_8$  is the conveyors activation time.

$$E_{\text{coolant}} = P_{\text{coolant}} \cdot \Delta t_7 \quad (33)$$

$$E_{\text{conveyor}} = P_{\text{conveyor}} \cdot \Delta t_8 \quad (34)$$

Power consumption of chiller and lubrication unit are also constant and depend to the machine tool, so the energy consumption of coolant and conveyor could also be determined multiplying the constant power consumption value by their activation time, which is shown in Equations (35) and (36) where  $P_{\text{chiller}}$  is chiller power consumption,  $\Delta t_9$  is the chillers activation time,  $P_{\text{Lubrication}}$  is the power consumption of lubrication unit and  $\Delta t_{10}$  is the activation time of lubrication unit.

$$E_{\text{chiller}} = P_{\text{chiller}} \cdot \Delta t_9 \quad (35)$$

$$E_{\text{Lubrication}} = P_{\text{lubrication}} \cdot \Delta t_{10} \quad (36)$$

### 3.3 Cutting energy

Cutting energy consumption, which is the tool tip energy, could be determined in various ways such as using specific cutting energy, deriving power consumption equations and etc. In a feature based energy consumption model the cutting energy would be the summation of energy consumptions of all features of a machining process which is shown in Equation (37).

$$E_{\text{cutting}} = E_{\text{Feature 1}} + E_{\text{Feature 2}} + E_{\text{Feature 3}} + E_{\text{Feature 4}} + \dots \quad (37)$$

Where  $E_{\text{Feature 1}}$  is the energy consumed during cutting feature 1 and so on. If there is  $n$  cutting feature in a machining process the cutting energy consumption could be determined as shown in Equation (38).

$$E_{\text{cutting}} = \sum_{i=1}^{i=n} E_{\text{Feature } i} \quad (38)$$

Total energy consumption model for a turn-mill system could be determined as given in Equation (39).

$$\begin{aligned}
\mathbf{E}_{\text{total}} = & \mathbf{P}_{\text{idle}} \cdot \Delta \mathbf{t}_1 + \int_0^{t_1} \mathbf{P}_{\text{main-spindle}} \mathbf{d} \mathbf{t} + \int_0^{t_2} \mathbf{P}_{\text{sub-spindle}} \mathbf{d} \mathbf{t} + \\
& \int_0^{t_3} \mathbf{P}_{\text{milling-spindle}} \mathbf{d} \mathbf{t} + \mathbf{E}_{\text{milling head-feed}} + \int_0^{t_5} \mathbf{P}_{\text{turret-feed}} \mathbf{d} \mathbf{t} + \int_0^{t_6} \mathbf{P}_{\text{tool change}} \mathbf{d} \mathbf{t} + \\
& \mathbf{P}_{\text{coolant}} \cdot \Delta \mathbf{t}_7 + \mathbf{P}_{\text{conveyor}} \cdot \Delta \mathbf{t}_8 + \mathbf{P}_{\text{chiller}} \cdot \Delta \mathbf{t}_9 + \mathbf{P}_{\text{lubrication}} \cdot \Delta \mathbf{t}_{10} + \\
& \mathbf{E}_{\text{cutting}}
\end{aligned} \tag{39}$$





## CHAPTER 4

### ENERGY CHARACTERIZATION OF MAZAK INTEGREGX I200-ST

#### TURN-MILL SYSTEM

As mentioned before an energy prediction model will be presented for Mazak integrex i200-ST turn-mill system. Performing energy characterization studies prior to creating energy prediction model of CNC machine is necessary. Within the framework of the energy characterization studies, experiments were conducted to reveal the energy consumption of the idle energy, auxiliary sub-units of CNC machine tool and cutting features. In order to determine energy consumption of each part in the model with respect to cutting parameters, equations are derived for obtained instantaneous power graphs.

#### 4.1 Machine tool properties

Experimental studies in this thesis scope were carried out on 5 axis Mazak integrex i-200ST machine tool existing in advanced manufacturing laboratory of TOBB University of Economics and Technology. The Mazak integrex i-200ST advanced Multi-Tasking machine delivers maximum versatility and throughput for medium to large complex parts. The machine combines the capabilities of a high-powered turning center and full-function machining center to produce parts in single setups. Mazak integrex i200-ST is more advanced compared with other turn-mill systems since it contains a turret and sub-spindle in addition to the main spindle and milling head of the machine tools. A front view of this machine tool is shown in Figure 11. This machine tool has 2 spindles, a main spindle, a sub spindle, a milling head and a turret. The milling head can travel in X, Y and Z axis and also it has the capability to rotate 240° on B axis and the turret can travel on X2 and Z2 axis. The main spindle and sub-spindle are also capable to rotate 360° on  $C_1$  and  $C_2$  axis. The machine tool contains direct measuring system for all axes so it allows the production of extremely high-precision parts in roundness, flatness,

circular shape precision and surface quality. Other specifications of the machine tool are listed in Table 4.



Figure 11 A view of Mazak integrex i200-ST

Table 4 Specifications of Mazak integrex i200-ST [65]

Specification		Bed Length - 1500U in
Capacity	Maximum Swing	25.91 in / 658 mm
	Maximum Machining Diameter	25.910 in / 658 mm
	Maximum Bar Work Capacity	2.6 in / 65 mm
	Maximum Machining Length	59.800 in / 1519 mm
Main spindle	Chuck Size	8 in
	Maximum Speed	5000 RPM
Sub-spindle	Chuck Size	8 in
	Maximum Speed	5000 RPM
Milling head	B-Axis Travel	240°
	Magazine Capacity	36
	Maximum Speed	12000 RPM
Feed axis	Travel (X Axis)	24.21 in / 615 mm
	Travel (X2 Axis)	9.06 in / 230 mm
	Travel (Y Axis)	9.84 in / 250 mm
	Travel (Z Axis)	62.40 in / 1585 mm
	Travel (Z2 Axis)	54.65 in / 1388 mm
	Travel (W Axis)	41.97 in / 1066 mm

## 4.2 Energy measurement method

In order to visualize the information about instantaneous power drawn by the machine tool within energy characterization studies, a Socomec DIRIS A40 branded multifunction energy meter was used. This energy meter provides the information of the instantaneous power, current, voltage and so on to the user by means of the LCD screen inserted on it. Energy meter sampling time is 1 second, the data received is once per second.

The IP address taken from modem is entered manually on the energy meter thus data transfer to the server can be provided via Ethernet connection. It should be considered that the server is compatible with its subnet or not while the IP address given through energy meters. Once this connection is established, data tracking is provided online through the server.

To store the data 'Wamp Server' has been established on the computer which the measurements will be stored. In order to transfer the information about instantaneous power and time during a metal cutting process to excel, first `http://localhost/phpmyadmin` address is entered in a web browser of the computer and user is signed in to server interface. After user sign in, in order to run the code which enables instantaneous power and time data collection `http://localhost/ecoman100` address will be written in a new tab of the same browser and instantaneous power consumption values are stored in rows on the server. When the tab is closed about data storage process is stopped and the accumulated data continues to be stored on the server. The data stored on the server interfaces can be saved in an excel file by selecting 'Export' and then selecting 'CSV for MS Excel' for the file format. Thus instantaneous power values of machine tools are transferred to an excel file. The stages of transferring the data received from the machine tools to the excel file format are shown schematically in Figure 12.

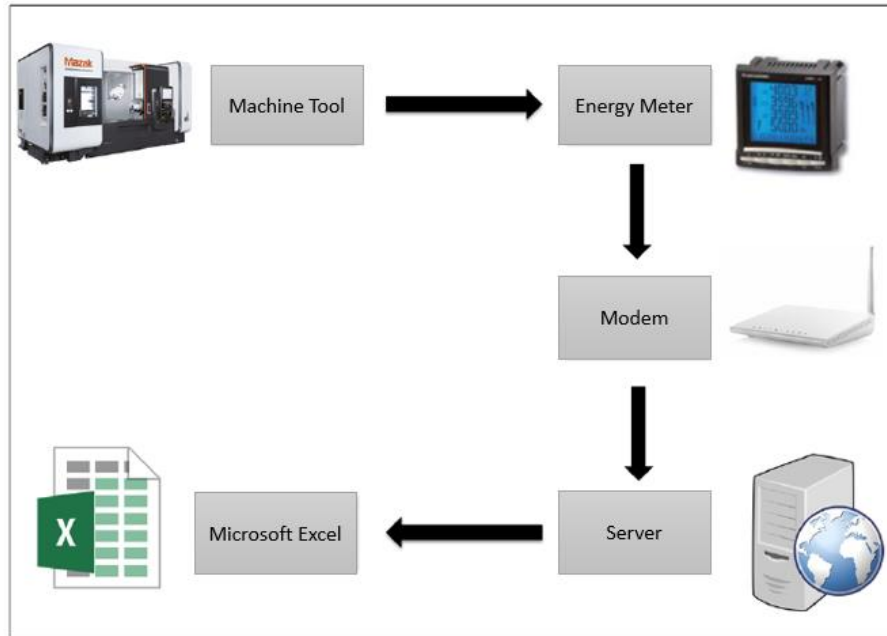


Figure 12 Schematic representation of the energy measurement methods

### 4.3 Idle energy

Idle energy is the energy that machine tool consumes in ready position after start-up waiting for the manufacturing process. In order to obtain idle energy consumption of Mazak integrex i200-ST machine tool, the average value of instantaneous power consumption of machine tool must be determined while idling. Idle energy consumption will be calculated by multiplying this value with the operation time. For this purpose, energy consumed during idling of the machine tool was measured using energy meters and instantaneous power-time graph is generated based on received data as shown in Figure 13.

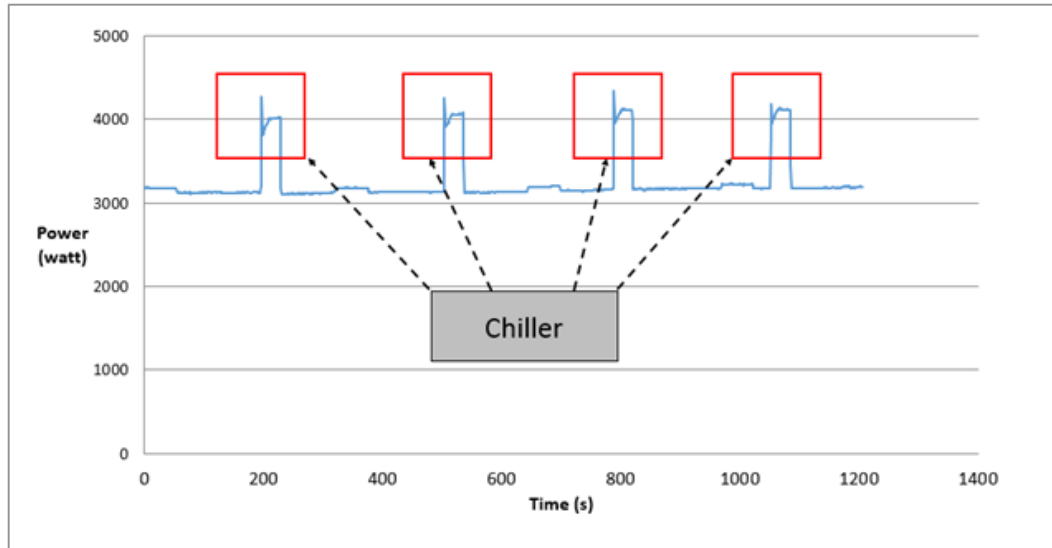


Figure 13 Instantaneous power - time graph for basic energy consumption

As seen in Figure 13 two different instantaneous power values are drawn when machine is waiting in ready position (idle). With the observations made during the test and contacting the manufacturer it is identified that the difference in power values has originated from the automatic operation of chiller. Chiller unit of the machine tool is responsible to keep the temperature of the machine tool at a constant degree which could be specified by user. There is timer that runs the chiller at certain time periods which can be seen in idling instantaneous power consumption graph but when machine tool is operating a cutting process, the temperature of the spindles increases and chiller automatically starts to work to decrease the temperature, so it is not possible to predict when chiller will starts to run. This approach can create problems in the consistency of the energy model estimates.

Examining idle energy consumption test data it is found that each time chiller is activated every 250 second on average it remains active for 32 seconds on average. The power that chiller is about 1KW which is a considerable amount. Average power consumption for idling when the chillers power consumption is not taken into consideration is 3161 watts.

Idling consumes power whenever the machine tool is started up or running and it will consumed energy till the machine turs off, so the energy consumption of idling will be determined multiplying 3161 watts by the machine tool activation time.

#### 4.4 Auxiliary energy

In order to model energy consumption of the machine tool in addition to idle energy the energy consumption of all auxiliary sub-units are measured and reported in this section. For this purpose auxiliary sub units was actuated in several speeds and feed rates manually using controller and instantaneous power consumptions are determined using energy meters. The sub-units of Mazak integrex i200-ST are shown in Figure 14.

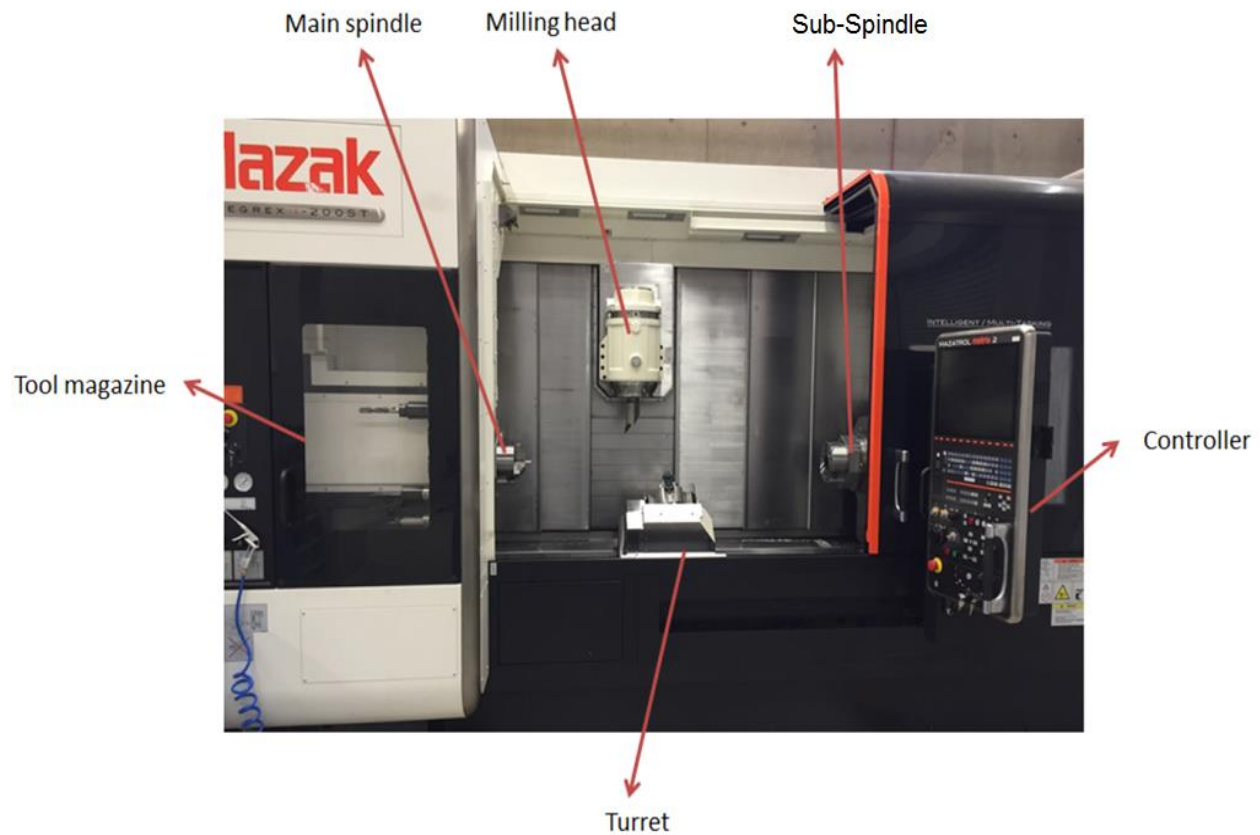


Figure 14 Subunits of Mazak integrex i200-ST

#### 4.4.1 Main Spindle

Both turning spindles of the Integrex i-200ST provide equal high performance with spindle speeds of 5000 rpm and C-axis turning control. The main spindle is the spindle on the left side of the machine tool which is shown in Figure 14. The main spindle was set to work at specific speeds when the machine was at the ready state in order to determine main spindle power consumption. Each experiment was carried out 3 times and the average of the instantaneous power values taken at stated speeds was calculated which are given in Appendix A. Using these values, an average power - speed graph was obtained which is shown in Figure 15. These values will be used for Energy Prediction model verification in this study. For example, if a metal cutting operation is carried out with a spindle speed of 3000 RPM, the power consumption amount of the main spindle will be 1470 watts. As seen in the figure, the average power consumption increases by raising the rotational speed, but there is a significant increase in the power consumption value at the speed of 1000 RPM, which is because of the activation of another motor in order to reach required speeds.

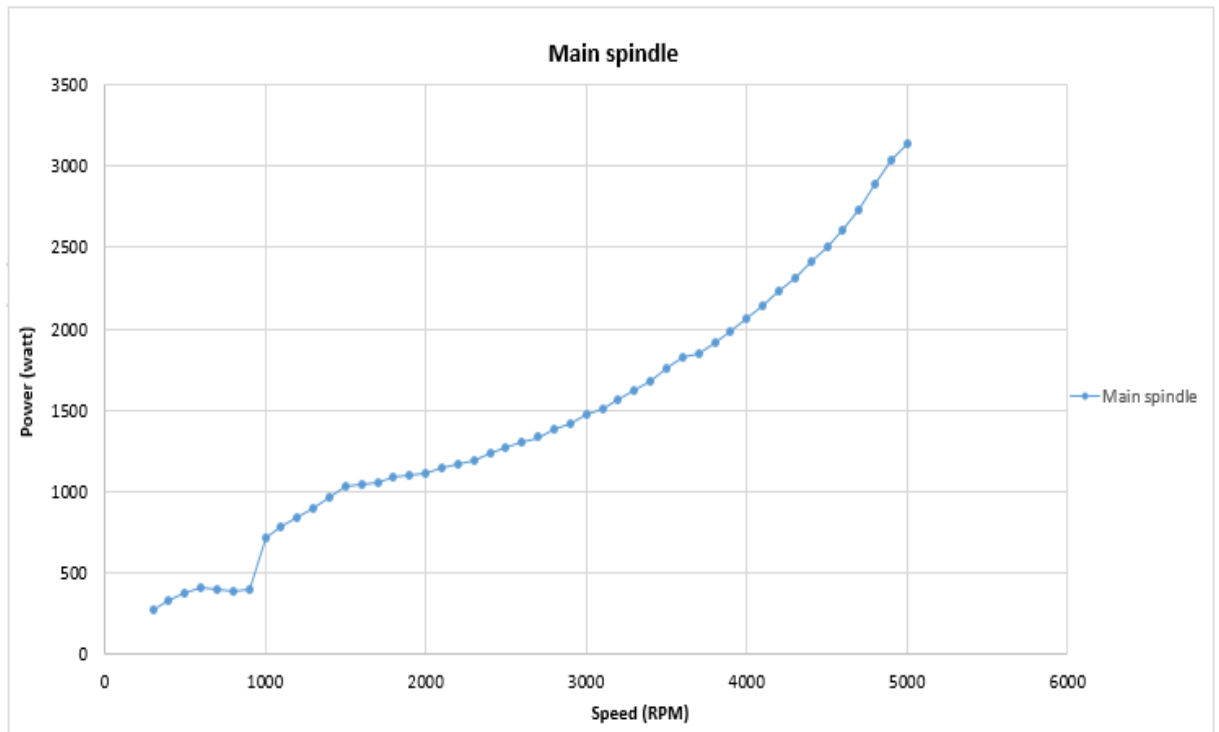


Figure 15 Average power consumption-speed graph for main spindle

In order to derive equation for power consumption of main spindle with respect to rotational speed (RPM) trend lines are added to the graph using Microsoft Excel. As mentioned above power consumption significantly increase at 1000 RPM so to get more accurate results the graph is divided to 2 parts at this point as shown in Figure 16. For each part desecrate trend lines and equations are obtained. For the first part, a second polynomial regression with R-squared value of 0.9581 and for the second part a third order polynomial regression with R-squared value of 0.9987 is applied.

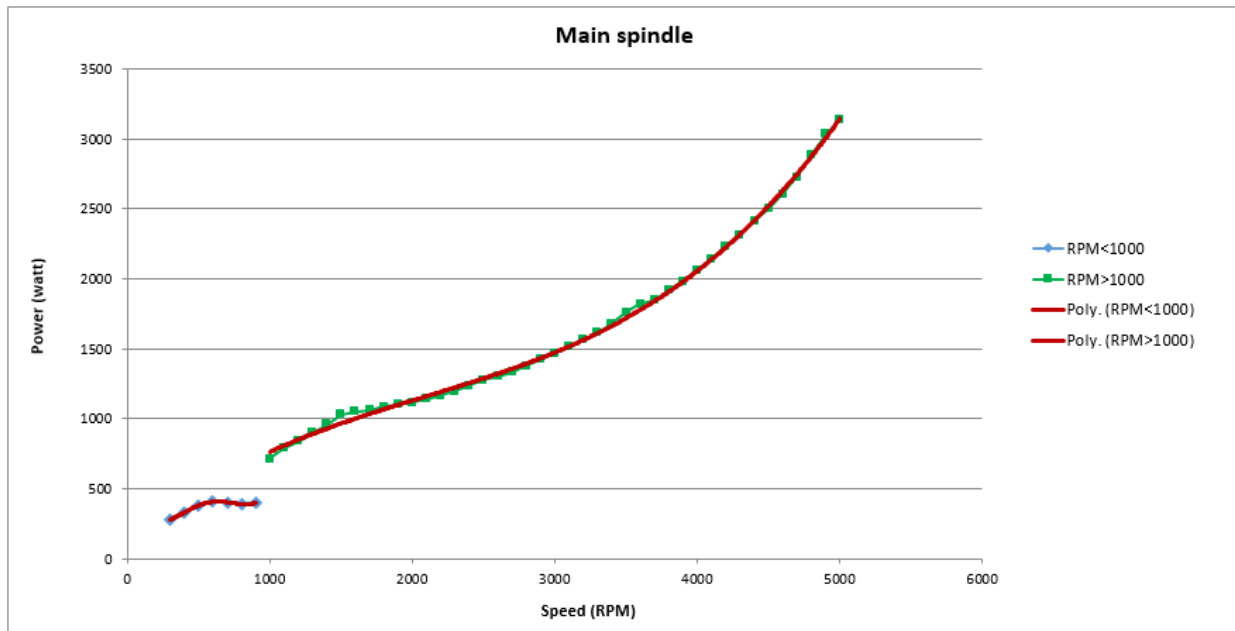


Figure 16 Trend lines of average power consumption-speed graph for main spindle

The trend lines are specified with red colors in the figure and derived equations are given in Equation (40) where  $P_{main-spindle}$  is average power consumption of main spindle and  $S$  is rotational speed of main spindle (RPM). The constant coefficients in the equations are rounded and the actual values of coefficients are given in Appendix B.

$$P_{main-spindle} = \begin{cases} -0.0007.S^2 + 1.0071.S + 42.381, & RPM < 1000 \\ 4E-08.S^3 - 0.0003.S^2 + 0.8845.S + 110.58, & RPM \geq 1000 \end{cases} \quad (40)$$



#### 4.4.2 Sub-Spindle

As mentioned before both turning spindles on the integrex i-200ST provide equal high performance with spindle speeds of 5000 rpm and C-axis turning control. Sub-spindle is the spindle on the right side of the machine tool which is shown in Figure 14. The procedure applied for main spindle is repeated for sub-spindle thus sub-spindle also was set to work at specific speeds while machine was waiting at the ready position. These tests were also repeated 3 times and the average of the instantaneous power values determined at stated speeds was calculated which are given in Appendix A. Using these values average power-speed graph was obtained which is shown in Figure 17. These values will be used for energy prediction model verification in this study as power consumption of sub-spindle. The average power consumption values of sub spindle also increases in high rotational speeds for, but here significant increase in the power consumption value occurs at the speed of 1100 RPM which can be seen in Figure 17 which is also because of activation of another motor in order to reach required speeds.

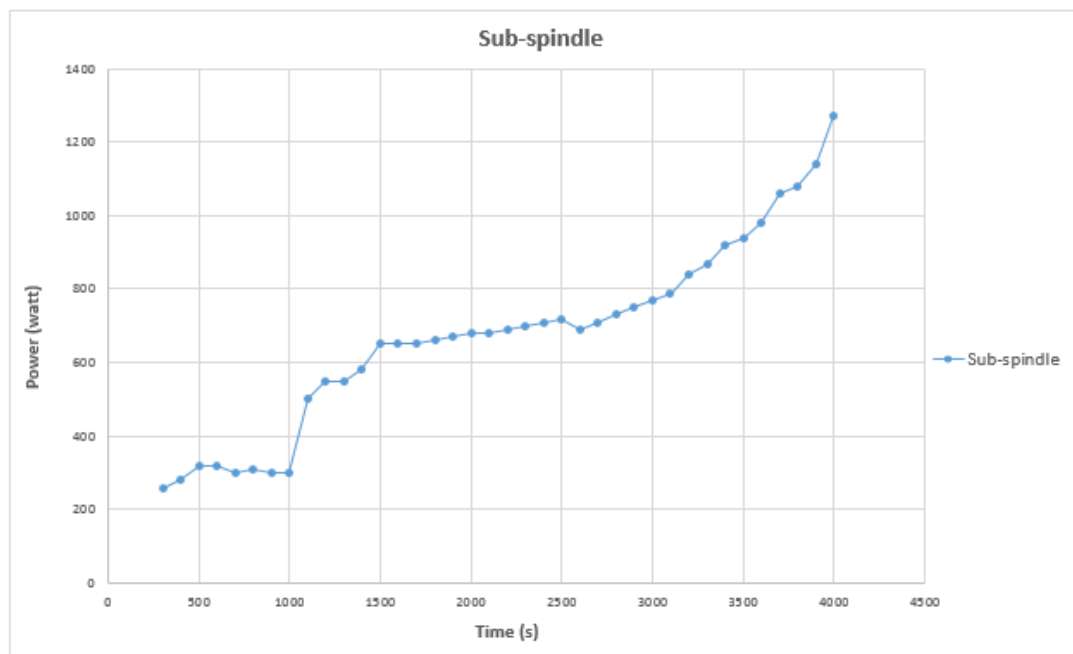


Figure 17 Average power consumption-speed graph for sub-spindle

Same procedure is applied for sub-spindle to derive equation for power consumption with respect to rotational speed (RPM). The graph is divided into 2 parts at the speed of 1100 RPM to obtain trend lines for each part separately as shown in Figure 18. For the first part a third order polynomial regression with R-squared value of 0.8455 and for the second part a third order polynomial regression with R-squared value of 0.9927 is applied. The trend lines are specified with red colors in the figure and derived equations are given in Equation (41). The constant coefficients in the equations are rounded and the actual values of coefficients are given in Appendix B.

$$P_{Sub-spindle} = \begin{cases} 8E - 07S^3 - 0.0018S^2 + 1.3383S - 2.619, & RPM < 1100 \\ 8E - 08S^3 - 0.0006S^2 + 1.2922S - 356.16, & RPM \geq 1100 \end{cases} \quad (41)$$

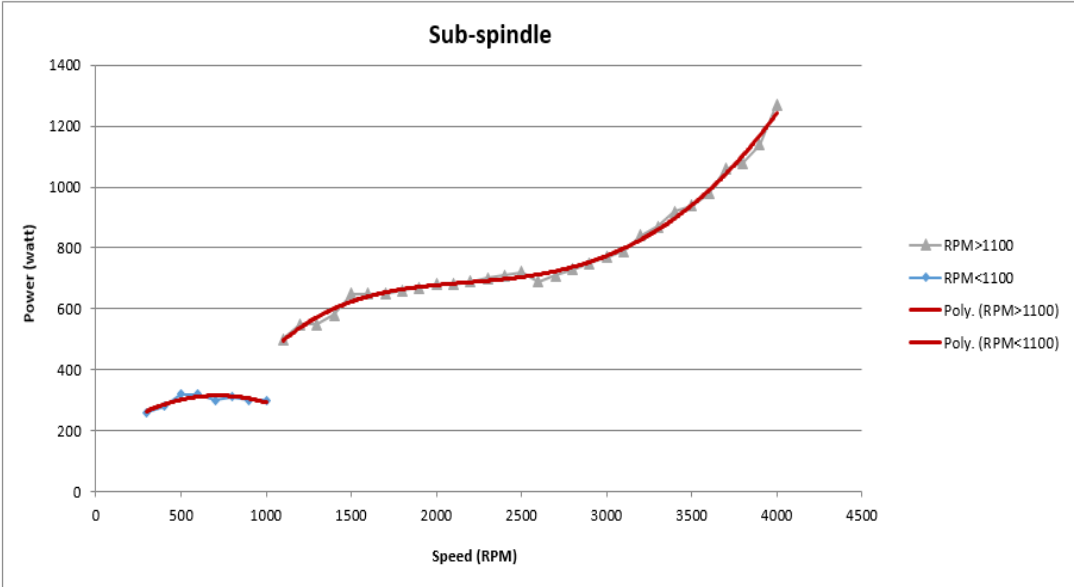


Figure 18 Trend lines of average power consumption-speed graph for sub-spindle

### 4.4.3 Milling Head

Mazak integrex i200-ST has a milling head on the top of the machine which is able to carry out both turning and milling operations. The spindle of milling head could be used up to maximum rotational speed of 12,000 RPM manually and as an option it

could reach 18,000 RPM if it is needed in running programs. Experiments were carried out on milling head in order to determine power consumption of spindle of milling head. For this purpose it was rotated at specific speeds and the average power - speed graph was obtained which are given in appendix A. Average power consumption-speed graph for milling spindle is shown in Figure 19. Comparing milling spindle with main spindle or sub-spindle, power consumption of milling spindle is much lower even at 12,000 RPM.

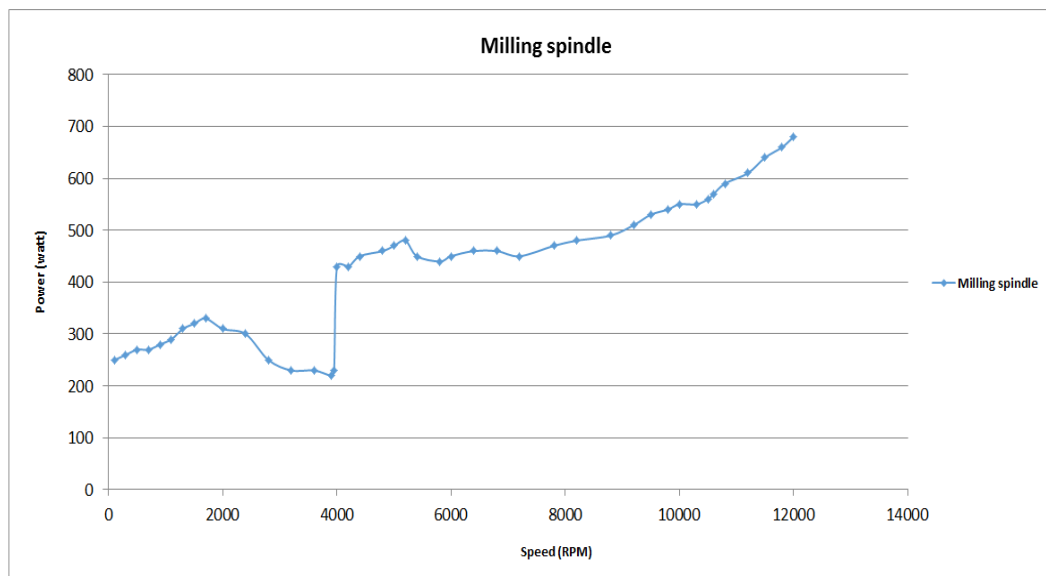


Figure 19 Average power consumption-speed graph for milling spindle

In milling spindle also there is a remarkable increase in power consumption amount at the speed of 4000 RPM, so the graph is separated into 2 parts at this point in order to derive equations separately to get better results. Trend lines of these parts are shown in Figure 20 where the trend lines are specified with red colors. For both parts fourth order polynomial regression with R-squared value of 0.9535 and 0.9839 is applied. Derived equations are given in Equation (42). The constant coefficients in the equations are rounded and the actual values of coefficients are given in Appendix B.

$$P_{\text{Milling-spindle}} = \begin{cases} 9E - 12.S^4 - 7E - 08.S^3 + 0.0001.S^2 - 0.0341.S + 255.51, & \text{RPM} < 4000 \\ -2E - 13.S^4 + 6E - 09.S^3 - 8E - 05.S^2 + 0.3953.S - 267.2, & \text{RPM} \geq 4000 \end{cases} \quad (42)$$

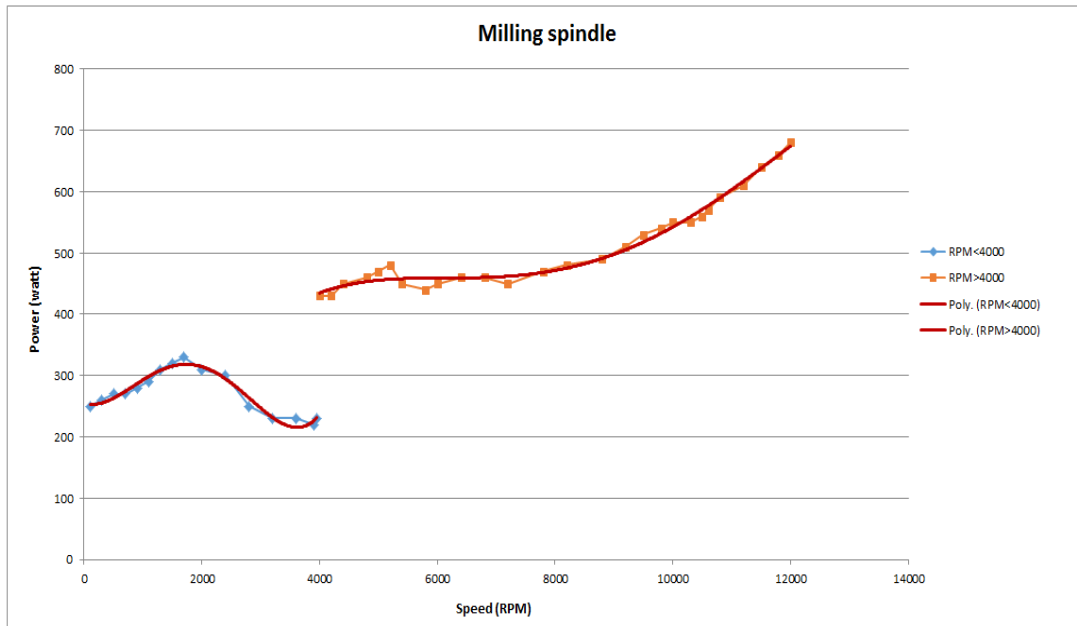


Figure 20 Trend lines of average power consumption-speed graph for milling spindle

The milling head can travel on X+ and X-, Z+ and Z- and also Y+ and Y- axis and also it can be rotated from 0 degree to 180 degree with 45-degree steps. The energy consumption of milling head travels was determined by moving feed axis at different feed speeds and recording consumed instantaneous power values which are given in appendix A. These values are obtained for each feed axes of milling head. All experiments are performed for rapid move (G00) and normal move (G01) separately. In these tests there is not much difference between Z+ and Z- direction or Y+ and Y- direction so an average value of power is determined for these axes. The effect of gravity on power consumption when moving in X- direction creates a large difference between the power consumption of the X- direction and X+ direction average power consumption so power consumption of X+ and X- directions are also calculated separately. Average Power - Feed rate graphs of milling head for G00 move and G01 move are obtained and given in Figure 21 and Figure 22. As seen in the figures rapid move of milling head consumes much more power than the normal (G01) move of milling head. When milling head travels in X- axis (in both G00 and

G01 mode) the values of power consumption which are obtained from the energy meter is even less than the idle power consumption of machine tool because of the effect of gravity. This is the reason of negative values of power consumption for X-axis of milling head in both G00 and G01 move. Comparing the power consumption amounts of feed axes of milling head, traveling in Z axis in both G00 and G01 mode consumes the most power.

The power consumption equations with respect to feed rates also derived for all axes separately. For all axis of milling head in both G00 and G01 mode linear regression is used. The trend lines are specified with red colors in the Figure 23 and Figure 24 and derived equations are given in Equations (43) and (44). The constant coefficients in the equations are rounded and the actual values of coefficients are given in Appendix B.



Figure 21 Average power consumption-feed rate graph for feed axis of milling head (G01)

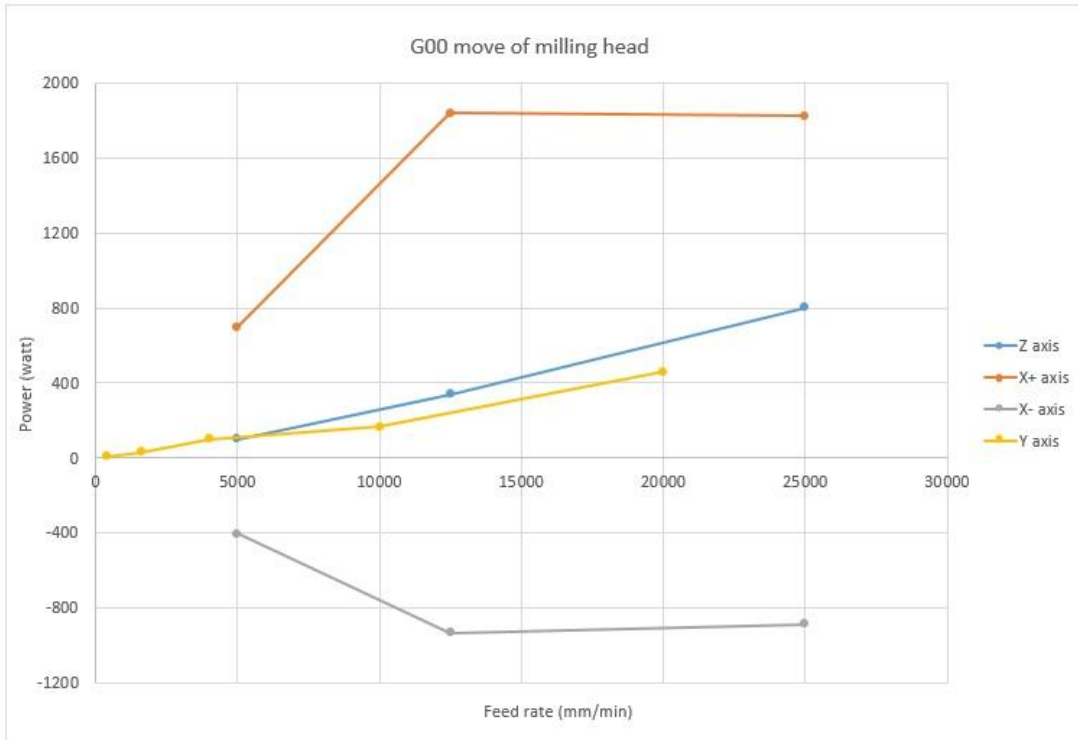


Figure 22 Average power consumption-feed rate graph for feed axis of milling head (G00)

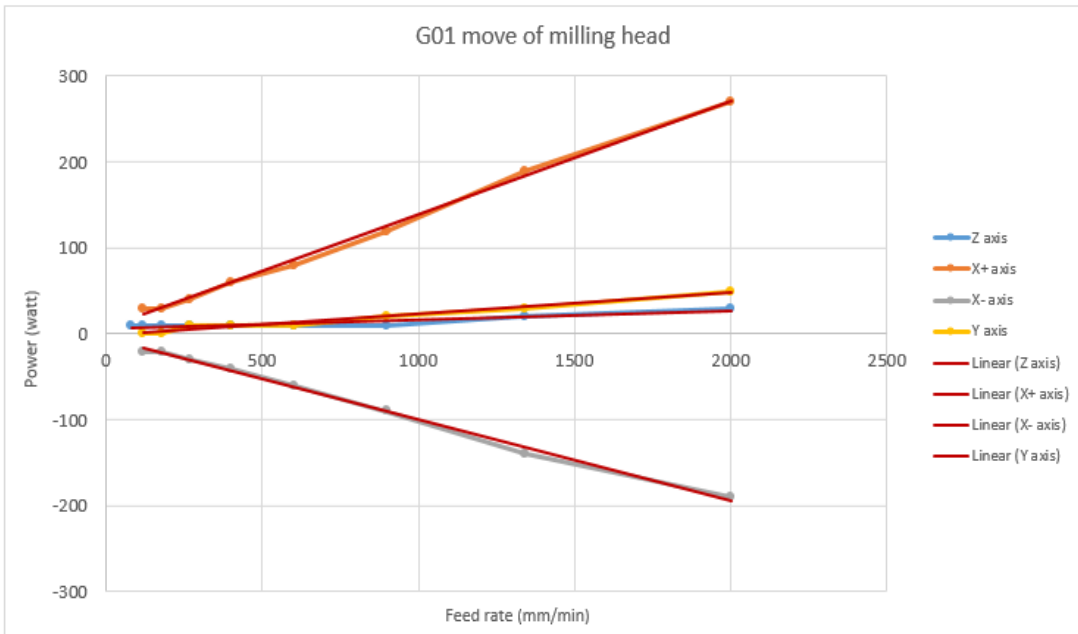


Figure 23 Trend lines of average power consumption-feed rate graph for milling head (G01)

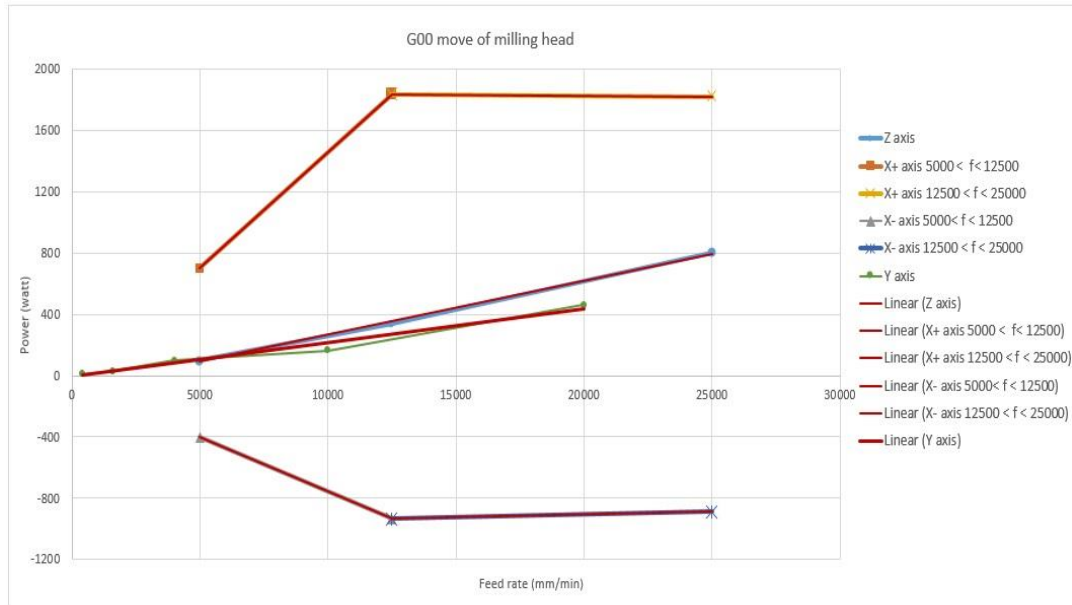


Figure 24 Trend lines of average power consumption-feed rate graph for milling head (G00)

$$P_{milling\ head\_G01} = \begin{cases} 0.1318.f + 6.762, & X + Axis \\ -0.0946.f - 5.0532, & X - Axis \\ 0.0099.f + 6.8254, & Z Axis \\ 0.0253.f - 2.1085, & Y Axis \end{cases} \quad (43)$$

$$P_{milling\ head\_G00} = \begin{cases} 0.152.f - 60, & X + Axis, 5000 < f < 12500 \\ -0.0014.f + 1857, & X + Axis, 12500 < f < 25000 \\ -0.0707.f - 49.167, & X - Axis, 5000 < f < 12500 \\ 0.0037.f - 978.33, & X - Axis, 12500 < f < 25000 \\ 0.0223.f - 7.746, & Y Axis \\ 0.0354.f - 86.496, & Z Axis \end{cases} \quad (44)$$

As mentioned above milling head could be rotated up to 180 degree with 45-degree steps. The energy consumption of rotation of milling head during each 45 degree is

determined by rotating milling head in different speeds and obtaining power consumption values. Average power consumption-degree graph for B axes of milling head in various speeds is shown in Figure 25. Different power consumption values in each rotation is due to effect of gravity dependent on position of milling head after each rotation. The energy consumed for rotation of milling head could be calculated by multiplying the power consumption by duration of the time that rotation occurs which is related to the rotation speed. As the power consumption amount is constant for each rotation, it can be selected from the Average power consumption-rotation graph.

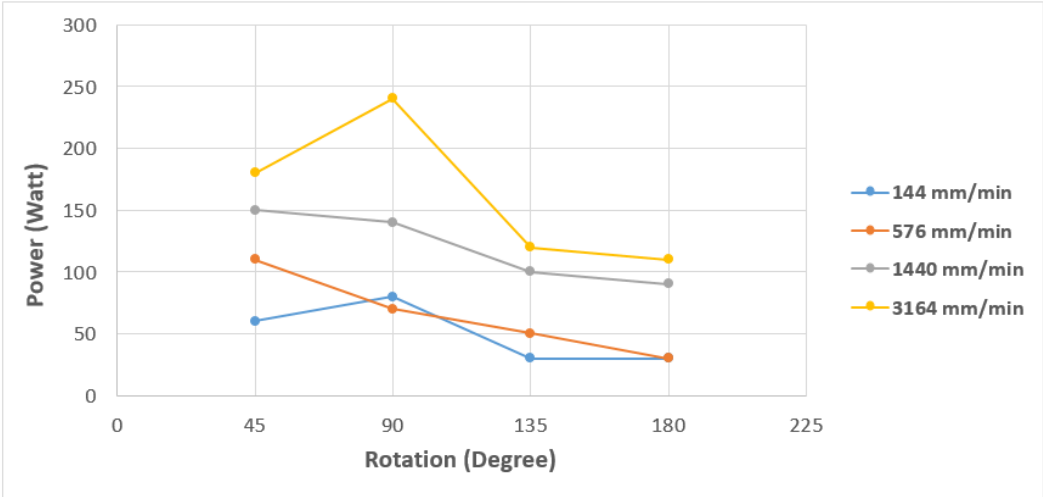


Figure 25 Average power consumption-rotation graph for B axes of milling head

**4.4.4 Turret**

Turret can travel on X+ and X-, Z+ and Z- axis. The energy consumption of turret was also determined by moving feed axis at different feed rates and recording consumed instantaneous power values which are given in appendix A. All experiments are performed for rapid move and normal move separately same as milling head. In these tests there is not much difference between Z+ and Z- direction so an average value of instantaneous power is determined for these axes but the



effect of gravity on power consumption in turret also makes a large difference between the power consumption of the X- direction and X + direction average power consumption so power consumption of X+ and X- directions are also calculated separately for turret. In addition, Average Power - Feed rate graphs of turret for rapid move and normal move are given in Figure 26 and Figure 27.

Power consumption equations with respect to feed rates also derived for all axis separately. Microsoft Excel is used to add trend lines to the graph which is shown in Figure 28 and Figure 29. For all axis of G01 move of milling head second order polynomial regression is used where for G00 move linear regressions are used. Trend lines are specified with red colors in the figure and derived equations are given in Equations (45) and (46). Some of the constant coefficients of these equations are rounded and actual values are given in Appendix B.

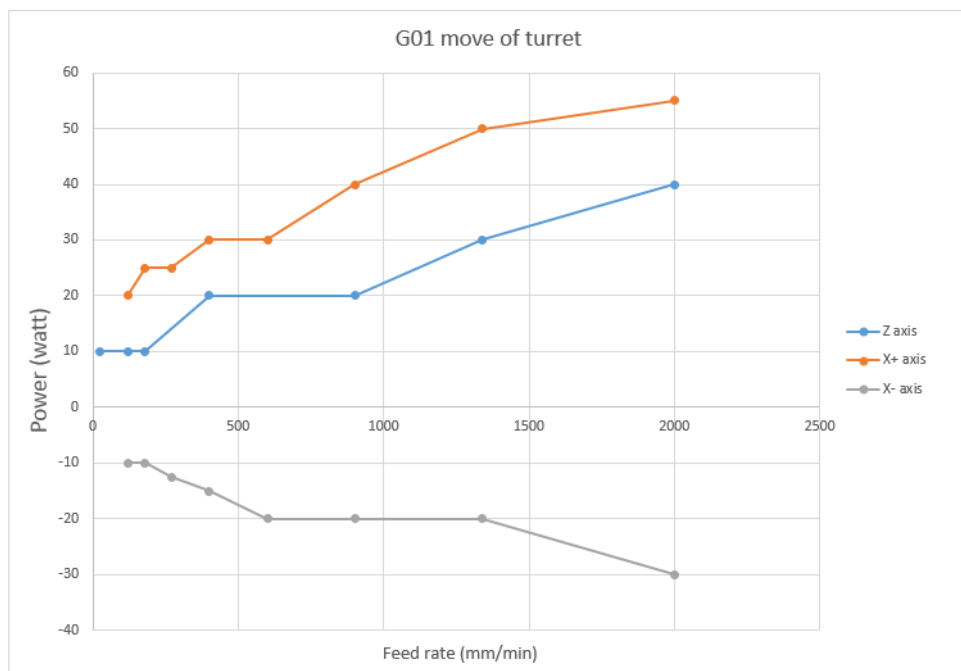


Figure 26 Average power consumption-feed rate graph for feed axis of milling head (G01)

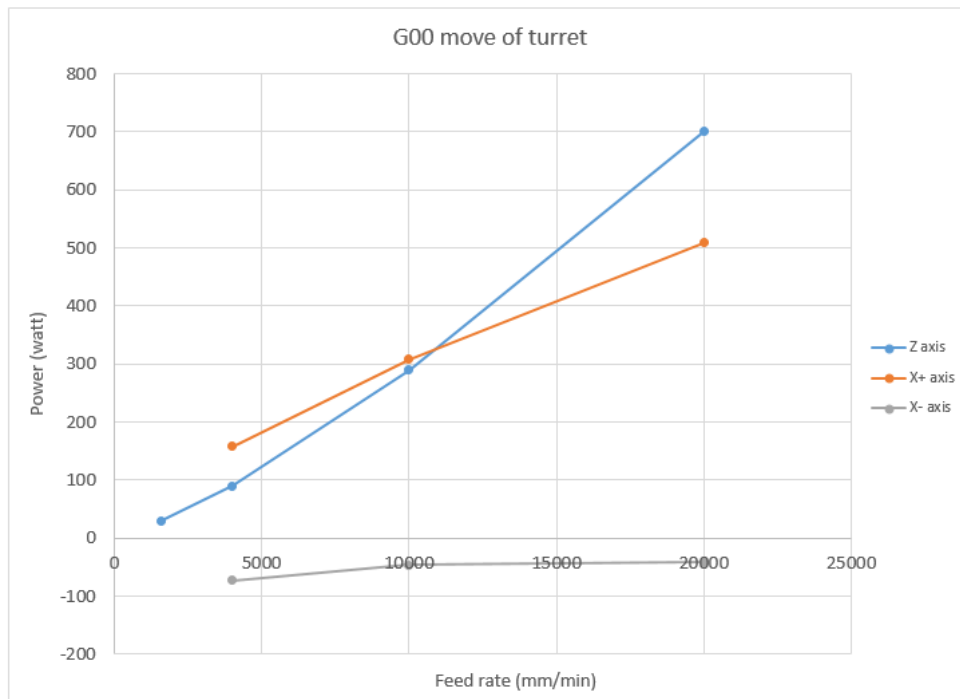


Figure 27 Average power consumption-feed rate graph for feed axis of milling head (G00)

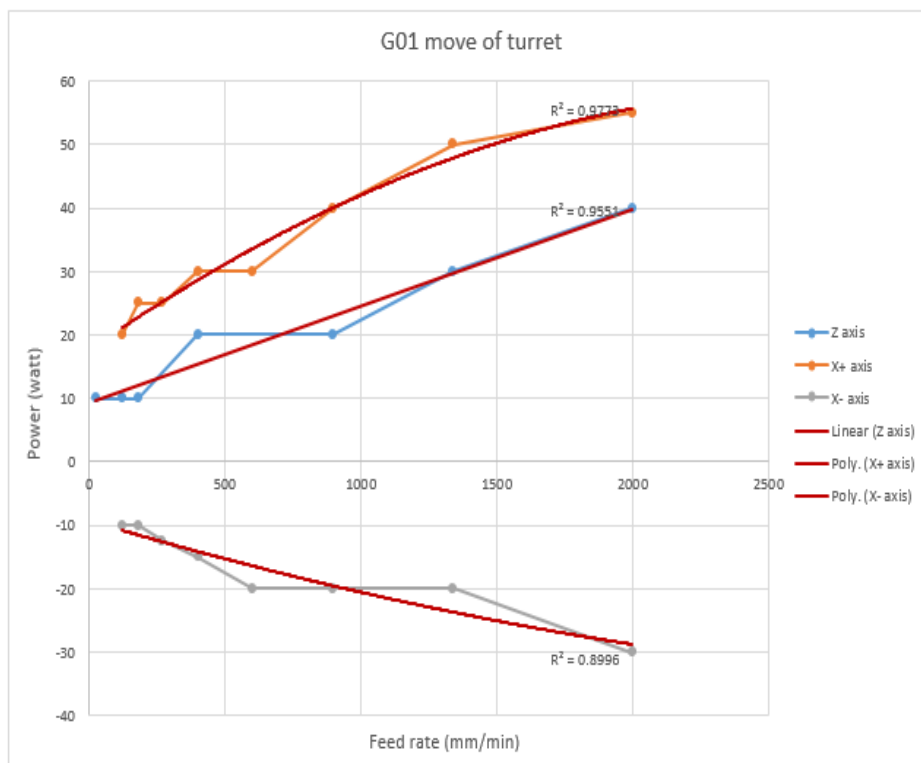


Figure 28 Trend lines of average power consumption-feed rate graph for turret (G01)

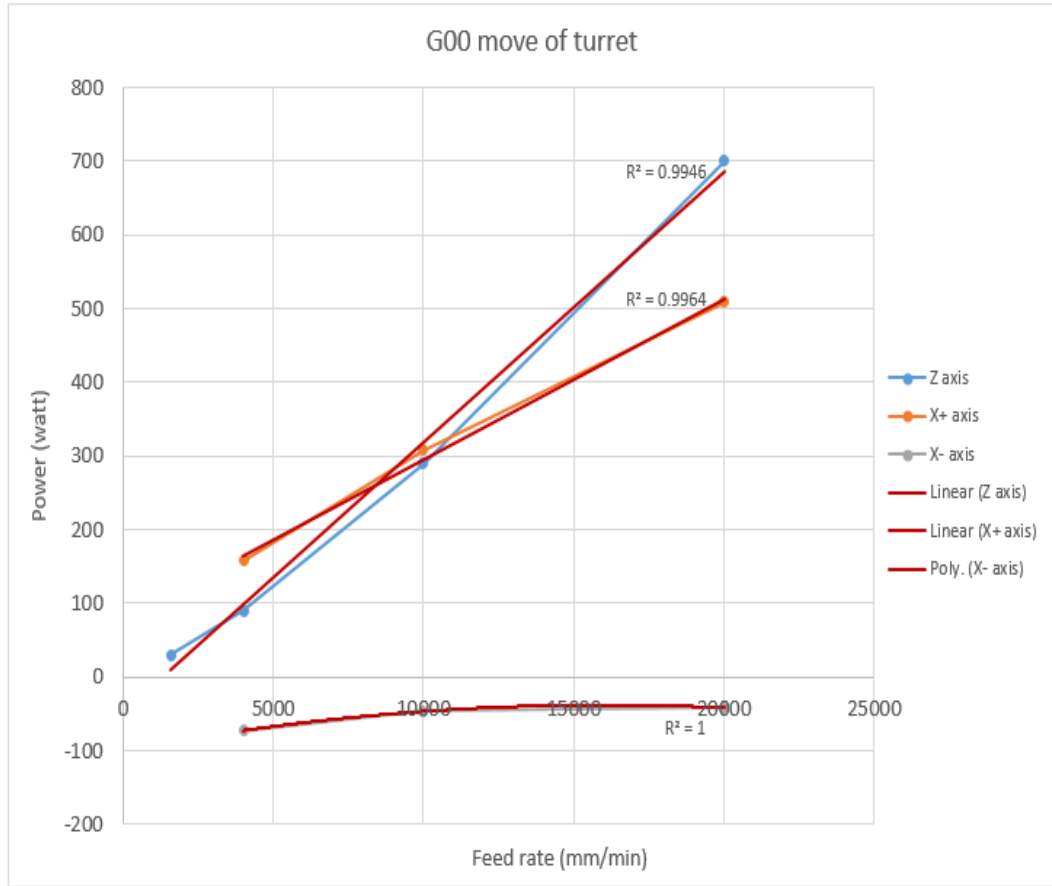


Figure 29 Trend lines of average power consumption-feed rate graph for turret (G00)

$$P_{Turret-G01} = \begin{cases} 5E - 06. f^2 + 0.0299f + 17.576 & X + Axis \\ 2E - 06. f^2 - 0.0128f - 9.2622 & X - Axis \\ 0.0152. f + 9.1929 & Z Axis \end{cases} \quad (45)$$

$$P_{Turret-G00} = \begin{cases} 0.0217. f + 78.07 & X + Axis \\ -2E - 07. f^2 + 0.0076. f - 99.236 & X - Axis \\ 0.0368. f - 50.272 & Z Axis \end{cases} \quad (46)$$

**4.4.5 Tool change**

In Mazak integrex i200-ST cutting tool changes automatically in both turret and milling head. For tool change in milling head there is a tool magazine at the left side of machine tool as shown in Figure 14 which has capacity to keep 36 cutting tools. For tool change all needed is to enter the number of the cutting tool in magazine so milling head get its position in 0 degree and approaches to tool magazine to take the requested cutting tool then goes back to its home position.

We have repeated the tool change for milling head 5 times in different speeds to obtain instantaneous power consumption which is shown in Figure 30.

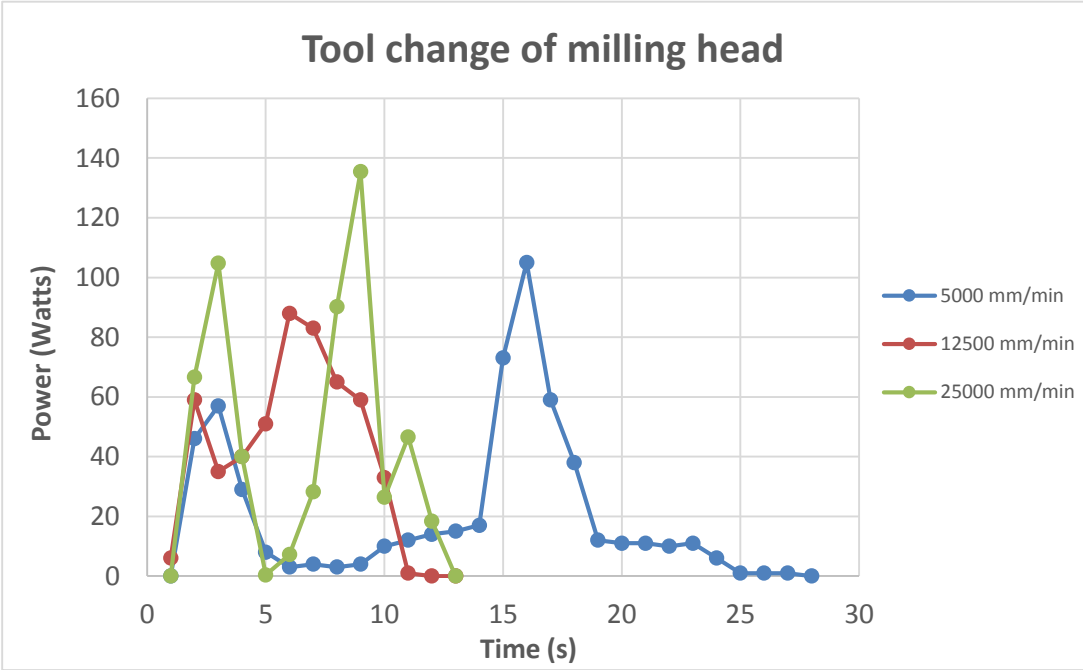


Figure 30 Average power consumption-time graph for tool change of milling head

The feed rate that is given for tool change could not be specified in MAZATROL or ISO programs and it could only be changed manually using the feed rate button on the controller. There are 3 feed rates that could be set for tool change. The process of tool change is same for all tools in milling head so the energy consumption is

constant for tool changes occurs on specific feed rates. Thus, the area under curve of power-time graph of tool change gives energy consumption of tool change for each feed rate which is given in Equation (47).

$$E_{TC-millinghead} = \begin{cases} 5610 \text{ Joules,} & f = 5000 \text{ mm/min} \\ 5330 \text{ Joules,} & f = 12500 \text{ mm/min} \\ 5642 \text{ Joules,} & f = 25000 \text{ mm/min} \end{cases} \quad (47)$$

Turret also has a rotational magazine where the cutting tool can be changed by rotating turret to reach the requested tool with a stop in each cutting tool. The rotational speed in turret is not adjustable. The instantaneous power consumed for rotating the turret magazine to the next tool is determined by changing the cutting tool of turret to the next tool in magazine and recording the instantaneous power value. Experiments are repeated 5 times and average power consumption-time graph is obtained and shown in Figure 31.

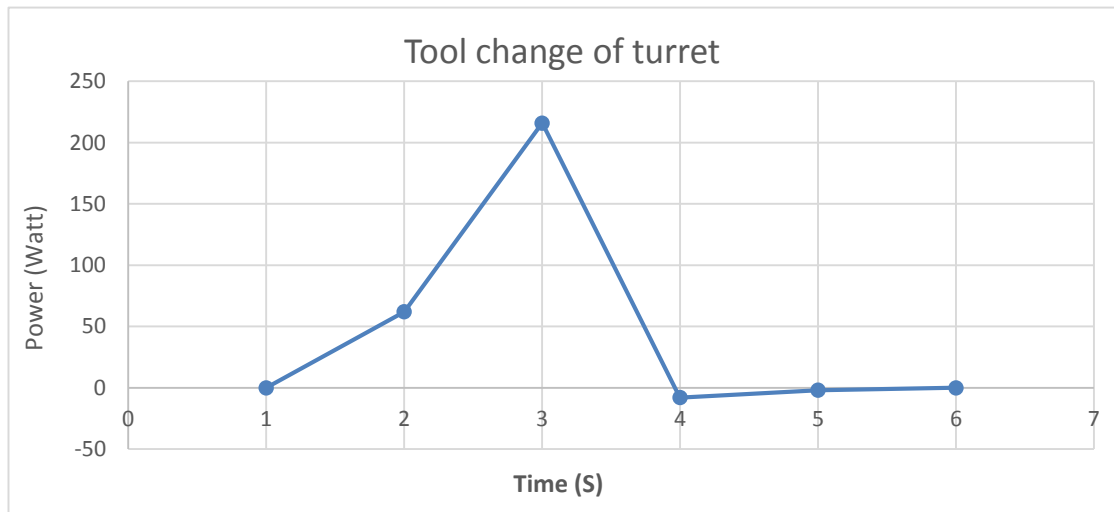


Figure 31 Average power consumption-time graph for tool change of turret

The area under the curve of power-time graph of turret tool change gives the energy consumption of tool change for one rotation which is about 268 joules. If more

rotations is needed to reach the requested cutting tool in turret, determined energy consumption should multiplied by number of rotations.

#### **4.4.6 Conveyor**

A conveyor exists on front side of the machine tool in order to remove chips from machining region; power consumption of conveyor is also measured by activating the conveyor and determining the instantaneous power consumption. As a result conveyor consumes about 160 watt every second when it is activated and this value remains constants during conveyor activation. Conveyor usually starts to work when program begins so the energy consumption of conveyor is calculated by multiplying power consumption of conveyor by its activation time or program's run time.

#### **4.4.7 Coolant**

Coolant systems pump liquids to cool and lubricate work pieces and cutting tools. A machine tool coolant system improves the performance of tools by delivering filtered coolants directly to the machining area at the proper temperature and pressure. The coolant system of Mazak integrex i200-ST turn-mill machine tool can pump liquids to different points of machine tool according to working auxiliary sub-units. There are 3 pumps for coolant system of the machine tool in order to activate different coolants which are turret coolant, milling head coolant, milling spindle-through coolant and shower coolant. One of the pumps is a 15-bar pump and the others are 5-bar pumps. All coolants are activated separately and power consumption of each coolant is obtained from the meter. The number of required pump for each coolant and the power consumptions of coolants are given in Table 5.

The power consumption amounts given in Table 5 are valid if mentioned coolants are activated separately. If two or more coolants works simultaneously these power consumption amounts would not be valid since one of the pumps will pump liquid for more than one coolant and one of the pumps works commonly the power consumption amounts will be different. Existing 5-bar pumps in the machine tool are different so the power consumption amount of them is also different. In Figure 32, 5-

bar pump1 and 5-bar pump2 names are given to the 5-bar pumps and it is specified that which pump is needed for which coolant.

Table 5 Pumps of coolant system of Mazak integrex i200-ST

	5-bar pump	15-bar pump	Power consumption (Watts)
Turret	2	0	920
Milling head	1	1	1920
Milling spindle-through	1	1	1840
Shower	1	0	700

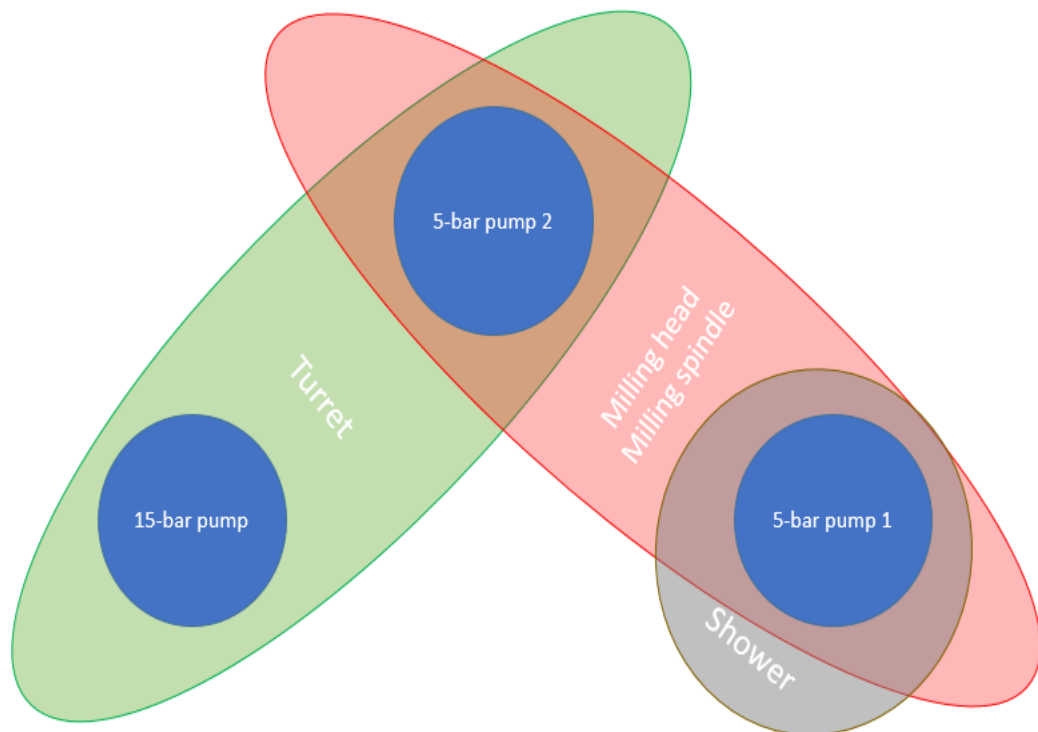


Figure 32 Pumps usage of coolant system of Mazak integrex i200-ST

For milling head and milling spindle-through and shower coolants there is a constant amount of energy consumption which is drawn by pump and also an amount of energy consumption which is dependent to activated coolant.

Table 6 Power consumption of coolant system

	5-bar pump1	5-bar pump2	15-bar pump	variable	Total
Turret	520	400	-	-	920
Milling head	-	400	1160	360	1920
Milling spindle- through	-	400	1160	280	1840
Shower	520	-	-	180	700

For example if turret coolant is activated the power consumption is 920 watts then if milling head is also activated at the same time, 5-bar pump2 is already running and only the 15-bar pump will be activated and also we have a 360 watts variable amount for milling head, so total power consumption amount will be:

$$P_{Total} = 920 + 1160 + 360 = 2440 \text{ watts}$$

Where 920W is the power consumption amount of turret coolant, 1160W is power consumption amount of 15-bar pump and 360W is the power consumption amount for milling head coolant.



#### **4.4.8 Chiller and lubrication unit**

Chiller of this turn-mill machine tool is located at the left side of the machine and it is responsible to keep the temperature of the machine tool at a constant degree. This temperature is specified by user. In Mazak integrex i200-ST this temperature is set to 25 degree. It means that when the temperature of the spindles increases over 25 degree the chiller unit starts to work and decrease the temperature of the spindles. There is also a timer that runs the chiller at certain time periods even when machine is idling which can be seen in idling instantaneous power consumption graph. The lubrication unit is responsible for lubricating the spindles and gears when it is needed.

As it is not possible to predict when the temperature of the spindles will increase over 25 degree or when lubrication is needed for lubricating the spindles or gears, so mathematical modeling or deriving an equation for Chiller and lubrication unit is not possible. The activation of these are realized by the sounds that this units makes while are working and also it is recognizable from power-time graph of the machine tool. According to obtained data from the meter during activation of chiller and lubrication unit, each of them consumes about 1KW power.

#### **4.5 Cutting energy**

In this section the cutting energy or tool tip energy of cutting processes is determined. In most of the previous studies specific cutting energy is used for modeling the cutting part of the energy prediction model. Specific cutting energy values are available for all work-piece materials, but it does not take the effect of cutting tool and cutting parameters such as cutting speed, depth of cut and feed rate into consideration, so it does not present a reliable and precise prediction. In this study, a methodology is presented to predict feature based cutting energy consumption with respect to cutting parameters. In order to validate this method, a number of features are selected based on STEP standard which are the most used turning and milling features and experiments were designed and performed for each feature to derive energy prediction equations with respect to cutting parameters.

As mentioned above, STEP features are utilized for modelling cutting energy consumption and metal-cutting power consumption in the model. The selected step features are shown in Figure 33.

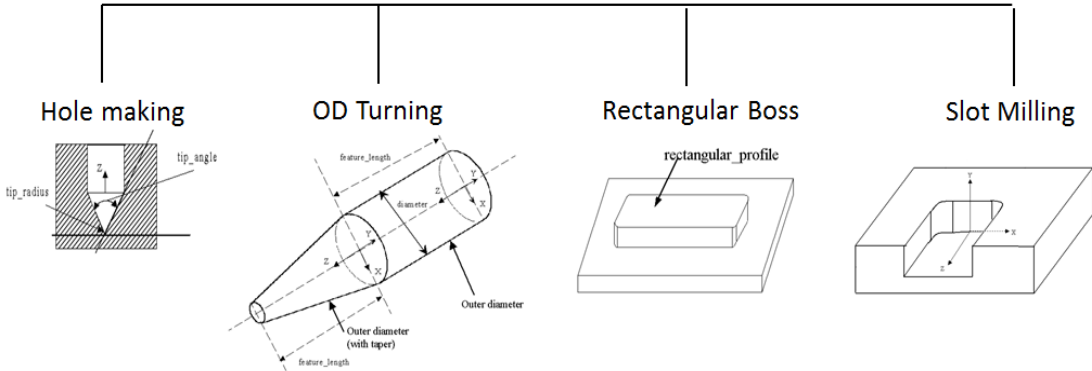


Figure 33 Selected STEP features

The workpiece used performed experiments is a 150mm length cylindrical workpiece with a diameter of 80 mm and the material is 304 stainless steel . The most widely used austenite steel of 300 Series is the 304, also known as 18/8 for its composition of 18% chromium and 8% nickel. The properties of 304 stainless steel is given in Table 7.

In this study, the cutting energy is modelled considering the effect of cutting parameters for each process separately. For this purpose, firstly the appropriate cutting parameters ( $a_p$ ,  $v$ ,  $f$ ) for cutting tool type and material is selected using tool catalogue of cutting tool manufacturer for each process.

Since too much experiments is required for examining all values of cutting parameters with all permutations to determine power consumption amount in various cutting parameter values, design of experiments (DOE) methods is utilized to perform a reasonable number of experiments.

Then, the correlation between cutting parameters and power consumption is obtained using the results of these experiments. Details of experiments of selected features is presented in the following sections.

Table 7 Properties of 304 stainless steel

Physical Properties		Component (Wt. %)	
Density	8 gr/cc	C	Max 0.08
Mechanical Properties		Cr	18 – 20
Hardness, Brinell	123	Fe	66.345 – 74
Hardness, Rockwell B	70	Mn	Max 2
Yield Stress	215 MPa	Ni	8 – 10.5
Modulus of Elasticity	193 – 200 GPa	P	Max 0.045
Poisson's Ratio	0.29	S	Max 0.03
Shear Modulus	86 GPa	Si	Max 1

#### 4.5.1 Outer Diameter turning (OD turning)

OD turning feature is one the most used features on cylindrical parts. In this section, the energy consumption of OD turning on 304 stainless steel is modelled. For performing experiments on mentioned workpiece material SECO tools selected. The grade of stainless steel in SECO tool catalogues is M and 304 type of stainless steel is M2. WNMG080408-M3, TP 2500 insert of SECO tools is selected for turning process. Medium rough and rough machining of steels is the main application area of this insert, also medium rough and rough machining of stainless steels are the

alternative application areas of the selected insert. The appropriate interval of cutting parameters for cutting 304 stainless steel using mentioned insert is given in Equation (44) where  $a_p$  is depth of cut,  $f_n$  is feed rate and  $v_c$  is cutting speed.

$$0.5 \text{ mm} < a_p < 4.0 \text{ mm}$$

$$\mathbf{0.15 \text{ mm/r} < f_n < 0.60 \text{ mm/r}} \quad (6)$$

$$325 \text{ m/min} < v_c < 435 \text{ m/min}$$

These 3 parameters are selected as cutting parameters for OD turning and 3 levels are chosen for each parameter for design of experiments as shown in Table 8.

Table 8 Levels of cutting parameters for design of experiments for OD turning

Exp.	$a_p$ (mm)	$f_n$ (mm/r)	$v_c$ (m/min)
Level 1	0.5	0.15	325
Level 2	2.25	0.4	380
Level 3	4	0.6	435

For design of experiments Taguchi's L9 orthogonal array is used which designs 9 experiments based on specified parameters levels. These 9 experiments carried out using coolant in different cutting parameters based on L9 orthogonal array which are shown in Table 9.

Since the selected interval was alternative application areas for stainless steels, at high cutting parameters, especially at experiment 9, the insert was abraded. So another L9 orthogonal array was designed by changing levels of the cutting parameters which is shown in Table 10.

Table 9 Taguchi's L9 orthogonal array for OD turning

Exp.	$a_p$ (mm)	$f_n$ (mm/r)	$v_c$ (m/min)
1	0.5	0.15	325
2	0.5	0.4	380
3	0.5	0.6	435
4	2.25	0.15	380
5	2.25	0.4	435
6	2.25	0.6	325
7	4	0.15	435
8	4	0.4	325
9	4	0.6	380

Table 10 Modified Levels of cutting parameters for design of experiments

Exp.	$a_p$ (mm)	$f_n$ (mm/r)	$v_c$ (m/min)
Level 1	0.5	0.15	325
Level 2	1	0.3	350
Level 3	2	0.45	375

The experiments were carried out again according to new array and the power consumption amounts were obtained from energy meters. As mentioned before, the energy meter sampling time is 1 second, so the length of each cut was selected according to feed rate in order to have a minimum of 5 second cut to get a minimum of 5 power consumption data. During the cutting process, in addition to idle power consumption the power consumption of active auxiliary subunits are calculated to

determine the power consumption of cutting process. The active auxiliary subunits during cutting process are spindle which rotated the workpiece, milling head and M8 coolant. Subtracting the auxiliary subunits and the idle power consumption values from the overall power consumption obtained from the meter during cutting gives the power consumption of cutting process which is calculated for each experiment and given in Table 11.

Table 11 Power consumption values of designed OD turning experiments

Exp.	$a_p$ (mm)	$f_n$ (mm/r)	$v_c$ (m/min)	P (Watt)
1	0.5	0.15	325	990
2	0.5	0.3	350	3160
3	0.5	0.45	375	4355
4	1	0.15	350	2800
5	1	0.3	375	4970
6	1	0.45	325	7180
7	2	0.15	375	6940
8	2	0.3	325	8555
9	2	0.45	350	17375

Analysis of obtained data is accomplished using MINITAB software. The regression equation which is shown in Equation (49) is obtained using response surface methodology.

$$P_{turning} = -1910 + 6167a_p + 209142 f - 270.8v + 5297a^2 + 90353 f^2 + 0.9827v^2 + 38589 a_p \cdot f - 79.03 a_p \cdot v - 835.9 f \cdot v \quad (7)$$

This equation gives the instantaneous power consumption for cutting process of 304 stainless steel in Mazak integrex i200-ST in various cutting parameters. Multiplying this value with cutting time will give the energy consumption of this cutting process as given in Equation (50) where  $P_{turning}$  is the power consumed for OD turning feature and  $t_9$  is the cutting time of OD turning.

$$E_{turning} = \int_0^{t_9} P_{turning} dt \quad (50)$$

#### 4.5.2 Slot milling

Slot milling is a milling feature which applicable in Mazak integrex i200-ST turn-mill machine tool. Cutting energy consumption of slot milling is determined in this section considering cutting parameters which are selected using tool catalogue of cutting tool manufacturer.

Appropriate cutting tool for machining the same workpiece material is selected for slot milling operation. JS5130803o-nxt tool of SECO tools is chosen to carry out experiments which is suitable to cut materials of grade M2 (304 stainless steel). The appropriate interval of cutting parameters for cutting 304 stainless steel using mentioned cutting tool is obtained from cutting tool catalogue and laboratory experiments which is given in Equation (51) where  $a_p$  is depth of cut,  $f_n$  is feed rate and  $v_c$  is cutting speed.

$$a_p \leq 4.0 \text{ mm}$$

$$0.05 \text{ mm/r} < f_n < 0.07 \text{ mm/r} \quad (51)$$

$$70 \text{ m/min} < v_c < 90 \text{ m/min}$$

Same as turning process for slot milling also these 3 parameters are selected as cutting parameters and 3 levels are chosen for each parameter for design of experiments as shown in Table 12. 9 experiment are designed using Taguchi's L9 orthogonal array with selected levels of cutting parameters which is shown in Table 13.

Table 12 Levels of cutting parameters for design of experiments for slot milling

Exp.	$a_p$ (mm)	$f_n$ (mm/r)	$v_c$ (m/min)
Level 1	1	0.05	70
Level 2	2.5	0.06	80
Level 3	4	0.07	90

Table 13 Taguchi's L9 orthogonal array for slot milling

Exp.	$a_p$ (mm)	$f_n$ (mm/r)	$v_c$ (m/min)
1	1	0.05	70
2	1	0.06	80
3	1	0.07	90
4	2.5	0.05	80
5	2.5	0.06	90
6	2.5	0.07	70
7	4	0.05	90
8	4	0.06	70
9	4	0.07	80

All the experiments are performed using coolant and the power consumption amounts were obtained from the energy meter. Since the selected feed rates of slot milling are lower comparing with turning experiments, sufficient data of power



consumption is obtained from energy meters even in shorter lengths of cutting, so reliable power consumption amounts are collected.

During the cutting process in addition to the idle power consumption, the power consumption of active auxiliary subunits are calculated to determine the power consumption of cutting process. The active auxiliary subunits during cutting process are spindle of milling head which rotates the cutting tool, milling head and M8 coolant. Subtracting the auxiliary subunits and the idle power consumption values from the overall power consumption obtained from meter during cutting gives the power consumption of cutting process which is calculated for each experiment and given in Table 14.

Table 14 Power consumption values of designed slot milling experiments

Exp.	$a_p$ (mm)	$f_n$ (mm/r)	$v_c$ (m/min)	P (Watt)
1	1	0.05	70	1975
2	1	0.06	80	1925
3	1	0.07	90	2010
4	2.5	0.05	80	1045
5	2.5	0.06	90	1180
6	2.5	0.07	70	1115
7	4	0.05	90	2330
8	4	0.06	70	1175
9	4	0.07	80	2415

Analysis of obtained data is accomplished using MINITAB software. The regression equation which is given in Equation (52) is obtained using response surface methodology.

$$P_{Slot-milling} = 4226 - 4245 a_p - 233752 f + 177.1 v + 472.3 a^2 + 40026000 f^2 + \quad (52)$$

$$0.7343 v^2 + 31680 a_p \cdot f - 1.902 a_p \cdot v - 4085 f \cdot v$$

This equation gives the instantaneous power consumption for cutting process of 304 stainless steel in Mazak integrex i200-ST in various cutting parameters. Multiplying this value with cutting time will give the energy consumption of this cutting process as given in Equation (53) where  $P_{Slot-milling}$  is the power consumption for slot milling feature and  $t_{10}$  is the cutting time of slot milling.

$$E_{Slot-milling} = \int_0^{t_{10}} P_{Slot-milling} dt \quad (53)$$

#### 4.5.3 Hole making

Hole making feature is performed on Mazak integrex i200-ST using the milling head of the machine tool in 0 degree. Cutting energy consumption of hole making is determined in this section using cutting parameters which are selected using tool catalogue of cutting tool manufacturer. SD205A-7.5-40-8R1 tool of SECO tools is selected for drilling materials of grade M2 (304 stainless steel). The appropriate interval of cutting parameters for cutting 304 stainless steel using mentioned cutting tool is obtained from cutting tool catalogue and laboratory experiments which is given in Equation (54) where  $a_p$  is depth of cut,  $f_n$  is feed speed and  $v_c$  is cutting speed.

$$a_p \leq 30 \text{ mm}$$

$$0.17 \text{ mm/r} < f_n < 0.21 \text{ mm/r} \quad (54)$$

$$80 \text{ m/min} < v_c < 100 \text{ m/min}$$

For hole making also these 3 parameters are selected as cutting parameters and 3 levels are chosen for each parameter for design of experiments as shown in Table 15. 9 experiments are designed using Taguchi's L9 orthogonal array with selected levels of cutting parameters which is shown in Table 16.

Table 15 Levels of cutting parameters for design of experiments for hole making

Exp.	$a_p$ (mm)	$f_n$ (mm/r)	$v_c$ (m/min)
Level 1	15	0.17	80
Level 2	20	0.19	90
Level 3	30	0.21	100

Table 16 Taguchi's L9 orthogonal array for hole making

Exp.	$a_p$ (mm)	$f_n$ (mm/r)	$v_c$ (m/min)
1	15	0.17	80
2	15	0.19	90
3	15	0.21	100
4	20	0.17	90
5	20	0.19	100
6	20	0.21	80
7	30	0.17	100
8	30	0.19	80
9	30	0.21	90

All the experiments are performed using coolant and the power consumption amounts were obtained from energy meters.

During the cutting process in addition to the idle power consumption the power consumption of active auxiliary subunits are calculated to determine the power consumption of cutting process. The active auxiliary subunits during cutting process are spindle of milling head which rotates the cutting tool, milling head and M8 coolant. Subtracting the auxiliary subunits and the idle power consumption values from the overall power consumption obtained from meter during cutting gives the power consumption of cutting process which is calculated for each experiment and given in Table 17.

Table 17 Power consumption values of designed hole making experiments

Exp.	$a_p$ (mm)	$f_n$ (mm/r)	$v_c$ (m/min)	P (Watts)
1	15	0.17	80	1290
2	15	0.19	90	2340
3	15	0.21	100	2150
4	20	0.17	90	1620
5	20	0.19	100	2970
6	20	0.21	80	2280
7	30	0.17	100	2980
8	30	0.19	80	3040
9	30	0.21	90	5110

Analysis of obtained data is accomplished using MINITAB software. Regression equation which is shown in Equation (55) is obtained using response surface methodology.

$$P_{Hole-making} = -330412 + 29692 a_p - 4884333f + 10753v - 664.7a^2 \quad (55)$$

$$- 63175000 f^2 - 255.5v^2 + 253383 a_p \cdot f - 494 a_p \cdot v + 251000 f \cdot v$$

This equation gives the instantaneous power consumption for cutting process of 304 stainless steel in Mazak integrex i200-ST in various cutting parameters. Multiplying this value with cutting time will give the energy consumption of this cutting process as shown in Equation (56) where  $P_{Hole-making}$  is the power consumption for hole making feature and  $t_{11}$  is the cutting time of hole making.

$$E_{Hole-making} = \int_0^{t_{11}} P_{Hole-making} dt \quad (56)$$

#### 4.5.4 Boss rectangular milling

Boss rectangular milling is also a milling feature which is applicable in Mazak integrex i200-ST turn-mill machine tool. Cutting energy consumption of boss rectangular milling is determined in this section considering cutting parameters which are selected using tool catalogue of cutting tool manufacturer.

Appropriate cutting tool for machining the same workpiece material is selected for slot milling operation. JS5130803o-nxt tool of SECO tools is chosen to carry out experiments which is suitable to cut materials of grade M2 (304 stainless steel). This tool is the same tool which is used for slot milling. For boss rectangular milling in addition to axial depth of cut radial depth of cut should also be taken into consideration. The schematic of axial depth of cut and radial depth of cut is clearly shown in Figure 34.

The appropriate interval of cutting parameters for cutting 304 stainless steel using mentioned cutting tool is obtained from cutting tool catalogue and laboratory experiments which is given in Equation (57) where  $a_p$  is depth of cut,  $f_n$  is feed rate,  $v_c$  is cutting speed and  $a_e$  is radial depth of cut.

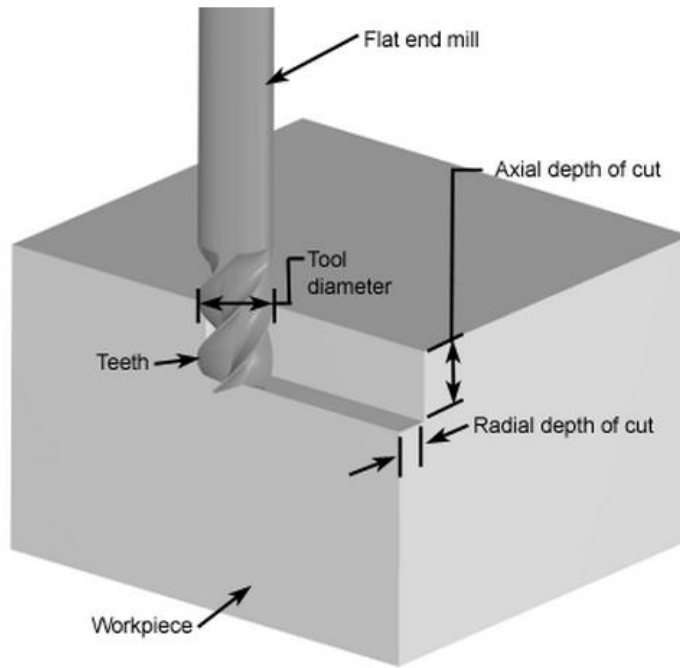


Figure 34 Schematic of axial depth of cut and radial depth

$$a_p \leq 5.0 \text{ mm}$$

$$0.05 \text{ mm/r} < f_n < 0.09 \text{ mm/r} \quad (57)$$

$$70 \text{ m/min} < v_c < 90 \text{ m/min}$$

$$1.0 \text{ mm} \leq a_e \leq 3.0 \text{ mm}$$

Unlike the previous feature for boss rectangular milling 4 parameters are selected as cutting parameters and 3 levels are chosen for each parameter for design of experiments as shown in Table 18. 9 experiment are designed using Taguchi's L9 orthogonal array with selected levels of cutting parameters which is shown in Table 19.

Table 18 Levels of cutting parameters for design of experiments for slot milling

	$a_p$ (mm)	$f_n$ (mm/r)	$v_c$ (m/min)	$a_e$ (mm)
Level 1	1	0.05	70	1
Level 2	3	0.07	80	2
Level 3	5	0.09	90	3

Table 19 Taguchi's L9 orthogonal array for slot milling

Exp.	$a_p$ (mm)	$f_n$ (mm/r)	$v_c$ (m/min)	$a_e$ (mm)
1	1	0.05	70	1
2	1	0.07	80	2
3	1	0.09	90	3
4	3	0.05	80	3
5	3	0.07	90	1
6	3	0.09	70	2
7	5	0.05	90	2
8	5	0.07	70	3
9	5	0.09	80	1

Coolant was not activated for performing these experiments. Power consumption amounts were obtained from energy meters. The power consumption of active auxiliary subunits and idle power consumption are calculated to determine the power consumption of cutting process. The active auxiliary subunits during cutting process are spindle of milling head which rotates the cutting tool, milling head. Subtracting auxiliary subunits and idle power consumption values from the overall power

consumption obtained from meter during cutting gives the power consumption of cutting process which is calculated for each experiment and shown in Table 20.

Table 20 Power consumption values of designed slot milling experiments

Exp.	$a_p$ (mm)	$f_n$ (mm/r)	$v_c$ (m/min)	$a_e$ (mm)	P (watts)
1	1	0.05	70	1	10
2	1	0.07	80	2	30
3	1	0.09	90	3	70
4	3	0.05	80	3	130
5	3	0.07	90	1	55
6	3	0.09	70	2	100
7	5	0.05	90	2	150
8	5	0.07	70	3	185
9	5	0.09	80	1	100

Analysis of obtained data is accomplished using MINITAB software. Regression equation which is given in Equation (58) is obtained using response surface methodology.

$$P_{Boss-rectangular-milling} = 530.2 + 33.33a_p - 1333 f - 13.67v + 43.33a_e - 1.042 a_p^2 + 8333 f^2 + 0.08333 v^2 - 1.667 a_e^2 \quad (58)$$

This equation gives the instantaneous power consumption for cutting process of 304 stainless steel in Mazak integrex i200-ST in various cutting parameters. Multiplying this value with cutting time will give the energy consumption of this cutting process



as shown in Equation (59) where  $P_{Hole-making}$  is the power consumption for hole making feature and  $t_{12}$  is the cutting time of boss rectangular milling.

$$E_{boss-rectangular-milling} = \int P_{boss-rectangular-milling} dt \quad (59)$$



## CHAPTER 5

### FIRST CASE STUDY; VERIFICATION OF TURN-MILL

#### ENERGY MODEL

In this section a mechanical part is designed and machined in order to verify the presented energy consumption model and obtain the accuracy of the prediction of the model. Selected STEP features are included in the part. Catia V5 is used to create part model which is shown in Figure 35.

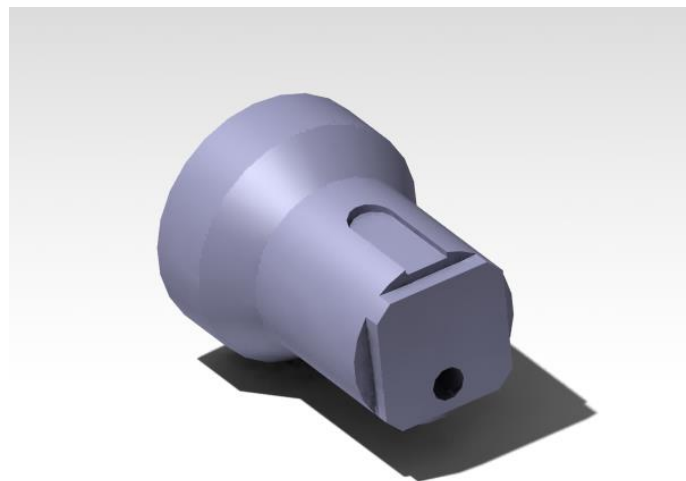


Figure 35 Part model of case study

As seen in the figure, the designed part contains OD turning, slot milling, hole making and boss rectangular features which were selected from STEP standard. This part is machined in Mazak integrex i200-ST turn-mill machine tool using the same tools which were used in Taguchi experiments of features.

Entire machining process of this part is programmed in MAZATROL programming system of Mazak machine tool and all feed rates are specified in the program which is given in Appendix C. The cutting parameters of machining features are selected different from the selected data points or levels in Taguchi's L9 orthogonal arrays in previous section in order to verify derived equations for cutting processes. The power consumption of whole process is obtained from energy meters. Figure 36 demonstrates the power consumption values during the manufacturing process of the part. Coolant was not used during cutting operation in order to determine and follow the movement of feed axis, tool change and cutting features.

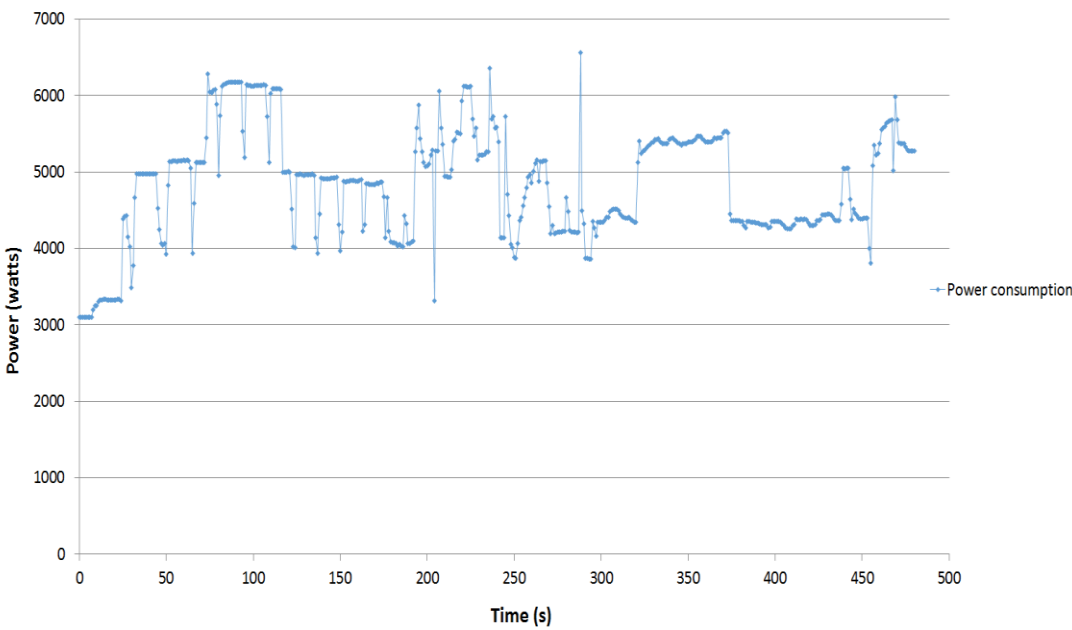


Figure 36 Power consumption during cutting operation of case study part

The sequence of processes are as following: OD turning, hole making, boss rectangular and slot milling at the end where the power consumption of each feature is shown separately in Figure 37.

The power consumptions of all sub-units and cutting processes are calculated using derived equations for sub-units and cutting feature with respect to cutting parameters used for machining of case study part. So, the average power consumption for whole

process is obtained. Activation time of each sub-unit or cutting processes is also determined and verified during cutting operation.

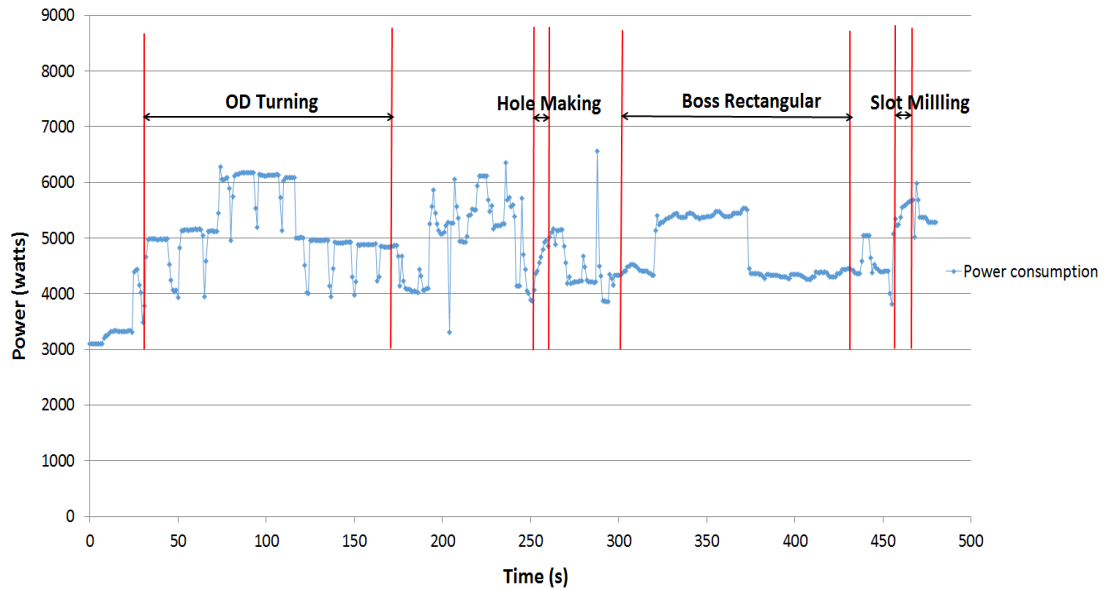


Figure 37 Power consumption and sequence of cutting features of case study part

An estimation graph for estimating power consumption of the operation is achieved. The estimated power consumption graph and the real power consumption data obtained from the energy meter is shown in Figure 38.

As mentioned above all data points are obtained from derived power equations. The time of activation of chiller unit and lubrication unit is obtained during cutting process and the power consumption amounts of these sub-units are added to the graph during the time of activation.

Overall accuracy of the prediction model comparing with real power consumption values obtained from the meter is about 95%. More detailed analysis for power consumption of cutting features is performed for each feature separately in following sections.

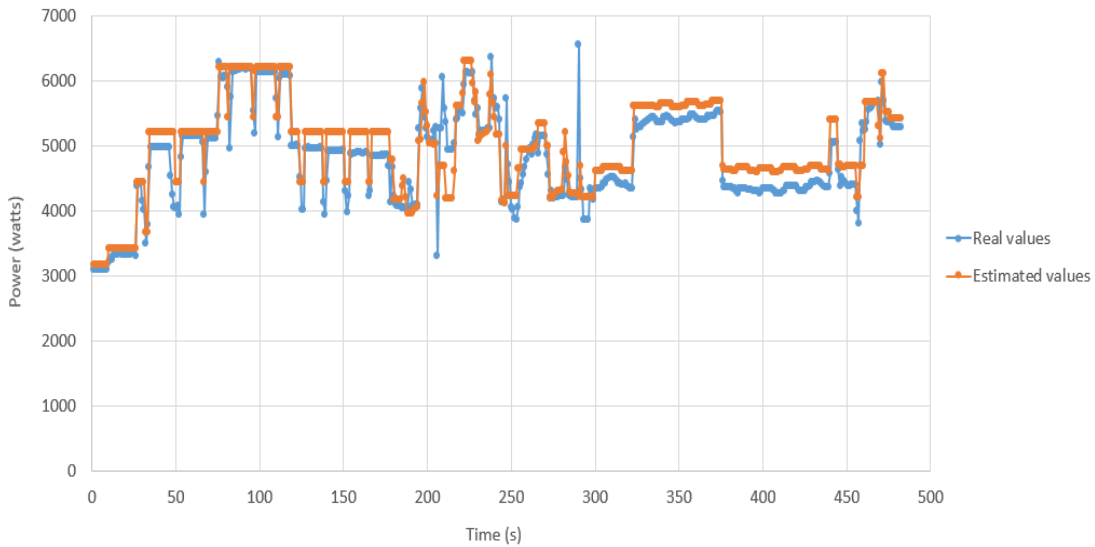


Figure 38. Estimated and real power consumption during cutting operation of case study part

### 5.1 Turning

First cutting operation performed on case study part is OD turning with a taper. OD turning is operated using milling head in 90 degree position. Figure 38 is the tool path of written program in MAZATROL for turning the case study part. Tapers are machined by decreasing the length of the cutting of normal OD turning in each pass in MAZATROL programming as shown in Figure 39.

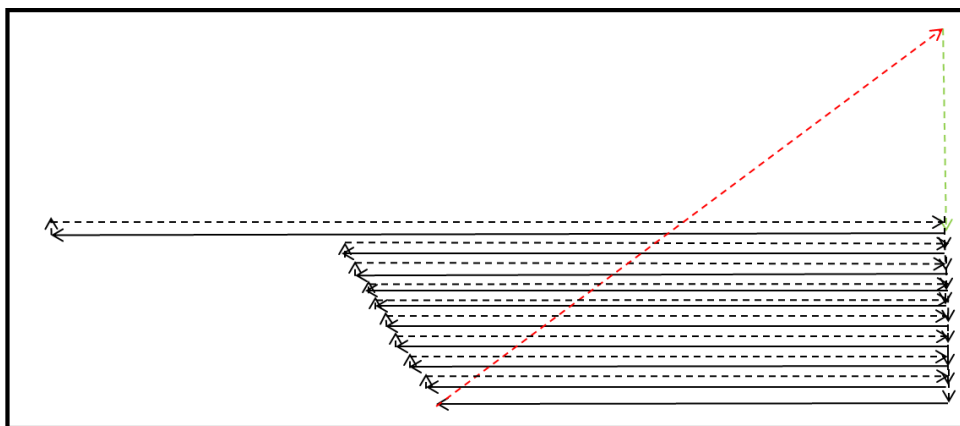


Figure 39 Tool path of OD turning of case study part

There are 10 passes where depth of cut for each pass is 0.75 mm with different lengths of cut. The solid lines in the figure demonstrate the tool path during cutting operation and dashes show the movement of tool on feed axis for positioning in order to start cutting operation of the next pass. The green dash shows the cutting tool approach to start the cutting and red dash shows the tool moving away from cutting region when turning operation is finished. Figure 40 shows the power consumed during turning operation. The cutting passes are also specified in the figure. The power consumed during 2 passes is the power consumption of feed axis for positioning. As shown in the figure, a chiller is activated at 41<sup>st</sup> second for about 45 seconds and consumed about 1KW power.

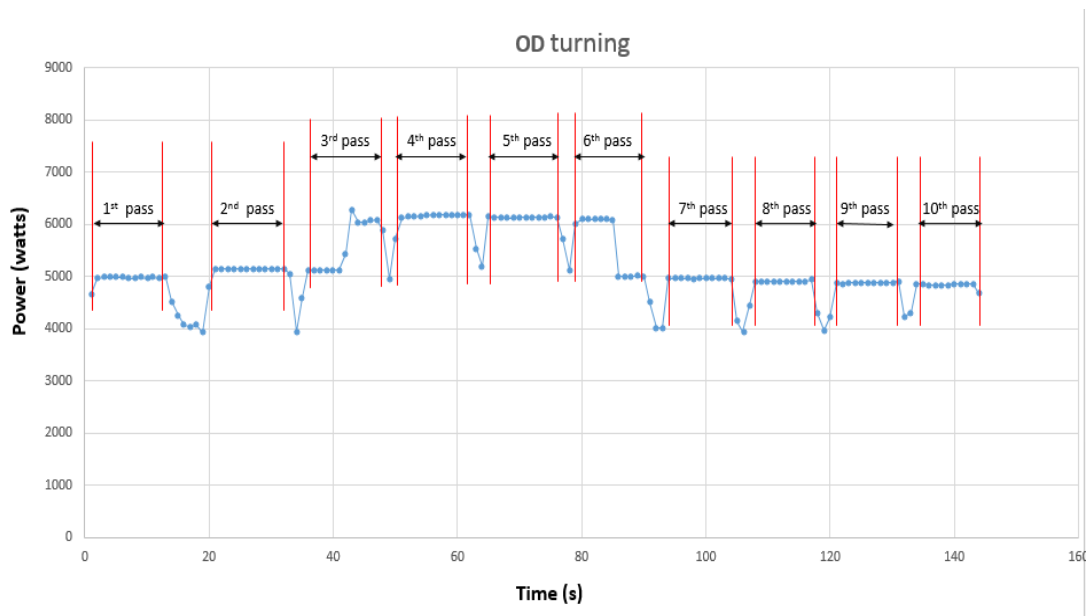


Figure 40. Power-time graph for OD turning

The real energy consumption amount is determined by calculating the area under the power-time graph for turning operation. After subtracting the energy consumption of sub-units, it is obtained that this OD turning operation consumes 124.162 KJ. Entering the cutting parameters used for this cutting in the derived equation for OD turning and considering the machining time the estimated energy consumption

amount is 137.567 KJ. It means that the accuracy of power consumption model for OD turning is about 89.1%.

### 5.2 Hole making

After OD turning operation the next feature is hole making. The diameter of the hole is the same with the diameter of the tool which is 7.5mm and the hole length is 15mm. prior to hole making operation a center drill operation is performed. This operation was performed before and the power consumed during center drilling was obtained. In this center drill operation the same cutting parameters and power consumption is used. In Figure 41 center drilling and hole making power consumption is specified in power-time graph of case study part. The power consumed between center drilling and hole making operations is for tool change and positioning.

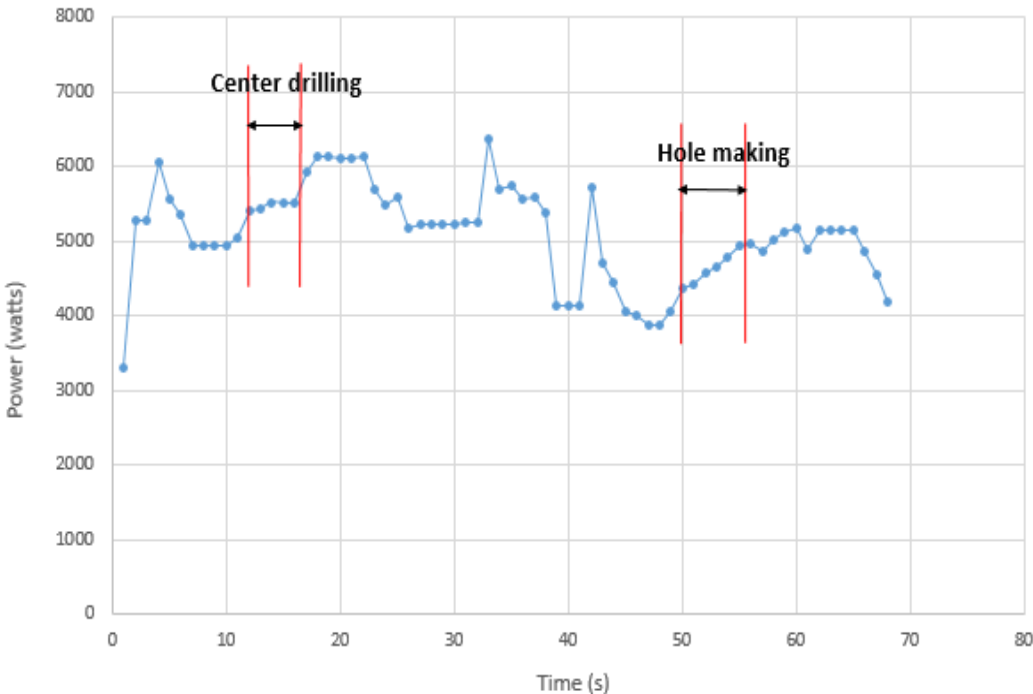


Figure 41 Power-time graph for center drilling and



Center drilling and hole making features were also performed using milling head in 0 degree. The real energy consumption amount is determined by calculating the area under the power-time graph for hole making operation. After subtracting the energy consumption of sub-units, it is obtained that hole making operation consumes 1.690 KJ. Entering the cutting parameters used for this cutting in the derived equation for hole making and considering the machining time, the estimated energy consumption amount is 1.567 KJ. So the accuracy of power consumption model for hole making is 92%.

### 5.3 Boss rectangular

Boss rectangular feature is performed prior to slot milling. For this operation milling head is used in 0 degree. Figure 42 demonstrated the tool path which will be applied on face of the workpiece. Solid lines in the figure demonstrates the tool path during machining operation and dashes shows the movement of tool on feed axis for positioning in order to start machining operation. The green dash shows the cutting tool approach to start the cutting and red dash shows the tool moving away from cutting region when turning operation is finished.

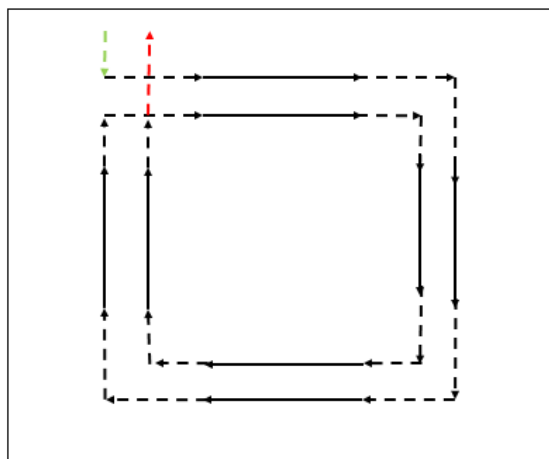


Figure 42 Tool path of boss rectangular milling of case study part

The real energy consumption amount is determined by calculating the area under the power-time graph for slot milling operation. After subtracting the energy consumption of sub-units it is obtained that slot milling operation consumes 4.187 KJ. Entering the cutting parameters used for this cutting in the derived equation for boss rectangular milling and considering the machining time, the estimated energy consumption amount is 3.690 KJ and consequently an accuracy about 88.1% is obtained for power consumption model of boss rectangular milling.

**5.4 Slot milling**

Final cutting feature is slot milling which applied simply using milling head in 90 degree. The real energy consumption amount for slot milling is also determined by calculating the area under the power-time graph for slot milling operation. Subtracting the energy consumption of sub-units the slot milling operation energy consumption is obtained which is about 7.602 KJ. Entering the cutting parameters used for this cutting in the derived equation for slot milling and considering the machining time, the estimated energy consumption amount is 8.340 KJ, so the accuracy of power consumption model for OD turning is 90.2%. The real energy consumption of cutting features and estimated energy consumption for features are shown and compared in Figure 43.

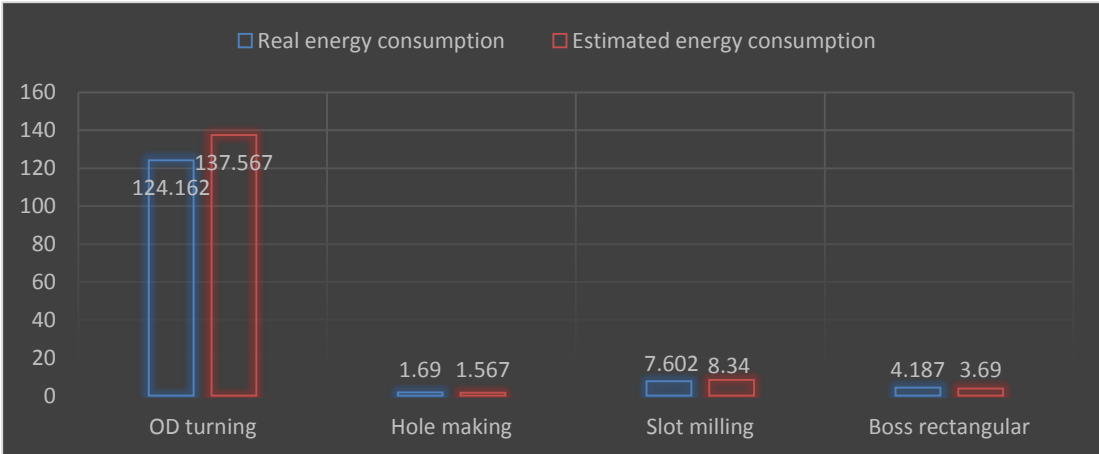


Figure 43 Real energy consumption and estimated energy consumption for cutting features

## CHAPTER 6

### SECOND CASE STUDY; INVESTIGATION OF THE ENERGY

#### CONSUMPTION OF TURN-MILLING PROCESSES

Turn-milling is not particularly demanding of the machine tool, but at minimum the process does require Y-axis motion. The workpiece rotation provides the C-axis motion that delivers the desired feed rate for the milling cutter. For turn-milling processes rotation speed of workpiece is much lower than the typical rotation speed in turning process. Y-axis motion is needed because the milling cutter has to do most of its cutting off-center. When the tool centerline intersects with the axis of rotation of the part then the tool would be cutting on the center of its face and not on its edges. To ensure that the cutting edges cut properly, the tool centerline should be offset from the work's axis of rotation by 1/4 of the cutter diameter. The mechanism of both orthogonal and co-axial turn-milling process is shown in Figure 44.

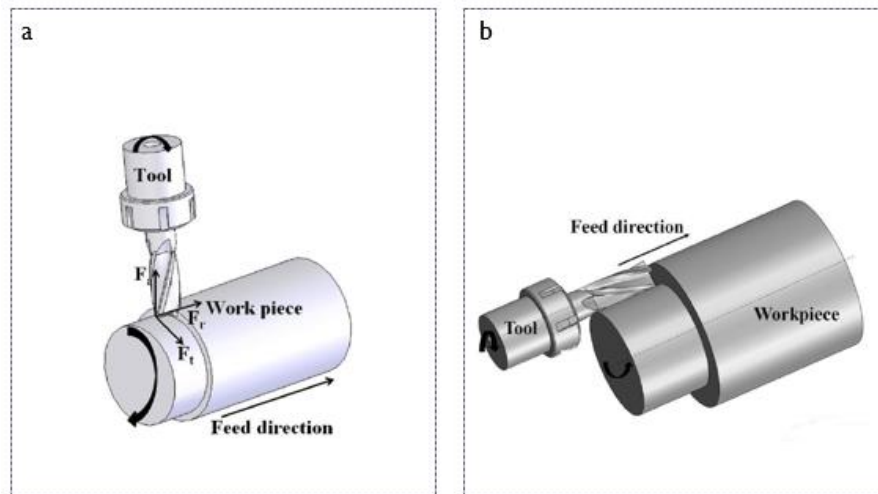


Figure 44 a) orthogonal turn-milling b) co-axial turn-milling

Here are some of the specific challenges that turn-milling can address:

- Milling cutting tools tend to do better than turning tool in interrupted cuts so using turn-milling process for interrupted cuts works better than turning.
- Turn milling process tend to be more efficient when a high amount of material is to be removed.
- Turn-milling can offer increased productivity for difficult-to-machine materials such as high temperature alloys as well as parts with large diameters which cannot be rotated at high speeds.
- In a hard-to-machine metal, a single turning insert might not be able to deliver enough tool life to last to the end of the cut where a milling tool can cut longer, since it has multiple inserts to divide the load. By enduring the complete cut, the milling tool can eliminate the risks involved with changing tools in mid-operation.

In this section turn-milling processes are performed in order to analyze the effect of cutting feature on power and energy consumption of the process. Power requirement and energy consumption of turn-milling processes are compared with conventional turning process in the same cutting condition to investigate the performance of turn-milling processes. Experiments are performed on Mazak integrex i200-ST and entire turn-milling process is programmed with ISO programming (G code) which is given in Appendix E where the conventional turning process is programmed in MAZATROL. Workpiece material is 304 stainless steel for both processes and cutting tool is a milling cutter with 3 inserts for turn-milling process. Power requirement of whole process is obtained using energy meter. Three set of experiments have been performed, in each set one cutting parameter is varying and others are constant during the process. So the effect of varying cutting parameter on power requirement and energy consumption is determined. The effect of rotational speed of cutting tool ( $N$ ), feed speed ( $f_z$ ) and depth of cut ( $a_p$ ) is analyzed and shown in Figure 45, Figure 46 and Figure 47 for both turn-milling process and conventional turning process. The rotational speed of workpiece is set to 20 rpm in all experiments.

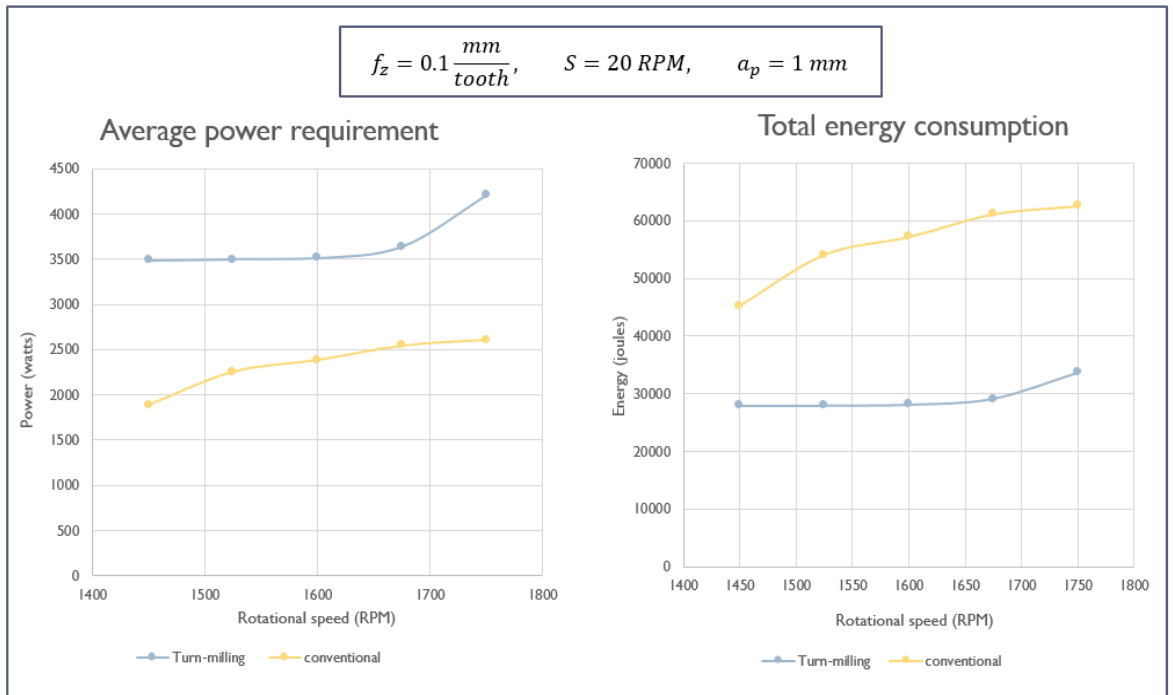


Figure 45 Effect of rotational speed on power requirement and energy consumption of turn-milling processes

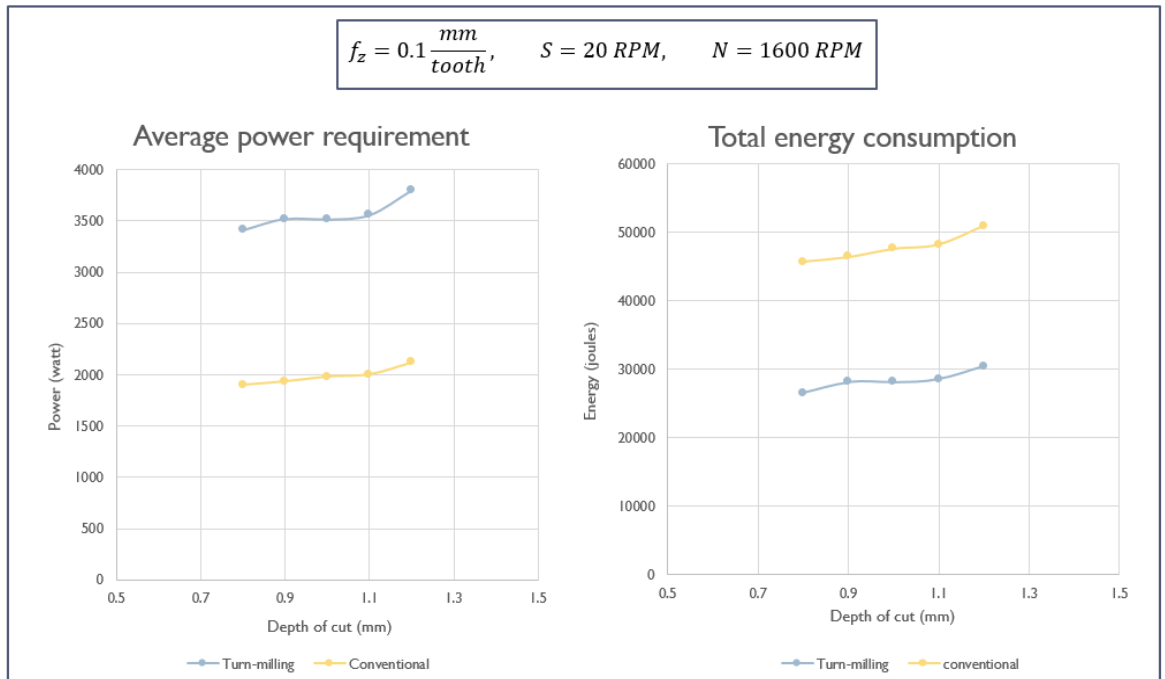


Figure 46 Effect of depth of cut on power requirement and energy consumption of turn-milling processes

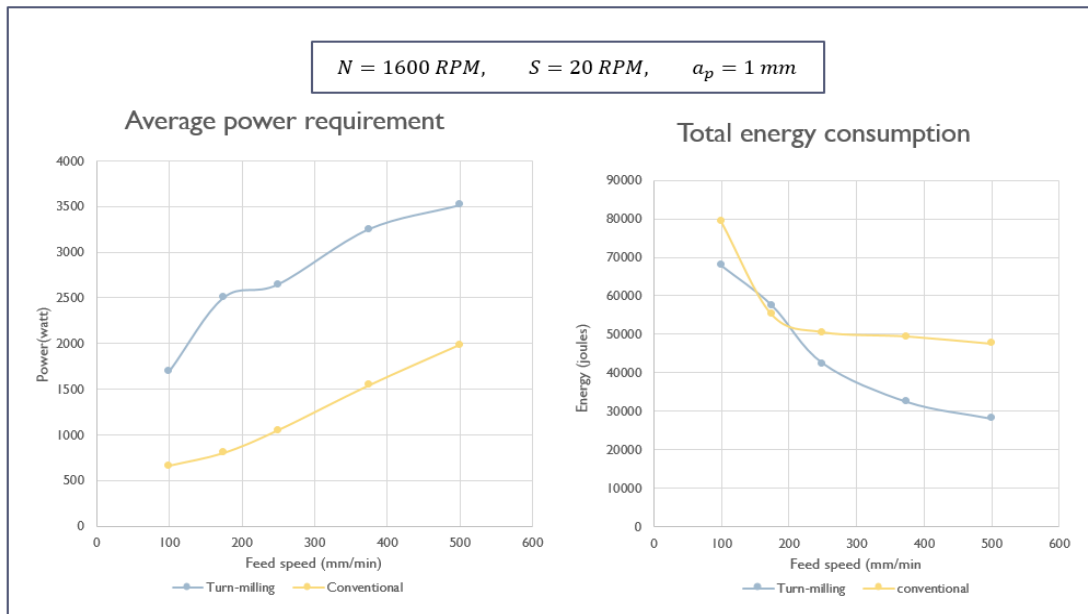


Figure 47 Effect of depth of cut on power requirement and energy consumption of turn-milling processes

As the rotational speed and depth of cut increases the power requirement and energy consumption also increases for both of processes. With increasing feed speed the power requirement increases. But as the cutting time decreases as feed speed increase, the energy consumption amount is much lower for high feed speeds.

Analyzing the turn-milling and conventional turning operations separately, power requirement of turn-milling operations is more than conventional turning operations. But as the cutting tool of turn-milling processes have 3 inserts, feed speed (mm/tooth) of milling cutting tool is 3 times more than the cutting tool of conventional turning. So the time required for conventional turning process to perform a cutting operation is 3 times more than the time required for turn-milling process and it results in less energy consumption amounts in turn-milling processes.

The effect of cutting parameters on power consumption of turn-milling processes is visible in Figure 48 which are 3D surface plots obtained using response surface methodology. Pictures of turn-milled parts are shown in Figure 49 in different feed speeds.

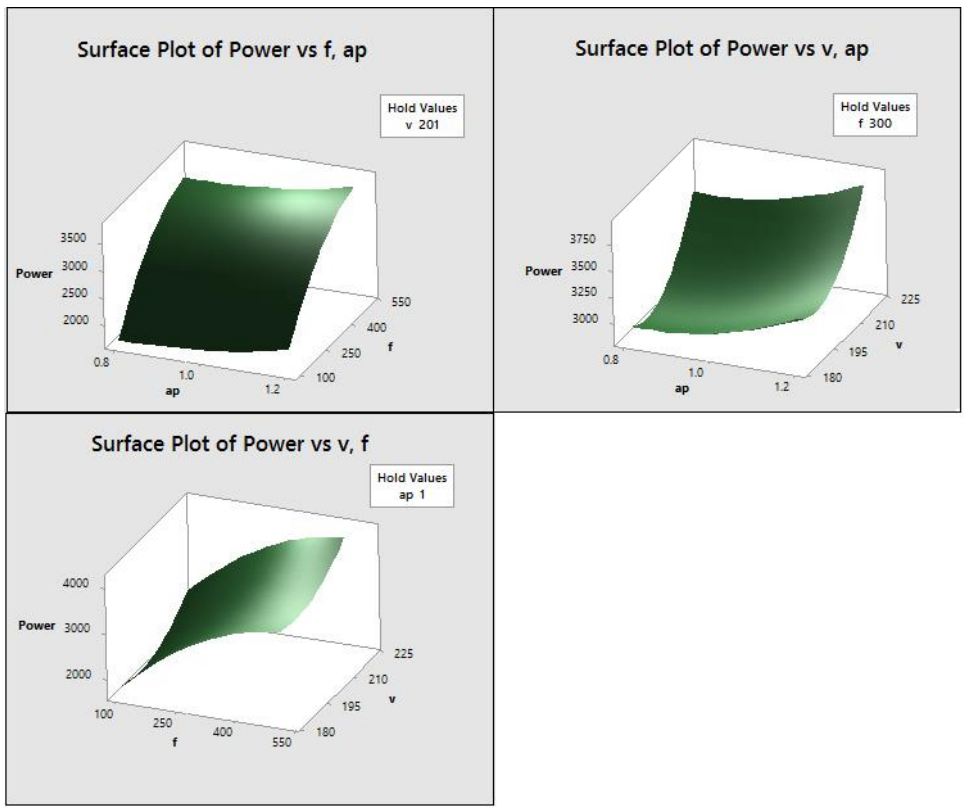


Figure 48. Surface plots for power consumption of orthogonal turn-milling process

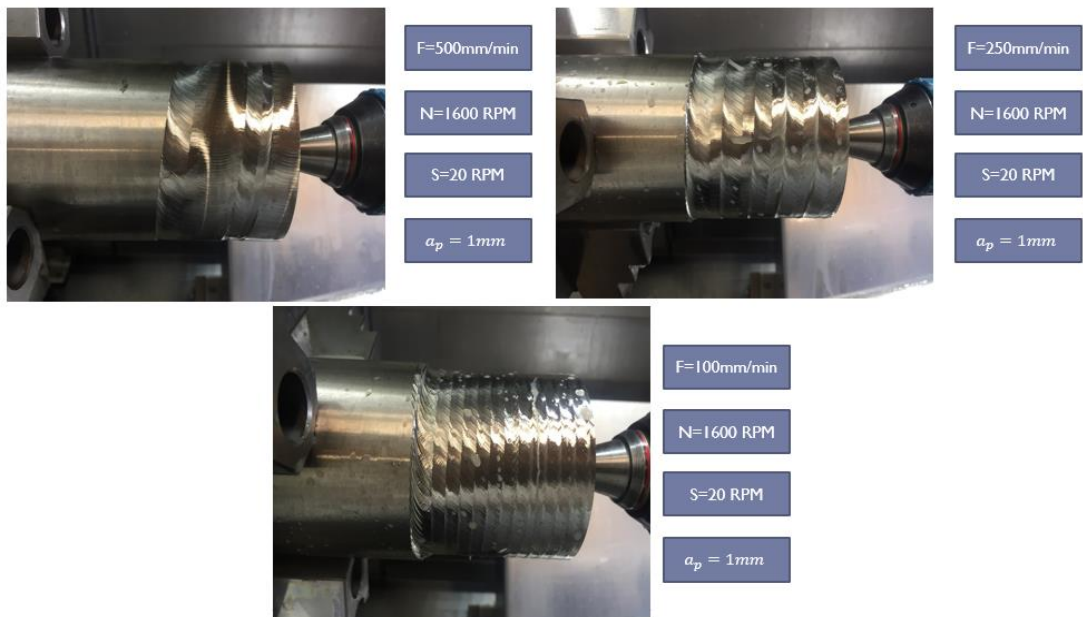


Figure 49 . Pictures of turn-milled parts





## CHAPTER 7

### DISCUSSION OF THE RESULTS

To discuss the results a breakdown of energy consumption during cutting operation of the case study part is obtained as seen in the Figure 50. The energy consumption share of active sub-unit is demonstrated based on percentages in the figure.

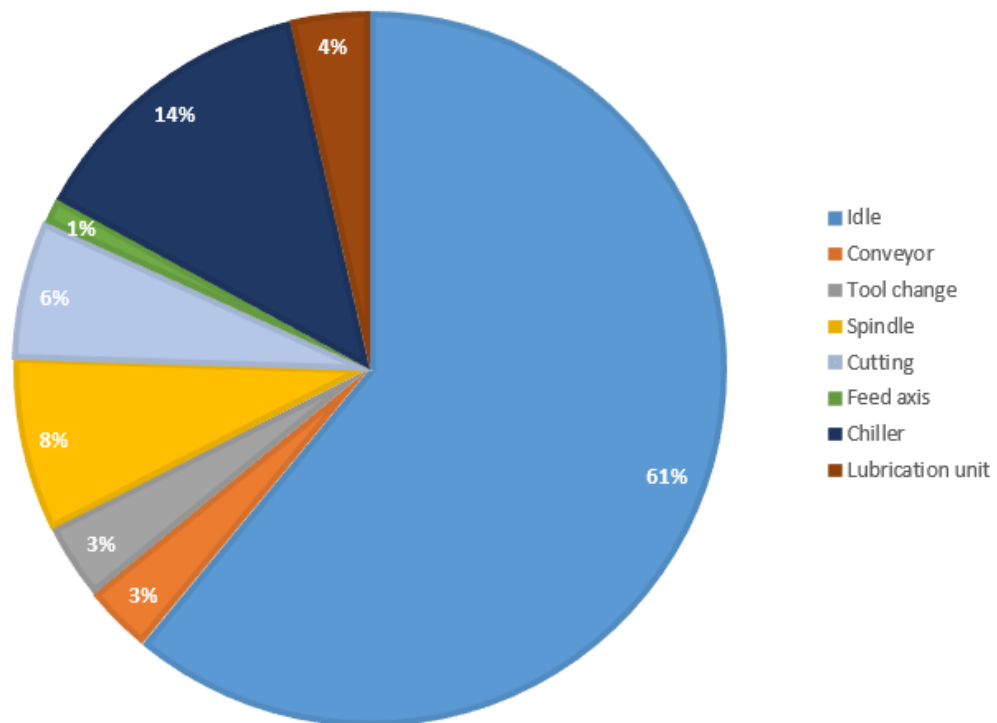


Figure 50 Breakdown of energy consumption for cutting operation of the case study part

During machining the case part, a considerable amount of the total energy consumption is consumed for idling. Idling consumed about 60% of the total energy consumed during this operation. This demonstrates the inefficiency of complicated systems since 61% of total energy consumption for a machining operation consumed

for keeping the machine tool in ready state without doing any operation. In addition the chiller is the next most energy consumer unit in the operation and this unit also consumes energy to keep the spindle in a specified temperature.

The spindle consumes about 8% of the total energy consumption. The energy consumption share of spindles is shown in Figure 51.

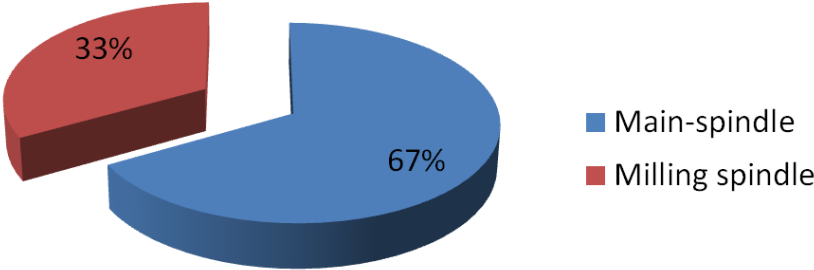


Figure 51 Energy consumption of spindle during machining processes of case study part

Although the activation time of milling spindle was much more than the main spindle and also the milling spindle was rotating at high RPMs comparing with the main spindle, main spindle consumes more energy.

The conveyor consumes about 4% of the total energy consumption which is activated while the program starts and consumes a constant amount of power every second during its activation time. 3% of the total energy consumption of the operation is for tool change. During the operation, automatic tool change is performed 3 times at low speeds. The feed axis consumed the least amount of energy compared to other sub units.

All the subunits are operated in order perform the cutting features, but cutting features consumes only 6% of the total energy consumption. This is another reason that clarifies the inefficiency of complicated machine tools. Among the performed

cutting features, the most of the energy is consumed for OD turning feature. The breakdown of cutting energy consumption is shown in Figure 52.

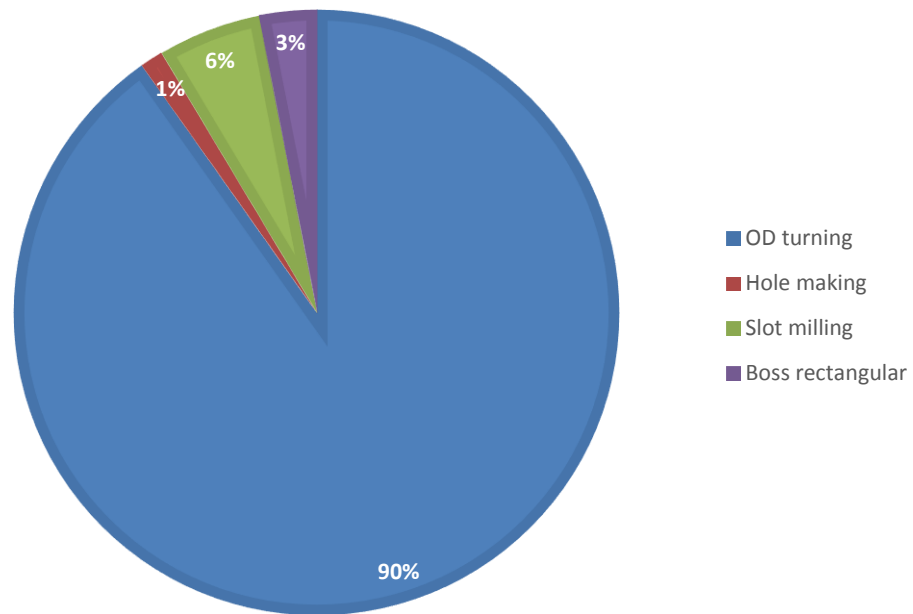


Figure 52 Breakdown of cutting energy consumption for case study

The reason is that turning operation lasts more than the other operations and also the volume removed by OD turning feature is much more than the other features. The volume removed by each feature is calculated Appendix D. The energy consumed in removing a unit volume of material is also determined for each feature separately. The calculated values are actually specific cutting energy which are specified for each feature. These values are given in Figure 53.

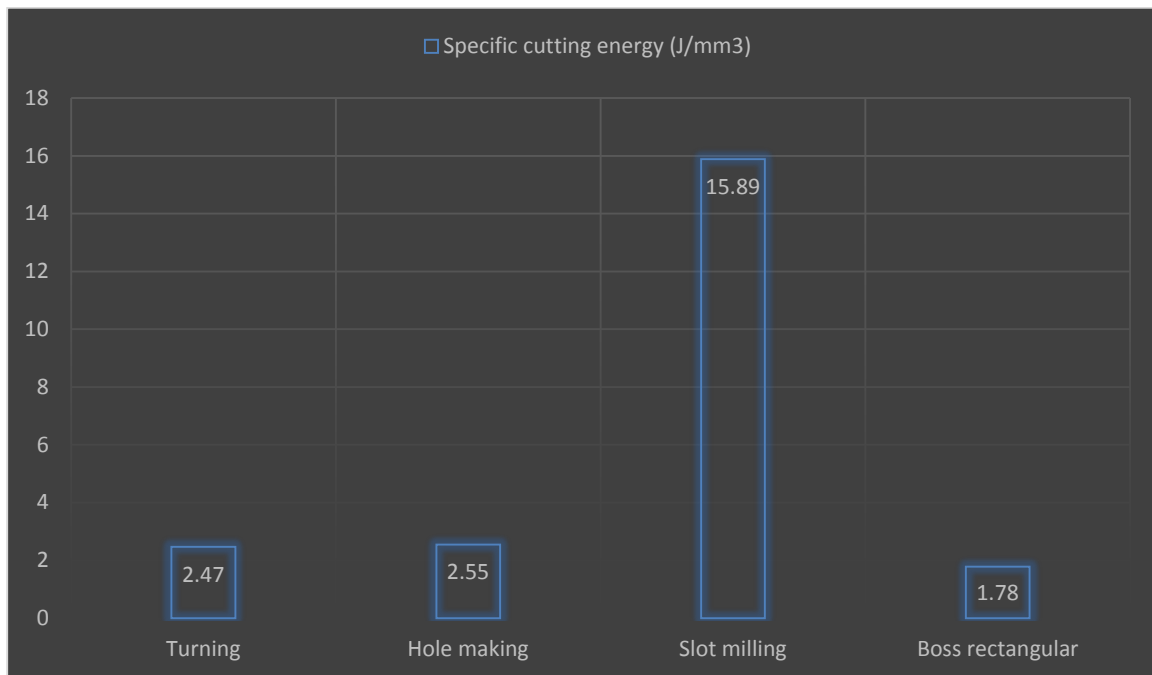


Figure 53 Specific cutting energy of the cutting features

## **CHAPTER 8**

### **CONCLUSIONS AND FUTURE WORKS**

This thesis work outlines an experimental study to generate an energy consumption model for turn-mill systems and investigating the energy consumption of orthogonal turn-milling processes.

Within this study a generic energy consumption model is derived for turn-mill systems considering the sub-units of turn-mill systems. Characterization studies are performed on Mazak integrex i200-ST and for this purpose experiments were designed in order to obtain power consumption amount of sub-unit and equations were derived for the sub-units which were dependent on cutting parameters.

The cutting parameters used for cutting operations and also cutting features considerably affect the energy consumption of material removal processes. In most of previous energy consumption modelling studies the cutting energy was modelled by specific cutting and as mentioned above specific cutting energy is the energy consumed to remove one unit volume of material regardless of cutting parameters or cutting features. It is estimated that one of the reasons of the low accuracy of energy consumption predictions while using specific cutting energy is not considering the cutting parameters and cutting features. In this study a methodology is presented to model cutting energy of cutting features separately and with respect to cutting parameters in order to increase the accuracy of cutting energy models. Taguchi and response surface methodology are both utilized and energy consumption models were derived for each of selected cutting features and an average accuracy of 90% is obtained for developed cutting energy models.

In first case study the power requirement of whole process is estimated using obtained equations in characterization studies and developed cutting energy models and an accuracy of 95% is obtained. The main reason of this accuracy is that the

major part of total energy consumption of manufacturing processes is consumed during idling which is a constant amount of energy and determined during characterization studies, so the main part of total energy consumption is predicted with a high accuracy.

Total energy consumption of the first case study manufacturing process is analyzed and it is obtained that the 61% of total energy consumptions consumed for idling which demonstrates the inefficiency of complicated machine tools. This demonstrates the inefficiency of complicated systems since 61% of total energy consumption for a machining operation consumed for keeping the machine tool in ready state without doing any operation. In addition the chiller is the next most energy consumer unit in the operation and this unit also consumes energy to keep the spindle in a specified temperature where the cutting process consumes only about 6% of total energy consumption.

Turn-milling processes are relatively novel processes and a few number studies have been presented in this area. Turn-mill process are performed in turn-mill machine tool with a wide interval for cutting parameters. The effect of cutting parameters on energy consumption of turn-milling energy consumption is obtained first time in the literature. Conventional turning operations was also performed in the same cutting conditions in order to compare the power requirement and energy consumption of turn-milling processes and conventional turning operations.

Since the cutting tool in turn-mill processes is milling cutting tool and has more than one insert, feed rate values I turn-milling processes are higher than conventional processes which results in higher material removal rates. Although the power requirement of turn-milling processes are more than the conventional turning processes but as the cutting time is lower in turn-milling processes due to higher feed rate amounts, turn-milling processes consumes less power comparing the conventional turning processes. So performing turn-milling processes on powerful machine tools will result in more energy efficient processes.

Presented energy consumption model is a feature based model considering cutting parameters. So the effect of cutting parameters and different feature are taken into consideration. Nevertheless, this model is still dependent to nevertheless workpiece material which considerably affect the energy consumption of cutting process and the presented model is valid for cutting operations of 304 stainless steel.

This study could be improved by using more enhanced energy meters to get more than one data every second. Also for modeling the energy consumption of cutting features, Taguchi's L9 orthogonal arrays was used, using L16 and L27 orthogonal arrays may considerably increase the accuracy of the model.

Many opportunities for future research exist which are given in following:

- One of the important improvements is developing a multi-objective optimization method to obtain optimal cutting parameters with objectives of minimum energy consumption and minimum cutting time.
- Compound machining processes which are applicable in complicated systems could be processes in order to examine efficiency of those type of processes.
- The presented model in the study is still dependent on workpiece material and cutting tool. A methodology could be provided to create a model which is independent of these factors.
- Energy consumption of co-axial turn-milling processes could be analyzed and compared with orthogonal turn-milling and conventional processes on turn-mill machine tools
- Surface quality of turn-milled parts could be modelled with respect to cutting parameters and optimum cutting conditions could be obtained in order to achieve best surface quality.





## REFERENCES

- [1] International Energy Annual (IEA), "World Energy Outlook 2013," International Energy Annual (IEA), [Online]. Available: <http://www.worldenergyoutlook.org/publications/weo-2013/>. [Accessed 2015].
- [2] Institution of Regulation of Energy Markets, "Petrol Piyasası Sektör Raporu 2013," [Online]. Available: [http://www.epdk.gov.tr//documents/petrol/rapor\\_yayin/2013\\_Petrol\\_Piyasasi\\_Sektor\\_Raporu.pdf](http://www.epdk.gov.tr//documents/petrol/rapor_yayin/2013_Petrol_Piyasasi_Sektor_Raporu.pdf). [Accessed 2015].
- [3] Electricity Generation Company, "Elektrik Üretim Sektör Raporu 2012," [Online]. Available: [http://www.enerji.gov.tr/yayinlar\\_raporlar/Sektor\\_Raporu\\_EUAS\\_2012.pdf](http://www.enerji.gov.tr/yayinlar_raporlar/Sektor_Raporu_EUAS_2012.pdf). [Accessed 2015].
- [4] TMMOB, "Türkiye'nin Enerji Görünümü," [Online]. Available: [http://www.tr.boell.org/downloads/turkiyenin\\_enerji\\_gorunumu\\_oguz\\_turkiyil\\_maz\\_2012.pdf](http://www.tr.boell.org/downloads/turkiyenin_enerji_gorunumu_oguz_turkiyil_maz_2012.pdf). [Accessed 2015].
- [5] EIA, "Annual Energy Review 2010" p. 38, 2010.
- [6] Black, J.T., Kohser, R. A., DeGarmo's Materials and Processes in Manufacturing, USA: John Wiley & Sons Inc., 2008.
- [7] D. Kordonowy, "A Power Assessment of Machining Tools," Bachelor of Science Thesis, Massachusetts Institute of Technology, Massachusetts, USA, 2002.
- [8] Gutowski, T.G., Dahmus, J.B., Thiriez, A., "Electrical Energy Requirements For Manufacturing Processes," Leuven, Belgium, 2006.
- [9] Dahmus, J.B., Gutowski, T.G., "An Environmental Analysis Of Machining," in The IMECE2004 ASME International Mechanical Engineering Congress and RD&D Expo, Anaheim, California USA, 2004.
- [10] Devoldere, T., Dewulf, W., Deprez, W., Willems, B., Duflou, J.R., "Improvement Potential for Energy Consumption in Discrete Part Production Machines," in 14th CIRP International Conference on Life Cycle Engineering, Waseda, Tokyo, Japan, 2007.
- [11] Rajemi, M.F., Mativenga, P.T., Aramcharoen, A., "Sustainable Machining: Selection of

- Optimum Turning Conditions Based On Minimum Energy Considerations," *J. Clean. Prod.*, vol. 18, pp. 1059-1065, 2010.
- [12] Mativenga P.T, Rajemi M.F., "Calculation of Optimum Cutting Parameters Based on Minimum Energy Footprint," *CIRP Annals - Manuf Technol*, vol. 60, pp. 149-152, 2011.
- [13] Schischke, K., Hohwieler, E., Feitscher, R., König, J., Kreuschner, S., Wilpert, P., Nissen, N.F., "Energy-Using Product Group Analysis - Lot 5," Task 5 Report – Technical Analysis BAT and BNAT, Berlin, 2012.
- [14] Li, W., Zein, A., Kara, S., Herrmann, C., "An Investigation into Fixed Energy Consumption of Machine Tools," in 18th CIRP LCE Conference, Braunschweig, 2011.
- [15] He, Y., Liu, F., Wu, T., Zhong, F.P., Peng, B., "Analysis and Estimation of Energy Consumption for Numerical Control Machining," *Proc IMechE Part B J Eng Manuf*, pp. 255-266, 2012.
- [16] Salonitis, K., Ball, P., "Energy Efficient Manufacturing from Machine Tools to Manufacturing Systems," in Forty Sixth CIRP Conference on Manufacturing Systems, 2013.
- [17] Calvanese, M.L., Albertelli, P., Matta, A., Taisch, M., "Analysis of Energy Consumption in CNC Machining Centers," in 20th CIRP International Conference on Life Cycle Engineering, Singapore, 2013.
- [18] Aramcharoen, A., Mative, P.T., "Critical Factors in Energy Demand Modelling for CNC Milling and Impact of Toolpath Strategy," *J. Clean. Prod.*, vol. 78, pp. 63-74, 2014.
- [19] Uluer M.U., Ünver H.Ö., Akkuş K., Kılıç S.E., "A Model for Predicting Theoretical Process Energy Consumption of Rotational Parts Using STEP AP224 Features," in 20th CIRP International Conference on Life Cycle Engineering, Singapore, 2013.
- [20] Mori, M., Fujishima, M., Inamasu, Y., Oda, Y., "A Study on Energy Efficiency Improvement for Machine Tools," *CIRP Annals - Manuf Technol*, pp. 145-148, 2011.
- [21] Diaz, N. , Redelsheimer, E. , Dornfeld, D., "Energy Consumption Characterization and Reduction Strategies for Milling Machine Tool Use," in Braunschweig, Germany, 2011, The 18th CIRP International Conference on Life Cycle Engineering.
- [22] Diaz, N., Helu, M., Jarvis, A., Tonissen, S., Dornfel, D., Schlosser, R., "Strategies for Minimum Energy Operation for Precision Machining," in The Proceedings of MTTRF

2009 Annual Meeting, 2009.

- [23] Kong, D., Choi, S., Yasui, Y., Pavanaskar, S., Dornfeld, D., Wright, P., "Software-based Tool Path Evaluation for Environmental Sustainability," *J Manuf Syst*, pp. 241-247, 2011.
- [24] Avram, O.L., Xirouchakis, P., "Evaluating the Use Phase Energy Requirements of a Machine Tool System," *J. Clean. Prod.*, pp. 699-711, 2011.
- [25] Neugebauer, R., Wabner, M., Rentzsch H., Ihlenfeldt, S., "Structure Principles of Energy Efficient Machine Tools," *CIRP Journal of Manufacturing Science and Technology*, vol. 4, pp. 136-147, 2011.
- [26] Hu, S., Liu, F., He, Y., Hu, T., "An on-line Approach for Energy Efficiency Monitoring of Machine Tools," *J. Clean. Prod.*, vol. 27, pp. 133-140, 2012.
- [27] Hu, S., Liu, F., He, Y., Peng, B., "Characteristics of Additional Load Losses of Spindle System of Machine Tools," *J Adv Mech Des Sys Manuf*, vol. 4, no. 7, pp. 1221-1233, 2010.
- [28] Balogun V.A., Mativenga P.T., "Modelling of Direct Energy Requirements in Mechanical Machining Processes," *J Clean Prod*, vol. 41, pp. 179-186, 2013.
- [29] Draganescu, F., Gheorghe, M., Doicin, C.V., "Models of Machine Tool Efficiency and Specific Consumed Energy," *J Mater Proc Technol*, vol. 141, pp. 9-15, 2003.
- [30] S. Kara, W. Li, "Unit Process Energy Consumption Models for Material Removal Processes," *CIRP Annals - Manufacturing Technology*, vol. 60, pp. 37-40, 2011.
- [31] Guo, Y., Loenders, J., Duflou, J., Lauwers, B., "Optimization of Energy Consumption and Surface Quality in Finish Turning," in *5th CIRP Conference on High Performance Cutting*, 2012.
- [32] Hae-Sung Yoon, Jong-Seol Moon, Minh-Quan Pham, Gyu-Bong Lee, Sung-Hoon Ahn, "Control of Machining Parameters for Energy and Cost Savings in Micro-scale Drilling of PCBs," *Journal of Cleaner Production*, vol. 54, pp. 41- 48, 2013.
- [33] Hae-Sung Yoon, Jang-Yeob Lee, Min-Soo Kim, Sung-Hoon Ahn, "Empirical Power-Consumption Model for Material Removal in Three Axis Milling," *Journal of Cleaner Production*, vol. 78, pp. 54-62, 2014.
- [34] Pervaiz S, Deiab I, Rashid A, "Prediction of Energy Consumption and Environmental Implications for Turning Operation Using Finite Element Analysis," *Proc IMechE part*

B J Eng Manuf, pp. 1-8, 2014.

- [35] Dietmair A, Verl A, "Energy Consumption Modeling and Optimization for Production Machines," in Proceedings of the IEEE International Conference on Sustainable Energy Technologies., 2008.
- [36] Dietmair A, Verl A, "A Generic Energy Consumption Model for Decision Making and Energy Efficiency Optimisation in Manufacturing," Int J Sustain Eng, vol. 2, no. 2, pp. 123-133, 2009.
- [37] Larek R, Brinksmeier E, Meyer D, Pawletta T, Hagendorf O, "A Discrete-event Simulation Approach to Predict Power Consumption in Machining Processes," J Prod Eng, vol. 5, p. 575–579, 2011.
- [38] D. Montgomery, Design and Analysis of Experiments, Wiley, New York, 1997.
- [39] Diaz N, Redelsheimer E, Dornfeld D, "Energy Consumption Characterization and Reduction Strategies for Milling Machine Tool Use," in The 18th CIRP International Conference on Life Cycle Engineering, Braunschweig, Germany, 2011.
- [40] Edwin R.U., Dean B., "Taguchi Approach to Design Optimization for Quality and Cost," in Annual Conference of the International Society of Parametric Analysts, 1991.
- [41] W.H. Yang, Y.S. Tarn, "Design Optimization of Cutting Parameters for Turning Operations Based on the Taguchi Method," Journal of Materials Processing Technology, p. 122–129, 1998.
- [42] Domnita Fratila, Cristian Caizar, "Application of Taguchi Method to Selection of Optimal Lubrication and Cutting Conditions in Face Milling of AlMg3," Journal of Cleaner Production, vol. 19, pp. 640-645, 2011.
- [43] Anirban Bhattacharya, Santanu Das, P. Majumder, Ajay Batish, "Estimating the effect of cutting parameters on surface finish and power consumption during high speed machining of AISI 1045 steel using Taguchi design and ANOVA," Journal of production engineering, vol. 3, pp. 31- 40, 2009.
- [44] Issam Hanafi, Abdellatif Khamlichi, Francisco Mata Cabrera, Emiliano Almansa, Abdallah Jabbouri, "Optimization of cutting conditions for sustainable machining of PEEK-CF30 using TiN tools," Journal of cleaner production, pp. 1-9, 2012.
- [45] G. E. P. Box, K. B. Wilson, "On The Experimental Attainment of Optimum Conditions," Journal of the Royal Statistical Society, vol. 13, 1951.

- [46] L. B. Abhang, M. Hameedullah, "Power Prediction Model for Turning EN-31 Steel Using Response Surface Methodology," *Journal OF Engineering Science and Technology Review*, vol. 3, no. 1, pp. 116-122, 2010.
- [47] Campatelli G, Lorenzini L, Scippa A, "Optimization of Process Parameters Using a Response Surface Method for Minimizing Power Consumption in the Milling of Carbon Steel," *J Clean Prod*, vol. 66, pp. 309-316, 2014.
- [48] R. K. Bhushan, "Optimization of Cutting Parameters for Minimizing Power Consumption and Maximizing Tool Life During Machining of Al alloy SiC Particle Composites," *Journal of Cleaner Production*, vol. 39, pp. 242-254, 2013.
- [49] Jihong Yan, Lin Li, "Multi-objective Optimization of Milling Parameters and the Trade-Offs Between Energy, Production Rate and Cutting Quality," *Journal of Cleaner Production*, vol. 52, pp. 462-471, 2013.
- [50] Aman Aggarwal, Hari Singh, Pradeep Kumar, Manmohan Singh, "Optimizing Power Consumption for CNC Turned Parts Using Response Surface Methodology and Taguchi's Technique—A Comparative Analysis," *Journal of Materials Processing Technology*, vol. 200, pp. 373-384, 2008.
- [51] Yung-Tsan Jou, Wen-Tsann Lin, Wei-Cheng Lee, Tsu-Ming Yeh, "Integrating the Taguchi Method and Response Surface Methodology for Process Parameter Optimization of the Injection Molding," *Applied Mathematics & Information Sciences*, no. 3, pp. 1277-1285, 2014.
- [52] Amaitik S. M., Kilic S. E., "STEP-based Feature Modeller for Computer-aided Process Planning," *International Journal of Production Research*, vol. 43, no. 15, pp. 3087-3101, 2005.
- [53] "Product Data Representation and Exchange – Part 224: Application Protocol: Mechanical Product Definition for Process Planning Using Machining Feature," International Standards Organization, ISO 10303-224 Industrial Automation Systems and Integration, Geneva, Switzerland, 2006.
- [54] Filho C., Martins J., "Prediction of Cutting Forces in Mill Turning Through Process Simulation Using a Five-axis Machining Center," *The International Journal of Advanced Manufacturing Technology*, vol. 58, pp. 71-80, 2012.
- [55] Schulz, H., Spur, G., "High Speed Turn-Milling — A New Precision Manufacturing Technology for the Machining of Rotationally Symmetrical Workpieces," *Ann ICRP Manuf Technol*, vol. 1, no. 39, pp. 107-109, 1990.

- [56] Schulz H., Kiensel T., "Turn-milling of Hardened Steel- An Alternative to Turning," Ann-CIRP, vol. 43, no. 1, pp. 93-96, 1994.
- [57] Choudhury, S. K., Mangrulkar, K. S., "Investigation of Orthogonal Turn-milling for the Machining of Rotationally Symmetrical Work Pieces," Journal of Materials Processing Technology, vol. 99, no. 1, pp. 120-128, 2000.
- [58] Choudhury, S. K., Bajpai, J. B. , "Investigation in Orthogonal Turn-milling Towards Better Surface Finish," Journal of Materials Processing Technology, vol. 170, no. 3, pp. 487-493, 2005.
- [59] Savas, V., Ozay, C., "Analysis of the Surface Roughness of Tangential Turn-milling for Machining with End Milling Cutter," Journal of Materials Processing Technology, vol. 186, no. 1, pp. 279-283, 2007.
- [60] Kopac, J., Pogacnik, M., "Theory and Practice of Achieving Quality Surface in Turn milling," International Journal of Machine Tools and Manufacture, vol. 307, no. 5, pp. 709-715, 1997.
- [61] Zhu, L., Haonan, L., Wansan, w., "Research on Rotary Surface Topography by Orthogonal Turn-milling," The International Journal of Advanced Manufacturing Technology, vol. 69, pp. 2279-2292, 2013.
- [62] Huang, C., Cai, Y. L., "Turn-milling Parameters Optimization based on Cutter Wear," Advanced Materials Research, vol. 602, pp. 1998-2001, 2013.
- [63] Neagu, C., Gheorghe, M., Dumitrescu A., "Fundamentals on Face Milling Processing of Straight Shafts," Journal of materials processing technology, vol. 166, no. 3, pp. 337-344, 2005.
- [64] Karagüzel, U., Uysal, E., Budak, E., Bakkal, M., "Analytical Modeling of Turn-milling Process Geometry, Kinematics and Mechanics," International Journal of Machine Tools and Manufacture, vol. 91, pp. 24-33, 2015.
- [65] "Mazak USA," 2015. [Online]. Available: <https://www.mazakusa.com/machines/integrex-i-200st/>. [Accessed June 2015].

## APPENDIX A

### AVERAGE POWER CONSUMPTION AMOUNT FOR AUXILIARY SUB-UNITS

Table 21 Average power consumption amounts for spindle speeds of main spindle

<b>RPM</b>	<b>Power (Watts)</b>	<b>RPM</b>	<b>Power (Watts)</b>	<b>RPM</b>	<b>Power (Watts)</b>
300	280	1900	1103.3	3500	1760
400	333.33	2000	1116.7	3600	1820
500	376.67	2100	1143.3	3700	1846.7
600	410	2200	1166.7	3800	1916.7
700	403.33	2300	1196.7	3900	1983.3
800	390	2400	1236.7	4000	2063.3
900	400	2500	1276.7	4100	2143.3
1000	713.33	2600	1303.3	4200	223.3
1100	790	2700	1333.3	4300	2316.7
1200	840	2800	1380	4400	2416.7
1300	900	2900	1423.3	4500	2503.3
1400	963.33	3000	1470	4600	2606.7
1500	1030	3100	1513.3	4700	2730
1600	1050	3200	1566.7	4800	2883.3
1700	1060	3300	1616.7	4900	3036.7
1800	1086.7	3400	1680	5000	3140

Table 22 Average power consumption amounts for spindle speeds of sub-spindle

<b>RPM</b>	<b>Power (Watts)</b>	<b>RPM</b>	<b>Power (Watts)</b>
300	260	2200	690
400	280	2300	700
500	320	2400	710
600	320	2500	720
700	300	2600	690
800	310	2700	710
900	300	2800	730
1000	300	2900	750
1100	500	3000	770
1200	550	3100	790
1300	550	3200	840
1400	580	3300	870
1500	650	3400	920
1600	650	3500	940
1700	650	3600	980
1800	660	3700	1060
1900	670	3800	1080
2000	680	3900	1140
2100	680	4000	1270



Table 23 Average power consumption amounts for spindle speeds of milling spindle

<b>RPM</b>	<b>Power (Watts)</b>	<b>RPM</b>	<b>Power (Watts)</b>
100	250	5200	480
300	260	5400	450
500	270	6000	450
700	270	6400	460
900	280	6800	460
1100	290	7200	450
1300	310	7800	470
1500	320	8200	480
1700	330	8800	490
2000	310	9200	510
2400	300	9500	530
2800	250	9800	540
3200	230	10000	550
3600	230	10300	550
3900	220	10500	560
3950	230	10600	570
4000	430	10800	590
4200	430	11200	610
4400	450	11500	640
4800	460	11800	660
5000	470	12000	680

Table 24 Average power consumption amounts for G00 moves of milling head

<b>Feed speed (mm/min)</b>	<b>Power (Watt)</b>		
	Z axis	X+ axis	X- axis
500	100	700	-402.5
12500	340	1840	-932.5
25000	803.3	1823	-886.7

Table 25 Average power consumption amounts for G00 moves of milling head

<b>RPM</b>	<b>Power (Watt)</b>
	Y axis
400	250
1600	260
4000	270
10000	270
20000	280

Table 26 Average power consumption amounts for G01 moves of milling head

<b>Feed rate (mm/min)</b>	<b>Power (Watt)</b>			
	Z axis	X+ axis	X- axis	Y axis
120	10	30	-20	0
180	10	30	-20	0
270	10	40	-30	10
400	10	60	-40	10
600	10	80	-60	10
900	10	120	-90	20
1340	20	190	-140	30
2000	30	270	-190	50

Table 27 Average power consumption amounts for rotation of milling head

<b>Feed speed (mm/min)</b>	<b>Power (Watt)</b>			
	0°-45°	45°-90°	90°-135°	135°-180°
144	60	80	30	30
576	110	70	50	30
1440	150	140	100	90
3164	180	240	120	110

Table 28 Average power consumption amounts for for G00 movess of turret

<b>Feed speed (mm/min)</b>	<b>Power (Watt)</b>		
	Z axis	X+ axis	X- axis
4000	90	157.5	-72.5
10000	290	307.5	-46.7
20000	700	508.3	-41.7

Table 29 Average power consumption amounts for for G01 movess of turret

<b>Feed speed (mm/min)</b>	<b>Power (Watt)</b>		
	Z axis	X+ axis	X- axis
120	10	20	-10
180	10	25	-10
400	20	30	-15
900	20	40	-20
1340	30	50	-20
2000	40	55	-30

## APPENDIX B

### DERIVED EQUATIONS FOR SUB-UNITS OF MAZAK

#### INTEGREX I200-ST

Table 30 Derived equations for sub-units of Mazak integrex i200-ST with respect to cutting parameters

Sub-unit		Derived Equation	
Main spindle	$RPM < 1000$	$-0.0007.S^2 + 1.0071x + 42.381$	
	$RPM \geq 1000$	$0.0000000439.S^3 - 0.0002749044.S^2 + 0.8845074804.S + 110.58283060$	
Sub-spindle	$RPM < 1100$	$0.00000078.S^3 - 0.00181818.S^2 + 1.33827561.S - 2.61904762$	
	$RPM \geq 1100$	$0.0000000825.S^3 - 0.0005526511.S^2 + 1.2922086784.S - 356.1590347299$	
Milling spindle	$RPM < 4000$	$0.0000000000091.S^4 - 0.0000000669423.S^3 + 0.0001291405303.S^2 - 0.0340515877945.S + 255.5146866024780$	
	$RPM \geq 4000$	$-0.00000000000018.S^4 + 0.00000000637724.S^3 - 0.00007765458948.S^2 + 0.39527484565071.S - 267.20002245144400$	
Turret	G01	X- axis	$0.00000154.f^2 - 0.01283123.f - 9.26223086$
	G01	X+ axis	$-0.00000542.f^2 + 0.02989522.f + 17.57628760$
	G00	X- axis	$-0.00000024.f^2 + 0.00763542.f - 99.23611111$



## APPENDIX C

### MAZARTOL PROGRAMMING OF FIRST CASE PART

Solutionware Corporation -- Mazak Print  
 Metric Mon, 24 Aug 2015, 01:05PM  
 Filename: C:\Users\taner.akkas\Desktop\1CASE.PBE  
 Machine: Matrix-e/i/j

WorkNumber: 1CASE  
 Size (number of blocks): 34  
 Machine: MatrixE

UNo.	MAT.	OD-MAX	ID-MIN	LENGTH	WORK-FACE	ATC-MODE	RPM
0	PASLANMZ	53.7	0.	103.	0.	0	1000
TPC Clearance TC37 TC38 TC39 TC40 TC62 Parameters							
0	0.	0.	0.	0.	0	1 0 0	0 0 0
0	0	0					
TPC Clearance TC37 TC38 TC39 TC40 TC62 Parameters							
0	0.	0.	0.	0.	0	1 0 1	0 0 0
0	0	0					

UNo.	UNIT	ADD.WPC	X	Y	Th	Z	C
1	WPC-	0	T.CENTER	T.CENTER	0.	-473.508	0.

UNo.	UNIT	TURN	POS X	TURN	POS Y	TURN	POS Z	ANGLE B	ANGLE C
2	INDEX	0.		0.		0.		90.	0.

UNo.	UNIT	PART	CPT-X	CPT-Z	FIN-X	FIN-Z						
3	BAR	OUT	53.65	0.	0.	0.						
SNo	TOOL	NOM.	No.	PAT.	DEP-1	DEP-2/NUM	DEP-3	FIN-X	FIN-Z	C-SP	FR	M
M	M											
R 1	GNL	OUT 25.	K	1	0.75	<>	<>	<>	<>	350	0.2	
FIG	PTN	S-CNR	SPT-X	SPT-Z	FPT-X	FPT-Z	F-CNR/\$	R/th	RGH			
1	LIN		<>	<>	38.65	40.		<>				
2	TPR		38.65	40.	52.9	50.						
3	LIN		<>	<>	52.9	65.		<>				

UNo.	UNIT	SHIFT-X	SHIFT-Y	SHIFT-Z	SHIFT-C	COORD.th	MIRROR
4	WPCSHIFT	26.825	0.	0.	0.	0.	0

UNo.	UNIT	TURN	POS X	TURN	POS Y	TURN	POS Z	ANGLE B	ANGLE C
5	INDEX			0.		0.		0.	0.

UNo.	UNIT	DIA	DEPTH	CHMF										
6	DRILLING	7.5	15.	0.										
SNo	TOOL	NOM-D	No	HOLE-D	HOLE-DEP	PRE-DIA	PRE-DEP	RGH	DEPTH	C-SP	FR	M	M	
M														
1	CTR-DR	3.	7.5	<>	<>	<>	90ø	CTR-D	18	0.08				
2	DRILL	7.5	7.5	15.	0.	100	PCK1	15.	40	0.06				
FIG	PTN	Z	X	Y	AN1	AN2	T1	T2	F	M	N	P	Q	R
1	PT	0.	-35.825	0.	<>	<>	<>	<>	<><>	<>	1	0	0	

UNo.	UNIT	DEPTH	SRV-Z	SRV-R	RGH	FIN-Z	FIN-R	START	END					
7	LINE-LFT	2.	2.	2.	9	0.	0.	OPEN	OPEN					
SNo	TOOL	NOM-D	No.	APRCH-X	APRCH-Y	TYPE	ZFD	DEP-Z	WID-R	C-SP	FR	M	M	M
R 1	E-MILL	10.	K	-6.975	-22.399	<>	G01	2.	<>	80	0.06			
FIG	PTN	X	Y	Rad/Th.	I	J	P	CNR	R-FEED					
RGH														
1*LINE		-9.5	17.325											

2	LINE	-9.5	-17.325
3	LINE	-44.15	-17.325
4	LINE	-44.15	17.325
5	LINE	-9.5	17.325
6	LINE	-11.5	15.325
7	LINE	-11.5	-15.325
8	LINE	-42.15	-15.325
9	LINE	-42.15	15.325
10	LINE	-11.5	15.325

UNO.	UNIT	TURN POS X	TURN POS Y	TURN POS Z	ANGLE B	ANGLE C
8	INDEX	0.	0.	0.	90.	0.

UNO.	UNIT	DEPTH	SRV-Z	S-WIDTH	BTM WAL	FIN-Z	FIN-R					
9	SLOT	9.5	2.	9.95	9 9	0.	0.					
SNO	TOOL	NOM-D	No	APRCH-X	APRCH-Y	TYPE ZFD	TYPE PK-DEP	DEP-Z	WID-R	C-SP	FR	
M	M	M										
R 1	E-MILL	10.	K	-5.	0.	CW	G01	<>	2.	<>	80	0.072
FIG	PTN	X	Y	Rad/Th.	I	J	P	CNR	R-FEED			
RGH												
1*	LINE	3.	0.									
2	LINE	24.	0.									

UNO.	UNIT	CONTI.	REPEAT	SHIFT	NUMBER	ATC	RETURN	Work-No.
EXECUTE								
10	END					0		
YES								



## APPENDIX D

### MATERIAL REMOVED DURING CUTTING FEATURES OF FIRST CASE STUDY

Table 31 Material removed during cutting features of first case study

<b>Feature</b>	<b>Material removed (<math>mm^3</math>)</b>
OD turning	50187.52
Hole making	662.68
Slot milling	478.54
Boss rectangular miling	2349.28



## **APPENDIX E**

### **ISO PROGRAMMING OF SECOND CASE PART**

G00 G59

G21 (METRIC)

G90 (ABSOLUTE)

G94 (F/MIN)

G109L1 (SELECT UPPER TURRET)

M902 (SELECT RIGHT SPINDLE)

T035 T0 M6 (TOOL CHANGE)

M300 (RIGHT SPINDLE MILLING MODE)

M03 S1600 (START MILLING CCW)

G94 G04 X5000

G01 X31. Z2. F2000

G01 X31. Z-35. F500

G01 X43. Z-35. F500

G01 X43. Z2. F2000

G01 X100. Z2. F2000

M05 (STOP SPINDLE)

M302 (DISCONNECT CAXIS RIGHT SPINDLE)

M950 (PROGRAM SYNC)

M30 (PROGRAM STOP)